Study of Inhibitory Properties of Small Molecule Compounds on Histone Deacetylases

A Major Qualifying Project Report

Submitted to the Faculty of the

Worcester Polytechnic Institute

In partial fulfillment of the requirements for the
Degree of Bachelor of Science
by

Christofer M. Welsh

Date: April 25, 2018
Approved:

X

Professor Destin Heilman
Major Advisor

Table of Contents

Abstract

Histones can undergo modifications, which regulate the accessibility of DNA. Modifications such as acetylation, methylation and phosphorylation alter the epigenetic landscape, which regulates the expression of different genes. (Kouzarides, 2013) Epigenetic regulations of genes have been linked to important developmental stages of cardiovascular development (Asnani, 2014). However, the process by which epigenetic regulations alter development is still not well understood. Still, some drugs have been shown to inhibit epigenetic regulators and affect development. (Kouzarides, 2013) Because of their large clutch sizes, and transparent embryos, zebrafish are a useful model for studying the effect of compounds believed to be epigenetic regulators (MacRae, 2015).

Therefore, the aim of this project was to screen a library of small molecule compounds targeting epigenetic regulators on zebrafish larvae, for their effect on circulatory function. The library was screened, and thereafter analyzed by *in vitro* and *in vivo* assays. Additionally, the effects of HDACs on cardiovascular development was investigated by *in* situ hybridization, and the development of a Cre-dependent *hdac1* mutant line of zebrafish. With these experiments it was determined that six of these compounds had varying inhibitory properties on HDAC enzymes, and that HDAC inhibition leads to malformation in arterial development in zebrafish embryos.

Introduction

In its normal state, genomic DNA is wrapped around histone proteins, which together make up nucleosomes, the main units of the chromatin structure. Histones can be post-translationally modified, which changes their structure and properties. These modifications alter the epigenetic landscape, which regulates the expression of different genes. (Kouzarides, 2013) Traditionally, histone modifications have been thought of as to either directly activate or repress a gene. However, these posttranslational modifications are now thought of as recruiters of enzyme complexes, which regulate transcription. In fact, several different modifications often interplay in their activation or repression of genes, and can mutually interfere with each other. (Berger, 2007) There are at least eight different main types of modifications that can be performed. Histones can undergo methylation, acetylation, phosphorylation, ubiquitylation, sumoylation, ADP ribosylation, deimination and proline isomerization. Of these, methylation, acetylation and phosphorylation of histones are best understood. Methylation is the process in which methyl groups are added to amino acid residues. Acetylation occurs at a lysine at the amino terminal domain, where an acetyl group is added to the residue. Acetylation neutralizes the basic charge of the lysines, which could lead to greater structural changes in the chromatin. Phosphorylation is the addition of a phosphate group, which occurs at either serines or threonines. Posttranslational modifications are dynamic; there are both enzymes that can add and enzymes that can remove these modifications. (Kouzarides, 2013)

Histone Deacetylases (HDACs) are enzymes that catalyze the hydrolysis of acetylated lysines, making the acetyl group leave. Though they are a major component of histone posttranslational modifications, in fact they mostly facilitate the deacetylation of lysines on other proteins. In mammals like humans HDACs are grouped in two different families, and four different classes. Classes I, II and IV all belong to the traditional HDAC family, while class III HDACs (also known as sirtuins) have different enzymatic mechanisms. Class I includes HDAC1, HDAC2, HDAC3 and HDAC 8, which are mostly located in the nucleus of many different cell types. However, they can be localized in the cytoplasm or specialized organelles, and HDAC3 have been found to be restricted to certain tissues. HDAC4, HDAC5 and HDAC6, HDAC7, HDAC9 and HDAC10 belong to class II HDACs. Often class II HDACs have been located to the cytoplasm, and have a much lower activity *in vitro* compared to class I HDACs. HDAC11 is the sole member of Class IV, which shares sequence homology of the catalytic site with both class I and II HDACs. Classes I, II and IV all require a zinc ion for their catalytic mechanism. Many HDACs are functionally redundant with other HDACs, even of different classes. Though substrate specificity of different HDACs exists, these are not well understood. A single HDAC can have different substrate specificity depending on what protein complex it is included in. (Seto, 2014) In zebrafish (*danio reiro*), HDAC class I consists of *hdac1*, *hdac3* and *hdac8* (ZFIN, 2018). Since HDACs 1 and 2 are very similar in their structure and activity, zebrafish hdac1 can fulfill the purpose of both enzymes (De Ruijter, 2003). Class II consists of *hdac*s 4, 5, 6, 7 (a and b), 9 (a and b) and 10. Class IV in zebrafish includes *hdac11*. It is also predicted that there is an *hdac12* in zebrafish. (ZFIN, 2018)

Previous studies have found that HDACs are important for cardiovascular development. In mice loss of HDAC2 leads to early death due to severe cardiovascular malformations (Haberland, 2009), while HDAC1 and HDAC2 redundantly regulate cardiac development (Montgomery, 2007). Another study showed that loss of both HDAC6 and HDAC9 in mice lead to defects in cardiovascular development (Haberland, 2009). HDACs have also been shown to lead to onset and progression of

cardiovascular diseases. For example, downregulation of HDAC2 has resulted in resistance to treatment against cardiac hypertrophy. (Yoon, 2016)

The activity of HDAC enzymes can be reduced by the application of different HDAC inhibitors. The first inhibitor was discovered in 1978, when Candido *et al.* showed that sodium butyrate (Nab) causes hyperacetylation of histones by inhibiting HDACs (Candido, 1978). Since then several other inhibitors have been discovered, some major ones including trichostatin A (TSA), suberoylanilide hydroxamic acid (SAHA) and valproic acid (VPA) (see Fig. 1). These inhibitors are divided into four different classes by their structure and mechanism of inhibition. TSA and SAHA are known as hydroxamates, since they both have the structure of hydroxamic acid. VPA belongs to the short-chain fatty acid class. (Seto, 2014) These inhibitors act similarly to the hydroxamates, by blocking water from entering the active site and performing a nucleophilic attack (Lloyd, 2013). The benzamide class includes inhibitors like MS-275. Their mode of inhibition makes the binding to HDAC enzymes semi-irreversible over time, which results in long-lasting histone acetylation levels after treatment with these compounds. The last class includes FK228, and these are known as cyclic peptides. These inhibitors coordinate zinc ions, with the help of electrophilic ketones and thiols, to inhibit the activity of HDACs. The target selectivity of these inhibitors is an important factor that varies between different HDACs. Hydroxmates tend to inhibit all class I, II and IV HDACS, while benzamides preferentially inhibit class I HDACs, except for HDAC8. Additionally, sodium butyrate, FK228, and MS-275 cannot inhibit HDAC6. (Seto, 2014)

Because of the selectivity, localization and specificity of different drugs in inhibiting enzyme *in vivo*, drug discovery has become an important study. However, the process consists of a complex set of experiments, from development of the drug, biochemical assays, toxicity and validation in animals and finally humans. (Zon, 2005) The initial problem for drug discovery is finding a compound that performs the desired effect, which can be done by two different methods. Target-based screens involve designing compounds to screen, that are modeled to affect specific targets. If the mechanism that the drug is supposed to effect is well understood, this method is very powerful in developing drugs. However, there are often unknown *in vivo* regulators that cannot be predicted. Phenotype-based screens involve screening different compounds *in vivo*, and analyzing the phenotype to deduce the effect of the compound. These screens are often performed in cell cultures, which can quickly give results, however cannot inform on the effect on multi-cellular organisms. Another problem that drug discovery faces is the late toxicity assays that are performed. Since toxicology studies using cell cultures are limited, they cannot effectively be used for these assays, and therefore animal models are often used. Toxicology in mammalian species, however, occurs relatively late, and is an expensive procedure. (MacRae, 2015)

Therefore, zebrafish are a powerful model system to use in the process of drug discovery. Phenotype-based screen can efficiently be performed on zebrafish embryos and larvae. Because of their small size, several embryos can easily fit in a single well in a 384-well plate. This allows for rapid screening of many different compounds, in a multi-cellular organism. By screening zebrafish embryos, a diverse set of biological processes can be analyzed, and since zebrafish possess a fully integrated vertebrate organ system, many relevant observations can be made. There are many relevant phenotypes that can be studied in zebrafish, like behavior, tumor metastasis and the cardiovascular system. However, there are many functions that cannot be relevantly screened on zebrafish. Since zebrafish are not mammalian, there are some limitations to these phenotype-based screens; however, it has also been shown that many rodent disease models also exhibit limitations in their accuracy with respect to human physiology. Therefore, as long as the limitations of zebrafish

as a model are known, they can be used to effectively validate potential drugs. For example, it has been found that there exist orthologues in zebrafish for about 71% of human genes. These genes are especially conserved within the active sites of the genes. Zebrafish possess recognizable organs, exhibiting conserved physiology. (MacRae, 2015) Additionally, the hematopoietic, cardiovascular and lymphatic systems in zebrafish are very similar to those of humans, and have been used as accurate models for these systems (Asnani, 2014). Zebrafish can also be used to deduce early insights into the toxicology of compounds. While performing target- or phenotype-based screens, the toxicity of the drugs will be observed, as death or severe abnormalities will be one of the potential results. There are several examples of zebrafish being used to successfully discover novel and existing drugs that can be used for therapeutics. For example, Dorsomorphin (which targets the bone morphogenetic protein receptor) was discovered in a screen to identify compounds that alter the basic body organization during early embryogenesis in zebrafish. Dorsomorphin is being investigated for therapies against fibrodysplasia ossificans progressiva and anemia of inflammation. (MacRae, 2015) Another screen on zebrafish discovered that TSA effects body curvature and laterality, which indicates a role for HDACs in pathogenesis of polycystic kidney disease (Cao, 2009). Additionally, zebrafish are useful models systems for discovery and validation of drugs, because of the wealth of powerful techniques by which genome engineering can be performed. With the use of such molecular tools as TALEN, CRISPR-Cas and Cre-dependent LoxP sites, mutant lines and conditional knockdowns can be developed. (MacRae, 2015) For example, with these tools zebrafish mutants which simulate the hypothesized effects of a drug can be developed. Additionally, null mutant lines can be established, which can subsequently undergo rescue screens.

The aim of this project was to screen a library of 1920 small molecule compounds for any morphological effects, in particular on cardiovascular development. The library of small molecule compounds were predicted to be inhibitors targeting epigenetic regulators, based upon modeling, due to their similarity to known inhibitors. The compounds were screened using zebrafish embryos, and additional re-screens were performed on compounds of interest. We identified six compounds, predicted to be HDAC inhibitors that caused defects in circulatory system function. Subsequent in vitro and in vivo biochemical assay verified that several of these compounds were able to inhibit HDAC activity both *in vitro* and *in vivo*.

Methods

Zebrafish maintenance and handling

Zebrafish were handled according to approved University of Massachusetts Medical School Institutional Animal Care and Use Committee protocols. Zebrafish embryos were generated by placing adult zebrafish males and females in separate chambers in a tank filled with egg water, the night before spawning. The following morning the females and males were put in the same chamber, while the released eggs are separated by a mesh insert. Zebrafish embryos were stored in a 28°C incubator for normal development.

Small molecule library screening

For the initial screens, compounds were diluted from 1 mM to 10 uM, and placed in 96-well plates in triplicate. Negative controls consisted of 1% DMSO solution. Zebrafish embryos between 6 and 8 hours post fertilization (hpf) were placed alone in a single well, performed in triplicate. The plates were stored at 28°C, and retrieved at 24 hpf. The general morphology, including head and tail development, as well as death, was scored for each compound. At 48 hpf the head and tail morphology, pigment, circulation and death was again scored for the different compounds. Compounds with two or more hits (same or similar results, or death) were screened again. For this screen four zebrafish embryos were placed together in 48-well plates, for the final concentrations of 1 and 10 uM of the compound. These embryos were screened in a similar fashion.

For the secondary screens, 10 embryos were placed at 6-8 hpf in a single well in 12-well plates. Each compound was screened in triplicate, for three different final concentrations: 1 uM, 5 uM and 10 uM. Negative controls consisted of 2% DMSO solution. Death, tail morphology, pigment, circulation and presence of edema was scored for each embryo at 24 and 48 hpf.

For the development screens, 10, 20 or 30 embryos at either 12, 24, 36 or 48 hpf were placed in 12-well plates. Each compound was screened in triplicate, at the final concentrations of 5 uM and 10 uM of the compound. Negative controls consisted of 2% DMSO solution. Death, tail morphology, pigment, circulation and presence of edema was scored for each embryo after different incubation periods.

HDAC *in vitro* assay

The HDAC *in vitro* assay was performed using an EMD Millipore HDAC Activity Assay Kit, following the supplied procedure. The positive control consisted of HDAC buffer instead of HeLa nuclear extract and treatment. The negative control consisted of HDAC buffer instead of treatment. TSA was diluted to a final concentration of 20 uM, VPA to a final concentration of 1mM, while the compounds were diluted to 100 uM and 1 mM from a stock of 10 mM. After 15 minutes of incubation, 1X HDAC Developer was added. After further incubation the fluorescence was measured with a Promega GloMax®-Multi Detection System at an excitation wavelength of UV 365 and emission wavelength of 415-445. Significant decrease in fluorescence was calculated by ANOVA, compared to the negative control

Cell treatment

Human Umbilical Endothelial Vein Cells (HUVEC) were seeded and incubated in Endothelial Basal Media (0.2% Bovine Brain Extract, 5 ng/ml rh EGF, 10mM L-glutamine, 0.75 Units/ml Heparin sulfate, 1 ug/ml Hydrocortisone hemisuccinate, 2% Fetal Bovine Serum, 50 ug/ml Ascorbic acid). After 24 hours of incubation, the cells were treated with compounds, negative and positive control. Compounds 1, 6 and 7 were first diluted to 1 mM from a stock of 10 mM (in DMSO). The cells were treated with compounds 1, 6 and 7 to a final concentration of 1 uM, compounds 2, 3 and 5 to a final

concentration of 10 uM, Sodium butyrate (Nab) to a final concentration of 5 mM for positive control and a final concentration of 0.1% DMSO for negative control. The cells were lysed with protease inhibitor in RIPA buffer, and the lysate collected.

Western blot analysis

Cell lysates with 1X laemmli buffer or 4 zebrafish embryo lysates with 1 X laemmli buffer were run on a 12% SDS-PAGE, after which the samples were transferred to a PVDF membrane pre-wetted with methanol. The membrane was blocked, and probed with an hdac1 antibody for the embryos, or an anti-hyperacetylated histone 4 (penta) antibody (acH4) (EMD Millipore cat#06-946) for the cell lysates. The membrane probed with acH4 was thereafter probed with a goat anti-rabbit IgG H&L (HRP) antibody (Abcam ab6721). The proteins were detected using a BIO-RAD ChemiDoc™ Touch Imaging System with chemiluminescence. The membrane was stripped with a stripping buffer (15 g Glycine, 10 g SDS, 10 mL Tween20, pH 2.2) and probed with anti-histone 4, pan, antibody (total H4) (EMD Millipore cat# 05-858). Lastly the membrane was probed again with ab6721 secondary antibody and detected with chemiluminescence.

The adjacent intensities of the bands were quantified using BIO-RAD Image Lab, and the relative acetylation calculated by comparing the intensities of acetylated histone to total histone. The percentage difference to the negative control was calculated by comparing each compound to the negative control in the framework of ANOVA using arcsine transformed ratio with a randomized block design.

Whole-mount *in situ* hybridization

Embryos were fixed at 24 hpf with 4% PFA overnight at 4°C. The embryos were washed with Phosphate-Buffered Saline with 0.1% Tween 20 (PBSt) and dehydrated with methanol, and stored overnight at -20°C. Then the embryos were rehydrated with PBSt, and digested with 10 ug/ml Proteinase K. Thereafter, the embryos were washed with PBSt, and re-fixed with 4% PFA, for at least 20 minutes, after which they were washed again with PBSt. The embryos were then washed with 50:50 PBSt and hybe buffer, and then pre-hybridized with hybe buffer at 65°C, for at least 1 hour. Then the embryos were probed with markers in hybe buffer (*efnb2a*, *flt4* or *fli1a*), overnight at 65°C. Thereafter the embryos were gradually washed with 0.2X SSC at 65°C, and then gradually washed with 100% MABt. The embryos were blocked with 2% Boehringer block for at least 1 hour, and then incubated with Anti-Digoxigenin-AP Fab fragments antibody in 2% Boehringer block overnight at 4°C. Thereafter, the embryos were washed with MABt in 6-well plates, equilibrated with fresh developing buffer (0.1 M Tris-HCl (pH 9.5), 0.1 M NaCl, 50 mM $MgCl_2$ and 0.1% Tween 20), and developed for at least five hours with a 50:50 developing buffer and BM Purple mixture. The reaction was stopped by washing with PBSt.

Development of cre-dependent *hdac1* mutant transgenic line

An equal number of female and male adult wild type (WT^{EK2}) zebrafish were separated and fin clipped, in order to sequence their genome at intron 1. To characterize the target site for the modified allele, primers for introns one and three were constructed and verified. Guide RNAs to facilitate homologous recombination and insertion of invertible cassette trap (Zwich) were constructed using CHOP-CHOP (http://chopchop.cbu.uib.no). Primers for constructing sgRNA for Cas9 and primers for constructing crRNA for Cpf1 were designed based upon their stability and proximity to a suitable target site. Thereafter the DNA templated were amplified with the help of the primers (sgRNA by plasmid transformation, and crRNA by simple PCR), purified and the RNAs synthesized by *in vitro* transcription using the Thermo Fisher Scientific MEGAscript® T7 Kit. The RNAs were co-injected with respective protein at one-cell stage zebrafish embryos. The embryos were

lysed at 24 hpf, and the DNA analyzed by amplification and digestion. The invertible cassette trap (Zwich) was designed as described by Sugimoto *et al*. (Sugimoto, 2017) The Zwich+3 plasmid (pZwith+3) was linearized and purified. Then the linearized pZwich and the two gBlocks, Hdac1 5' and 3' homologous arms, underwent HiFi assembly for 1 hour at 50°C. The HiFi assembly was electroporated, validated by PCR and digestion, and then sequenced. Successful plasmids were pooled, and microinjected into zebrafish embryos at the one-cell stage, with and without lbCpf1, and crRNA21. Two days post fertilization the embryos were checked for CryGFP expression. These embryos were lysed, and the genome amplified around the homologous arms and target site, and subsequently digested.

Results

Initial small molecule library screen

In order to identify small molecule inhibitors of epigenetic regulators that have an effect on cardiovascular development, the library of small molecule compounds was screened on zebrafish embryos. The library consists of 24 96-well plates with 80 compounds each, to a total of 1920 compounds. Single zebrafish embryos at 6-8 hours post fertilization (hpf) were placed in a well, each well corresponding to one of 80 compounds in each 96-well plate, to a final concentration of 10 uM. Additionally, 8 wells per plate had 1% DMSO in them for negative controls. Each plate was screened in triplicate, at 24 and 48 hpf. At 24 hpf general morphology for death or malformation was observed. At 48 hpf pigment, heartbeat and circulation in head and tail can be seen in the transparent larvae.

The first screening found 35 potential hits: compounds that lead to morphological defects or death. Nine of these compounds only lead to death, while three had at least half of the embryos die, other phenotypes including loss of circulation and loss of tail. Other common phenotypes were curved tails and reduced or no pigment.

In order to confirm consistent effects on the zebrafish embryos, all compounds with two or more hits were screened again. For this screen four embryos were placed together in 48-well plates, in triplicate. Solutions of the compounds were added, to final concentrations of 1 and 10 uM. The embryos were again screened at 24 and 48 hpf.

This second screen revealed that several of the hits were false positives, while some were highly toxic. Five compounds had normal phenotype, and nine compounds resulted in death or severe morphological abnormalities, not necessarily the same as for the first screen. The rest of the compounds had a mixture of previous phenotypes, as well as abnormalities in tail formation, circulation and pigment. From these, seven candidates of interest (from here on known as compounds 1-7) were selected. Compounds 2, 3 and 4 resulted mainly I loss of pigment, while 5 and 7 resulted mainly in death, but also loss of circulation. Compound 6 resulted in tail abnormalities, while compound 1 resulted in embryos with no pigmentation, curved tail and loss of circulation. Even though other compound also had positive hits in their second screen, these seemed the most promising, and they were commercially available. Compounds 1, 2, 3 and 5 were predicted to be inhibitors of HDAC1, while compounds 6 and 7 were predicted to inhibit HDAC2. Compound 4 was predicted to inhibit DNMT3a.

Secondary small molecule library screen

In order to confirm that the compounds inhibit Histone Deacetylases (HDACs), they were re-screened and compared to the development of *hdac1* mutant zebrafish (Fig. 2A-H). By crossing heterozygous *hdac1* parents (*hdac1*$^{+/-}$), around a fourth of the embryos had a phenotype, which was found to correlate to homozygous *hdac1* mutants (*hdac1*$^{-/-}$), which is noticeable with a simple microscope by 48 hpf. *Hdac1*$^{-/-}$ embryos have a loss of pigment, edema, curved tails and loss of circulation in the tail at 48 hpf. Additionally, in order to confirm loss of *hdac1* in the *hdac1*$^{-/-}$ zebrafish, a western blot was performed with an *hdac1* probe on lysates of embryos from an *hdac1*$^{+/-}$ cross (Fig. 2I). In order to further validate the hypothesis that these compounds are HDAC inhibitors, the embryos were screened at 24 and 48 hpf, and compared to the development of the *hdac1*$^{-/-}$ embryos. 10 morphologically normal zebrafish embryos were placed at 6-8 hpf in one well in 12-well plates. Compound solution was added to a final concentration of 1, 5 and 10 uM, in triplicate.

Compounds 1, 2, 3, 5, 6 and 7 had similar effects by 48 hpf at concentrations 5 and 10 uM, but not 1 uM. At 5 and 10 uM, embryos treated with compound 1 had no pigment and curved tails, while some 10 uM embryos had edema and loss of circulation in the tail. Also, at this concentration more embryos die (Fig. 3). For compound 2, embryos treated at 5 uM either died, or had reduced pigment and no circulation in the tail. At 10 uM all of the embryos had died by 48 hpf (Fig. 4). Embryos treated with 5 uM compound 3 had reduced pigment and loss of circulation in the tail, while embryos treated with 10 uM had about a third dead, a third reduced/loss of pigment and loss of circulation in the tail, and the rest were normal (Fig. 5). Compound 4, which was not modeled to be an inhibitor of HDACs, was found to be highly toxic, and was therefore discarded from further analysis (Fig. 6). At 5 uM embryos treated with compound 5 had tail malformations, however they were otherwise normal. At 10 uM the embryos had loss of pigment, tail malformations including loss of circulation and edema (Fig. 7). After only 24 hpf, both 5 and 10 uM of compound 6 resulted in curved tails in the embryos. After 48 hpf the embryos had tail malformations, and embryos treated with 10 uM had reduced pigment and edema (Fig. 8). Treatment with compound 7 resulted in a high rate of dead embryos, and those that survived had loss of pigment and no circulation in the tail (Fig. 9). This data suggests that compounds 1, 2, 3, 5, 6 and 7 have less active HDACs. The phenotypes seen in embryos treated with these compounds were in many ways similar to those of *hdac1*. Especially at 10 uM embryos treated with the compounds (except compound 4) had loss of circulation in the tail, reduced or no pigment and curved tails, while some compounds also resulted in edema. Compounds 2, 6 and 7 were also more toxic than the other compounds.

Time screen

In order to deduce if the compounds had any particular effect at a certain point in development, time screens were performed. In this case the compounds were added to the embryos at different stages, to final concentrations of 5 and 10 uM.

Compound 1 was added to embryos at 24 and 48 hpf. Embryos treated at 24 hpf ended up with a typical *hdac1*$^{-/-}$ phenotype by 55 hpf, and were dead after 72 hpf (Supplementary Fig. 1). With treatment at 48 hpf, the embryos were mostly either normal or dead by 72 hpf (Supplementary Fig. 2). Embryos that were treated with compound 2 had the compound added at 12, 24, 36 and 48 hpf. For embryos treated at 12 hpf, there was a high level of deaths, while the surviving embryos had a typical *hdac1*$^{-/-}$ phenotype (Supplementary Fig. 3). For 24 hpf, the embryos were essentially dead by 48 hpf if treated with 10 uM, while half of the embryos treated with 5 uM were wither dead, or had a typical *hdac1*$^{-/-}$ phenotype (Supplementary Fig. 4). Embryos treated at 36 hpf had a great level of dead embryos, while the remaining had reduced pigment, curved tails and edema by 60 hpf (Supplementary Fig. 5). Treatment at 48 hpf resulted in mostly dead embryos at 72 hpf (Supplementary Fig. 6). Compound 3 was added at 24 and 48 hpf. Treatment at 24 hpf resulted in a typical *hdac1*$^{-/-}$ phenotype for 5 uM, while embryos treated with 10 uM were all dead (Supplementary Fig. 7). Embryos treated at 48 hpf all had a typical *hdac1*$^{-/-}$ phenotype at 72 hpf, except they had normal pigment development (Supplementary Fig. 8). Embryos that were treated with compound 5 had the compound added at 24 hpf. These embryos had a typical *hdac1*$^{-/-}$ phenotype for 10 uM at 48 hpf, and 5 uM at 72 hpf, while 10 uM treatment resulted in death by 72 hpf (Supplementary Fig. 9). Compound 6 was applied to embryos at 24 hpf, and at 48 hpf both 5 and 10 uM treatment resulted in a typical *hdac1*$^{-/-}$ phenotype, while at 72 hpf the embryos were all dead (Supplementary Fig. 10). Embryos were treated with compound 7 only at 24 hpf. These embryos had reduced pigment, some loss of circulation and edema, while 10 uM treatment also resulted in curved tails, at 48 hpf. After 72 hpf most embryos were dead, the surviving embryos being similar to symptoms seen

at 48 hpf (Supplementary Fig. 11). The data indicates that the typical *hdac1*$^{-/-}$ phenotype can be seen in embryos treated up to 36 hpf, however the toxicity of the compounds do seem to increase with a later treatment. An exception is treatment with compound 3, which resulted in an *hdac1*$^{-/-}$ phenotype even after treatment at 48 hpf, even though they had pigment, which forms at 48 hpf.

In vitro HDAC assay

In order to assess the abilities of the compounds to directly inhibit HDACs, an *in vitro* assay was performed. The assay involves the binding of HDACs from HeLa nuclear extract to a substrate which fluoresces while bound. When HDAC is inhibited by a known inhibitors, or one of the compounds, the substrate is released, which leads to a lower level of fluorescence. The assay was performed for the six compounds, no HDAC, no treatment, and treatment with Trichostatin A (TSA) or Valproic acid (VPA). The compounds were applied at 1 mM and 100 uM, while TSA was diluted to 5 uM and VPA was diluted to 1 mM. The *in vitro* assay was performed in triplicate (Fig. 10).

TSA suppresses fluorescence (by inhibiting HDACs) to a higher degree than VPA, making it a greater inhibitor *in vitro*. Compound 1 had a similar effect on fluorescence as VPA at 1 mM ($P<0.0001$), while none at 100 uM. Compound 2 had similar effects as TSA at 1 mM ($P<0.0001$), with only little effect at 100 uM ($P<0.05$). Compound 3 also had a similar effect as VPA at 1 mM ($P<0.0001$), while little effect at 100 uM ($P<0.05$). Compound 5 had no effect on fluorescence *in vitro* at either concentration. Compound 6 had very strong *in vitro* inhibition at 1 mM ($P<0.0001$), greater than TSA, while inhibition at 100 uM ($P<0.0001$) was in between that of TSA and VPA. Compound 7 had similar effects as TSA at 1 mM ($P<0.0001$), while similar effects as VPA at 100 uM ($P<0.0001$). While the *in vitro* assay suggests that all the compounds except compound 5 had inhibitory effects on HDAC, especially compounds 2, 6 and 7 were remarkably efficient at reducing the fluorescence, and therefore the activity of HDACs. Compounds 6 seems to be a great inhibitor of HDAC, *in vitro*, while compounds 2 and 7 seem to be good inhibitors at high concentrations (Fig. 10).

In vivo assay of relative level of acetylation of histone H4

In order to validate the *in vivo* inhibitory properties of the compounds, the relative level of acetylation of histone H4 in Human Umbilical Vein Endothelial Cells (HUVEC) was determined by Western blot analysis. HUVECs were treated with compounds 1, 2, 3, 5, 6 and 7, as well as Sodium butyrate (Nab) as a positive control, and 0.1% DMSO as a negative control, in triplicate. Cells were treated with 10 uM of compounds 2, 3 and 5, and 1 uM of compounds 1, 6 and 7. Nab was added to a final concentration of 5 mM. The cells were lysed and run with a 12% SDS-PAGE. Thereafter the proteins were transferred to a PVDF membrane. The membranes were probed with a primary acetylated H4 antibody, and after imaging, they were stripped and re-probed with a primary total H4 antibody. The adjacent intensities were quantified with ImageLab, and the relative acetylation calculated by comparing the intensities of acetylated histone to total histone. The percentage difference to the negative control was calculated by comparing each compound to the negative control in the framework of ANOVA using arcsine transformed ratio with a randomized block design.

According to our analysis, the acetylation of H4 in the cells treated with compounds 2, 6 and 7 were significantly increased relatively to the negative control, which indicates decreased HDAC activity (Fig. 11). Cells treated with compounds 2 and 6 were somewhat significantly more acetylated ($P<0.1$) than the negative control, which suggests that these compounds are weaker inhibitors. Since cells treated with compound 7 was significantly more acetylated ($P<0.05$) than the negative control to a greater degree it can be inferred that this compounds is a stronger HDAC inhibitor. However, cells treated with these compounds are all less significant than the positive control Nab ($P<0.01$), which indicates that they are all weaker inhibitors than Nab.

Whole-mount in situ hybridization

To analyze the effect HDACs and the compounds have on expression of genes important for vascular development, whole-mount *in situ* hybridization was performed. Wild type (WT) (treated and untreated) and embryos of an *hdac1*$^{+/-}$ cross were fixed at 24 hpf. The embryos were probed with either *efnb2a*, *flt4* or *fli1a*. *Efnb2a* is an arterial endothelial cell marker, with which arterial development can be investigated (Weinstein, 2002). *Flt4* is expressed in sprouting endothelial cells; and is used as a marker for the lymphatic and vascular systems (Shin, 2016). *Fli1*a can be used as an endothelial specific vascular marker, to check for expression of both arterial and venous endothelial cells (Weinstein, 2002).

Based upon their *efnb2a* patterns, the embryos from the *hdac1*$^{+/-}$ cross were divided into three different groups, (see Fig. 12). The largest group (Fig. 12B) has the same pattern as WT embryos (Fig. 12A): spots on each side in the head-area, as well as a streak in the tip of the tail. The second largest group has the same pattern in the head-area, but little to no expression in the tail (Fig. 12C). The last group had no expression in the tail or head (Fig. 12D).

The *in situ* hybridization with *flt4* gave a similar pattern between WT and *hdac1*$^{+/-}$ cross embryos (see Fig. 13). The WT embryos have a streak at the tip of their tail, and this pattern was also seen in all embryos of the *hdac1*$^{+/-}$ cross.

The *fli1a* marker also showed a similar pattern between *hdac1*$^{+/-}$ cross and wild type embryos (Fig. 14). WT embryos have expression in both the head region and along the tail, and this could be seen in the *hdac1*$^{+/-}$ cross embryos as well.

For embryos treated with compounds 1, 2, 3 and 6 there was *efnb2a* expression in the head area but little none in the tail (Fig. 15A-C, E). Embryos treated with compound 7 had very little *efnb2a* expression in the head (Fig. 15F), while treatment with compounds 5 resulted in normal *efnb2a* expression (Fig. 15D); however, treatment with compound 5 leads to abnormal development generally at 24 hpf. There was normal *fli1a* as well as normal *flt4* expression in embryos treated with any of the compounds (Fig. 15G-R); however, *flt4* expression for embryos treated with compound 5 was not obviously normal, for the reason stated above.

These *in situ* experiments suggest that *hdac1* is involved in arterial development. It seems like loss of *hdac1* might reduce or wipe out *efnb2a* expression entirely in the tails of the zebrafish embryos. This is also supported by the fact that there is a loss of circulation in the tails of zebrafish larvae at 48 hpf.

Development of a Cre-dependent hdac1 mutant transgenic line

In order to assess the developmental effect on HDACs on zebrafish, the establishment of a conditional allele for a mutant *hdac1* line of zebrafish was initiated. First, in order to sequence the genome in sites of interest (*hdac1*, intron 1), 12 pairs of Wild Type EK2 (WT^{EK2}) adult zebrafish were fin clipped. Then a Cre-dependent invertible cassette, a so-called Zwitch, was constructed, with which an alternative splicing-site can be introduced. By tamoxifen treatment, Cre recombinase, an enzyme that causes recombination between paired LoxP or Lox5171 sites, is activated, leading to an inversion of the cassette (Sugimoto, 2017). In this case, this means that an early alternative splicing site is introduced, which leads to a truncated *hdac1*. Additionally, the cassette contains a CryGFP with promoter, with which the presence of the cassette can be visualized (see Fig. 16A). In order to inject and induce Homologous Repair (HR) by CRISPR, RNA sequences were designed and synthesized (Fig. 16B-C). Four sets of RNAs were designed: two using the Cas9 enzyme (sg12 and sg27), and two using the lbCpf1 enzyme (cr17 and cr21). The RNAs were validated by digestion with Hpy188I (for sg12 and cr17) and StuI (for sg27 and cr21), and prepared for microinjection (Fig.

17A). After microinjection into zebrafish embryos at the one-cell stage, the success of the RNAs was validated by PCR and digestion by Hpy188I or StuI on zebrafish genome. Of these, the IbCpf1 crRNAs were more successful in introducing HR, and especially crRNA21 was the most effective (Fig. 17B). Thereafter, the invertible cassette was synthesized. First the correct plasmid, pZwitch+3, was selected, modeled after the cassette designed by Sugimoto *et al* (Sugimoto, 20117). In order to not introduce a frameshift pZwitch+3 was selected. Then, in order to linearize the plasmid, it was digested with NheI and ClaI. Thereafter the correct 5' and 3' homologous arms were synthesized into the cassette by HiFi assembly. The 5' and 3' homologous arms were designed so as to match the *hdac1* intron 1 sequences. The cassette was introduced into a plasmid by electroporation with TOP10 EC cells, and validated by PCR and digestion with EcoRI, as well as StuI and XhoI (Fig. 17C). Then, in order to check for any fatal point mutations, the plasmids were sent for sequencing. Successful plasmids were pooled, and microinjected into zebrafish embryos with and without IbCpf1, and crRNA21. Two days post fertilization the embryos were checked for CryGFP, which resulted in a few positive injections, but high death-rate (data not shown). In order to validate the precession of the injections, these embryos were lysed, and the genome amplified around the 5' and 3' homologous arms as well as the target site, and digested (data not shown).

Discussion

Seven compounds from the small molecule compounds library were determined to be initial hits. Of these, six compounds were predicted to be HDAC1 or HDAC2 inhibitors. HDAC1 and HDAC2 are very similar, often performing redundant activity, and in zebrafish there is only one *hdac1* in place of both enzymes in humans. Therefore the compounds' inhibitory properties against *hdac1* were investigated. With a secondary screen it was confirmed that all compounds 1, 2, 3, 5, 6 and 7 had varying, but similar phenotypes to an *hdac1*$^{-/-}$ mutant line. These concentrations were achieved at either 5 uM or 10 uM. Compounds 2, 6 and 7 were also found to be more toxic at 10 uM. Additionally, time screens were performed, which indicated that the affects were achievable up to treatment at 36 hpf. Treatment at 48 hpf resulted in either death or normal development after treatment with compounds 1 and 2; however, treatment with compound 3 at 48 hpf was still able to achieve most of the phenotypes associated with *hdac1*$^{-/-}$ zebrafish. Thereafter, an *in vitro* assay was performed. This assay revealed that most compounds, all but compound 5, have some inhibitory properties at least at 1 mM. The *in vitro* assay also suggested that compound 6 is an excellent inhibitor at both concentrations. Additionally, the assay indicates that compounds 2 and 7 are good inhibitors at high concentrations, *in vitro*. Analysis of western blots of HUVECs treated with the compounds revealed that compounds 2, 6 and 7 were able to significantly increase the level of acetylation with respect to the negative control, which indicates that they inhibit HDACs *in vivo*. Compounds 2 and 6 were somewhat significantly more acetylated ($P<0.1$) than the negative control, which indicates that HDACs are less active. Compound 7 was significantly more acetylated ($P<0.05$) than the negative control to a greater degree. However, all these compounds are all less significant than the positive control sodium butyrate ($P<0.01$). This suggests that these compounds are not very strong inhibitors. Lastly, the *in situ* hybridization experiments indicate that loss of *hdac1* leads to defects in arterial development. The only marker that is affected in the embryos from the *hdac1*$^{+/-}$ cross is *efnb2a*, which is an arterial marker. The vascular and lymphatic markers *flt4* and *fli1a* had normal expression for all embryos. This expression pattern was also seen in embryos treated with the compounds, which indicates that *hdac1* activity is involved in *efnb2a* expression and arterial formation. The only exception was embryos treated with compound 5, but this compound was also the only compound which failed to significantly reduce fluorescence for the *in vitro* assay.

To further study the inhibitory properties of these drugs, and the effect they have on cardiovascular development, additional experiments should be performed. For screens, more time screens could be performed for compounds 5-7, especially at 36 and 48 hpf. This would confirm if treatment is (normally) effective only up to 36 hpf. Another interesting experiment would be to more carefully record the malformations of arterial development of the larvae. This could be done both in embryos treated with compound at a normal time point (6-8 hpf) and *hdac1*$^{-/-}$ mutant zebrafish, or for time screen embryos, and the Cre-dependent alternative allele line of zebrafish. To confirm the *in situ* experiments, that indicate that perhaps loss of *hdac1* leads to malformation of arterial development, the embryos of an *hdac1*$^{+/-}$ cross would need to be genotyped. If it is confirmed that all the embryos that have little to no *efn2ba* expression in the tail are found to be *hdac1*$^{-/-}$ embryos, and the other embryos *hdac1*$^{+/?}$, it can be inferred that *hdac1* activity is important for arterial formation in the tail in zebrafish.

Bibliography

Asnani A, Peterson RT. The zebrafish as a tool to identify novel therapies for human cardiovascular disease. *DMM Disease Models and Mechanisms*. 2014;7:763-767.

Berger SL. The complex language of chromatin regulation during transcription. *Nature*. 2007;447:407-412.

Candido EPM, Reeves R, Davie JR. Sodium butyrate inhibits histone deacetylation in cultured cells. *Cell*. 1978;14:105-113.

Cao Y, Semanchik N, Lee SH, et al. Chemical Modifier Screen Identifies HDAC Inhibitors as Suppressors of PKD Models. *Proceedings of the National Academy of Sciences of the United States of America*. 2009;106:21819-21824.

Haberland M, Olson EN, Montgomery RL. The many roles of histone deacetylases in development and physiology: implications for disease and therapy. *Nature Reviews Genetics*. 2009;10:32-42.

Kouzarides T. Chromatin Modifications and Their Function. *Cell*. 2007;128:693-705.

Lloyd KA. A scientific review: mechanisms of valproate-mediated teratogenesis. *Bioscience Horizons*. 2013;6:hzt003-hzt003.

MacRae CA, Peterson RT. Zebrafish as tools for drug discovery. *Nature reviews. Drug discovery*. 2015;14:721-731.

Montgomery RL, Davis CA, Potthoff MJ, et al. Histone deacetylases 1 and 2 redundantly regulate cardiac morphogenesis, growth, and contractility. *Genes and Development*. 2007;21:1790-1802.

De Ruijter, Annemieke J. M, Van Gennip AH, Caron HN, Kemp S, Van Kuilenburg, André B. P. Histone deacetylases (HDACs): Characterization of the classical HDAC family. *Biochemical Journal*. 2003;370:737-749.

Seto E, Yoshida M. Erasers of histone acetylation: the histone deacetylase enzymes. *Cold Spring Harbor perspectives in biology*. 2014;6:a018713-a018713.

Shin M, Male I, Beane TJ, et al. Vegfc acts through ERK to induce sprouting and differentiation of trunk lymphatic progenitors. *Development (Cambridge)*. 2016;143:3785-3795.

Sugimoto K, Hui S, Sheng D, Kikuchi K. Dissection of zebrafish shha function using site-specific targeting with a Cre-dependent genetic switch. *ELIFE*. 2017;6.

Weinstein BM, Lawson ND. Arteries and veins: making a difference with zebrafish. *Nature Reviews Genetics*. 2002;3:674-682.

Yoon S, Eom GH. HDAC and HDAC Inhibitor: From Cancer to Cardiovascular Diseases. *Chonnam Medical Journal*. 2016;52:1-11.

ZFIN. Hdac. *ZFN.org*. 2018.

Zon LI, Peterson RT. In vivo drug discovery in the zebrafish. *Nature reviews. Drug discovery*. 2005;4:35-44.

Figures

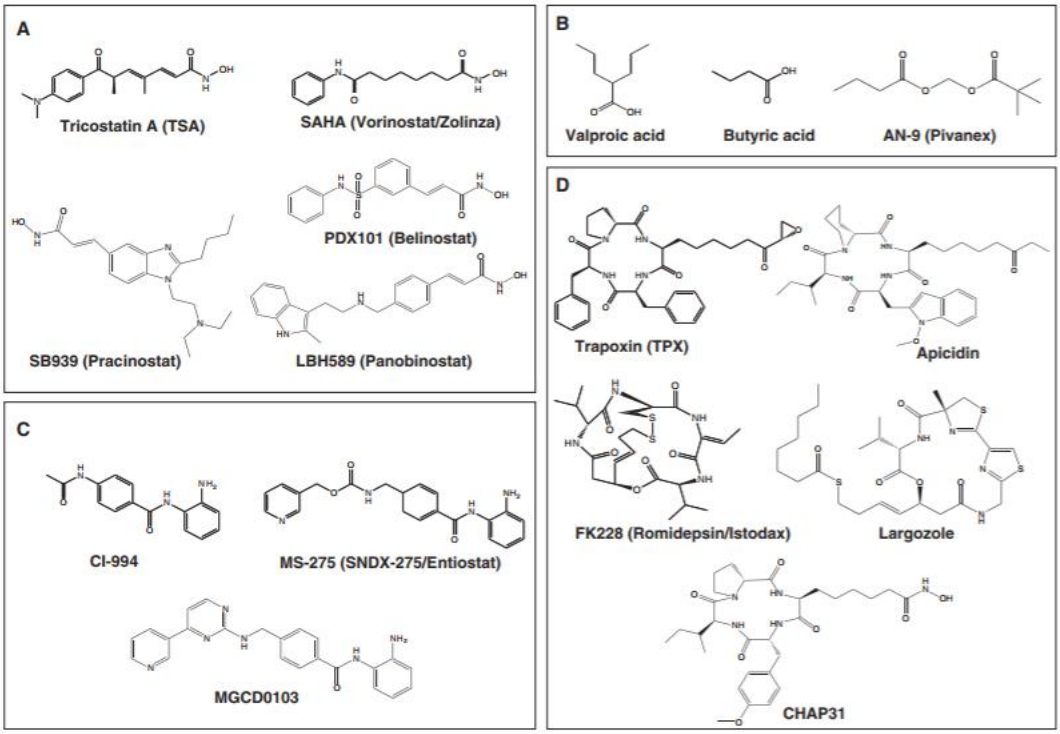

Figure 1: The four different classes of HDAC inhibitors. Hydroxamates **A**), short-chain fatty acids **B**), bezamides **C**) and cyclic peptides **D**). (Seto, 2014)

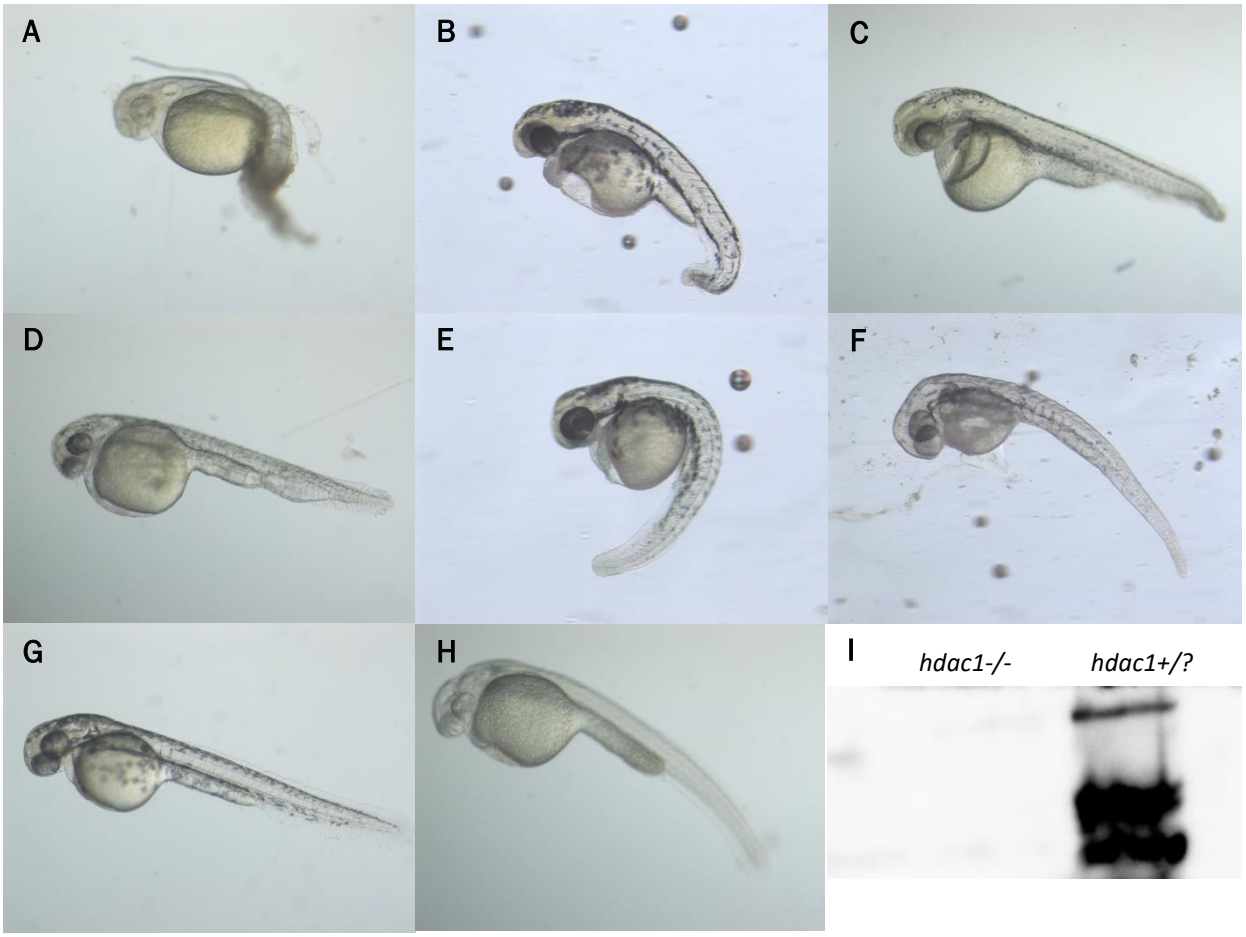

Figure 2: Embryos at 48 hours post fertilization (hpf) and conformation of mutant. Embryos were treated at 6-8 hpf with either compounds of interest (treatment), or DMSO (negative control) (**A-G**). The embryos were treated with 10 uM Compound 1 **A**) 10 uM Compound 2 **B**) 10 uM Compound 3 **C**) 10 uM Compound 5 **D**) 5 uM Compound 6 **E**) 5 uM Compound 7 **F**) and negative control 2% DMSO **G**). Positive control consists of *hdac1*$^{-/-}$ mutant embryos from cross between *hdac1*$^{+/-}$ zebrafish **H**). Western blot of *hdac*$^{+/-}$ cross embryos, probing for *hdac1*. Embryos that were homozygous *hdac1* mutant did not have any *hdac1* expression, while those that were either heterozygous or homozygous wild type had clear *hdac1* expression **I**).

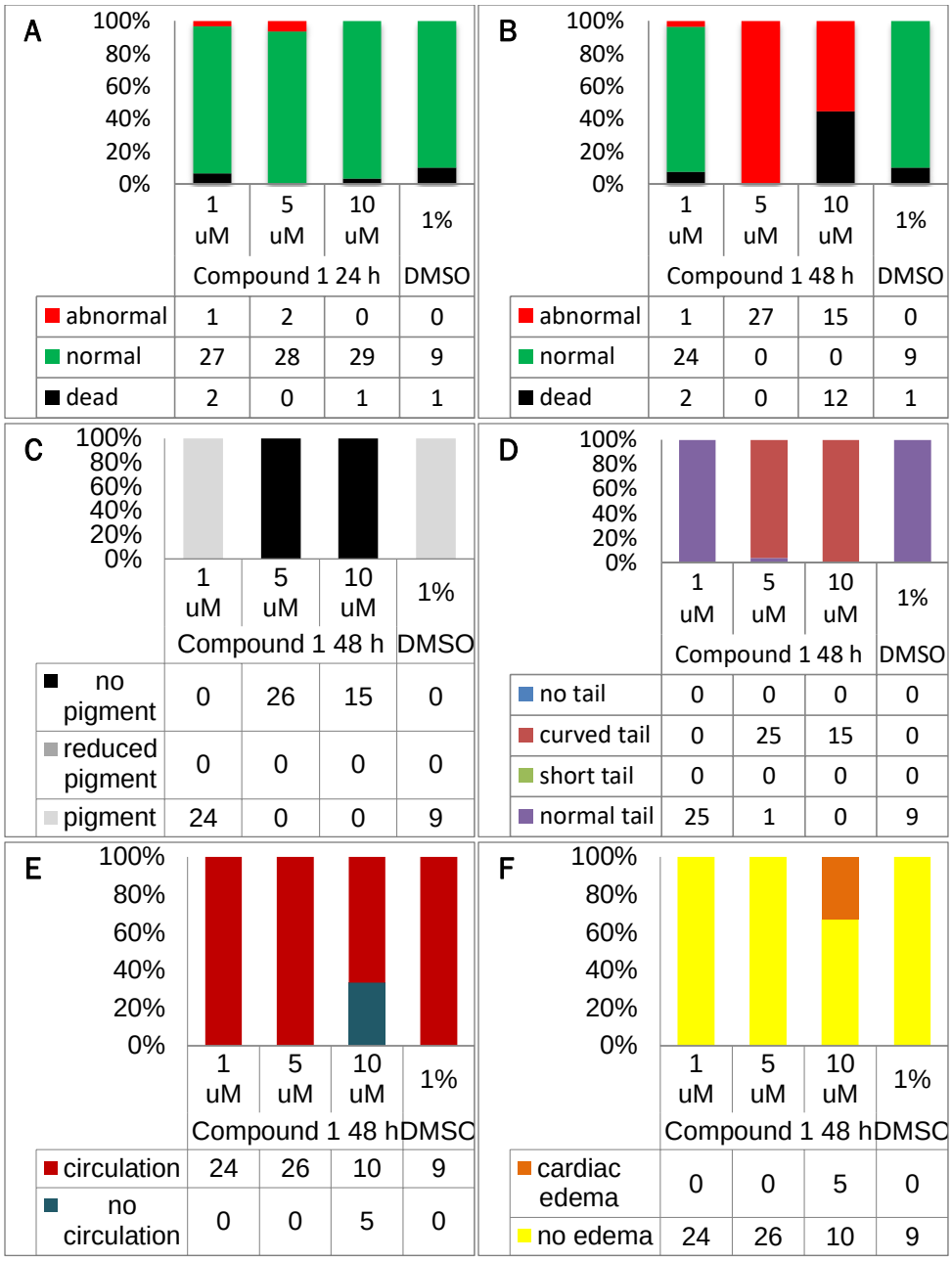

Figure 3: Screen compound 1 at different concentrations. General morphological observations of compound 1 at 24 hpf **A**) and 48 hpf **B**). Observations of pigment **C**), tail morphology **D**), circulation E) and presence of edema **F**) at 48 hpf.

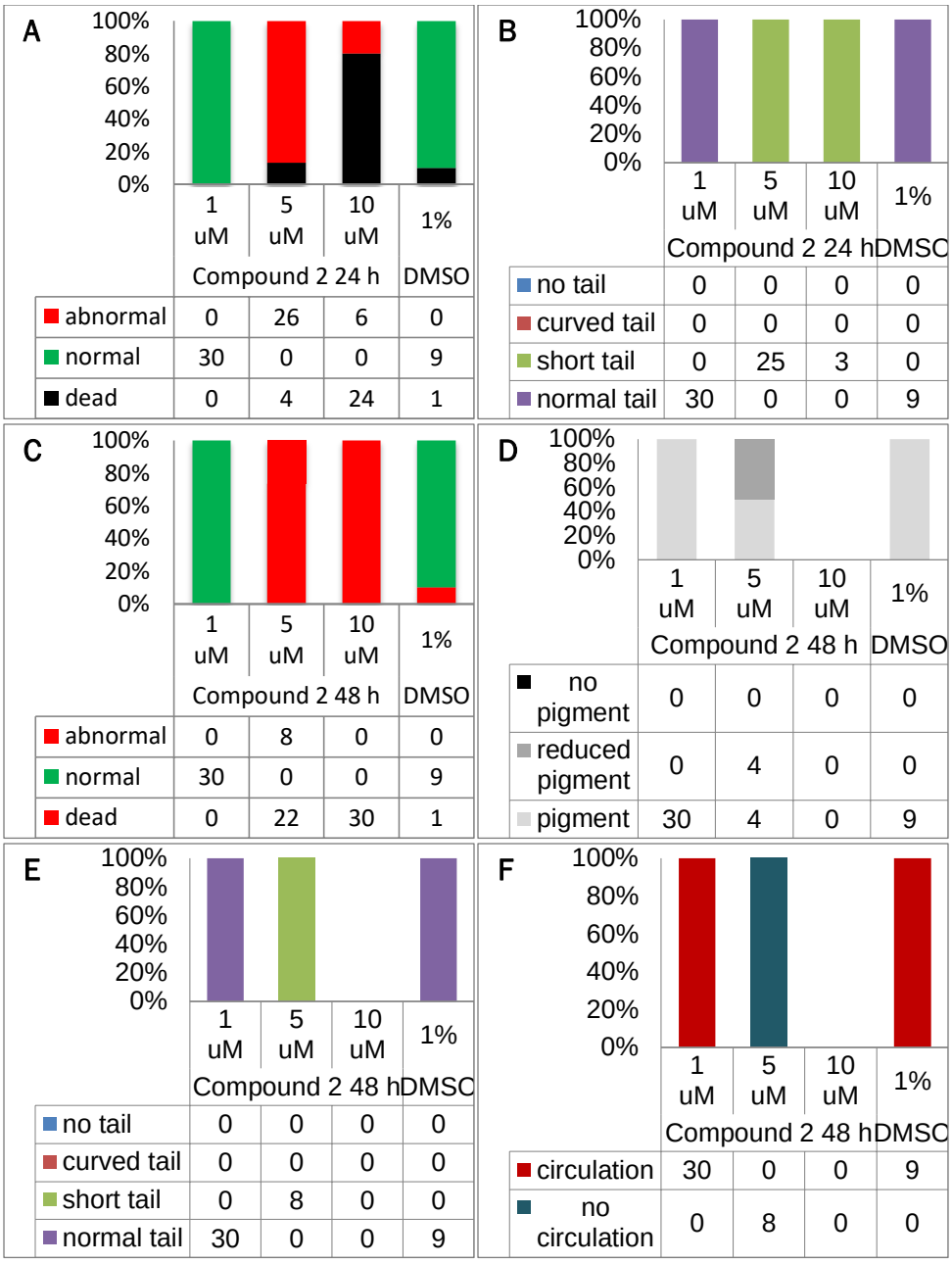

Figure 4: Screen compound 2 at different concentrations. General morphological observations of compound 2 at 24 hpf **A**) and 48 hpf **C**). Observations of tail morphology at 24 hpf B) and pigment **D**), tail morphology **E**) and circulation **F**) at 48 hpf.

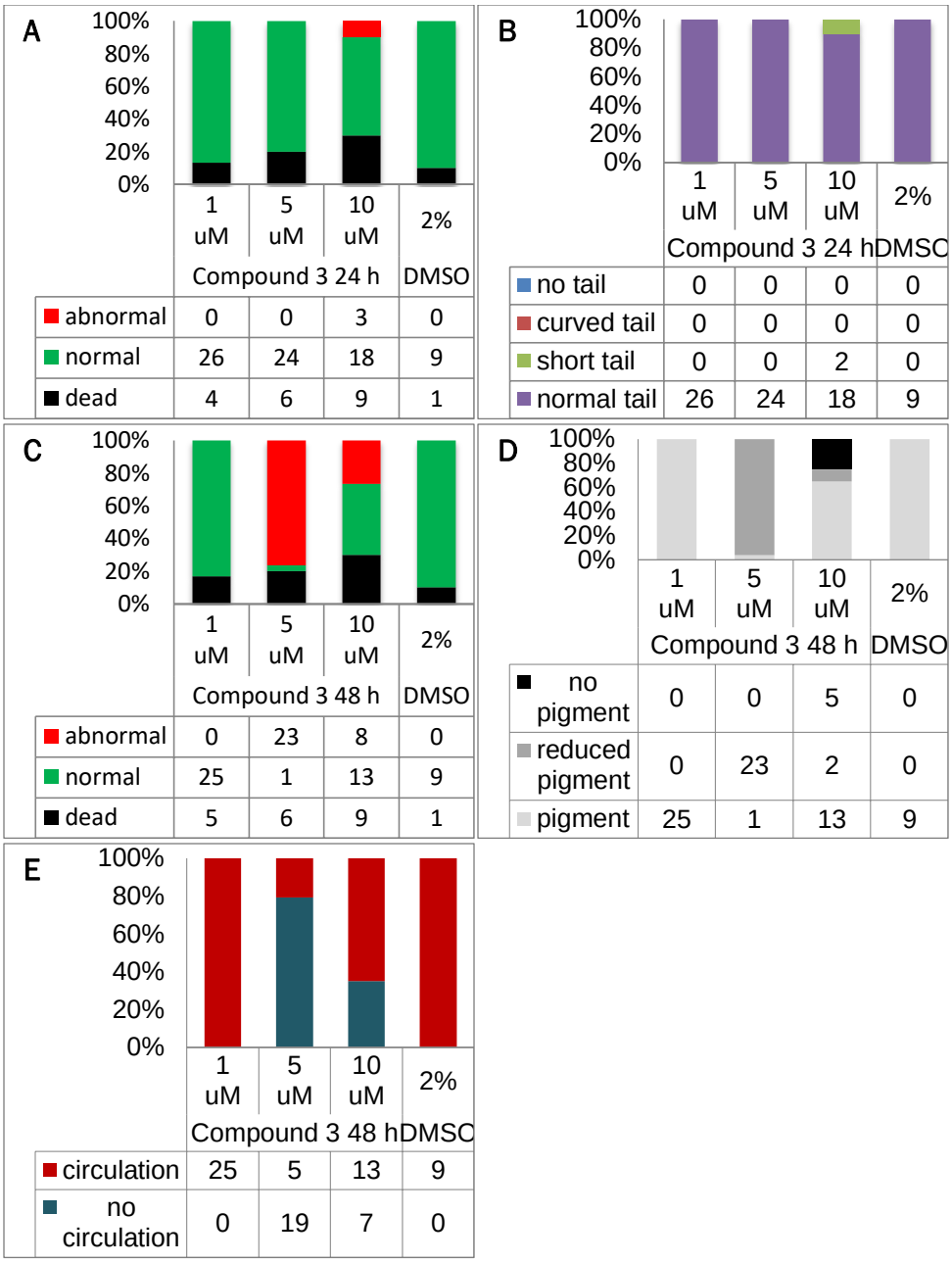

Figure 5: Screen compound 3 at different concentrations. General morphological observations of compound 3 at 24 hpf **A**) and 48 hpf **C**). Observations of tail morphology at 24 hpf B) and pigment **D**) and circulation **E**) at 48 hpf.

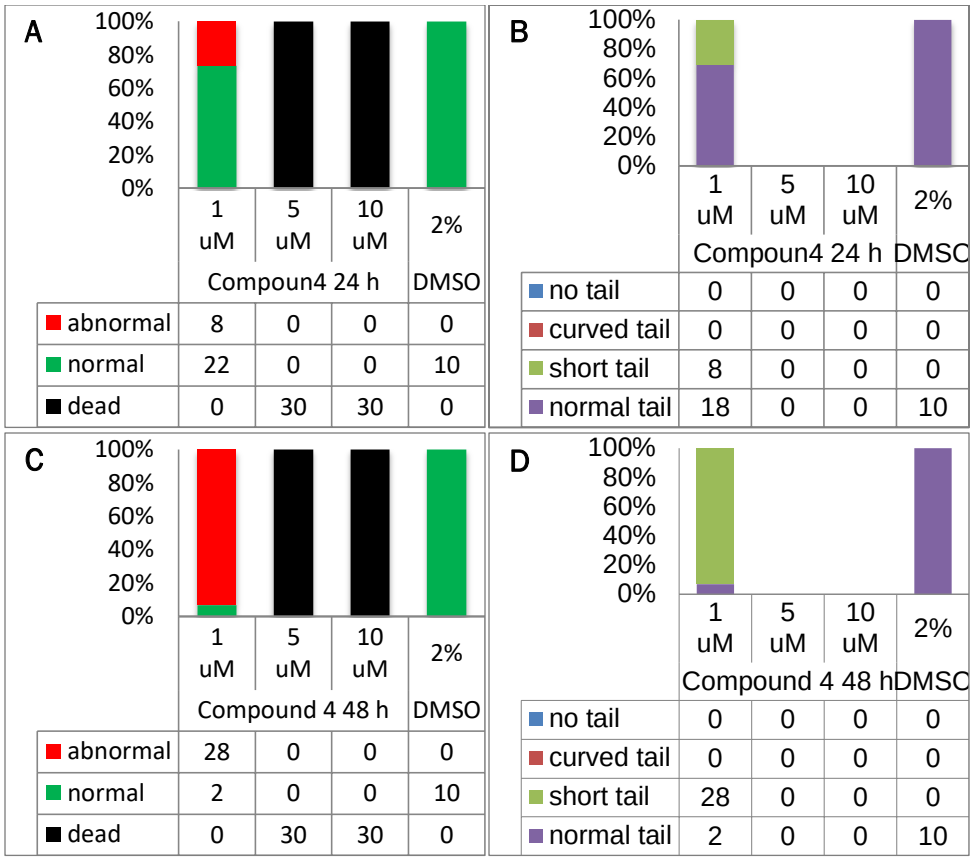

Figure 6: Screen compound 4 at different concentrations. General morphological observations of compound 4 at 24 hpf **A**) and 48 hpf **C**). Observations of tail morphology at 24 hpf B) and 48 hpf **D**).

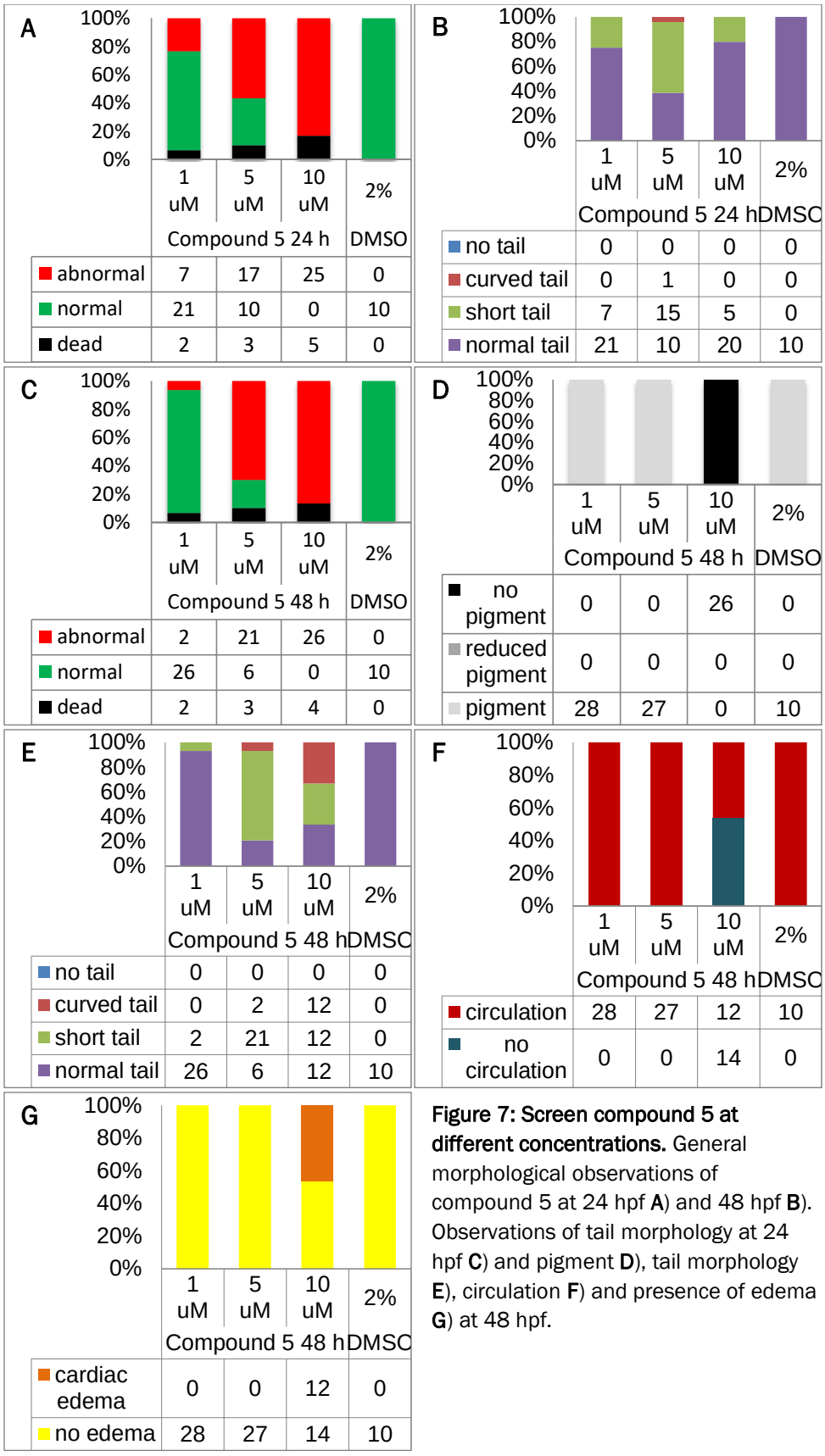

Figure 7: Screen compound 5 at different concentrations. General morphological observations of compound 5 at 24 hpf **A**) and 48 hpf **B**). Observations of tail morphology at 24 hpf **C**) and pigment **D**), tail morphology **E**), circulation **F**) and presence of edema **G**) at 48 hpf.

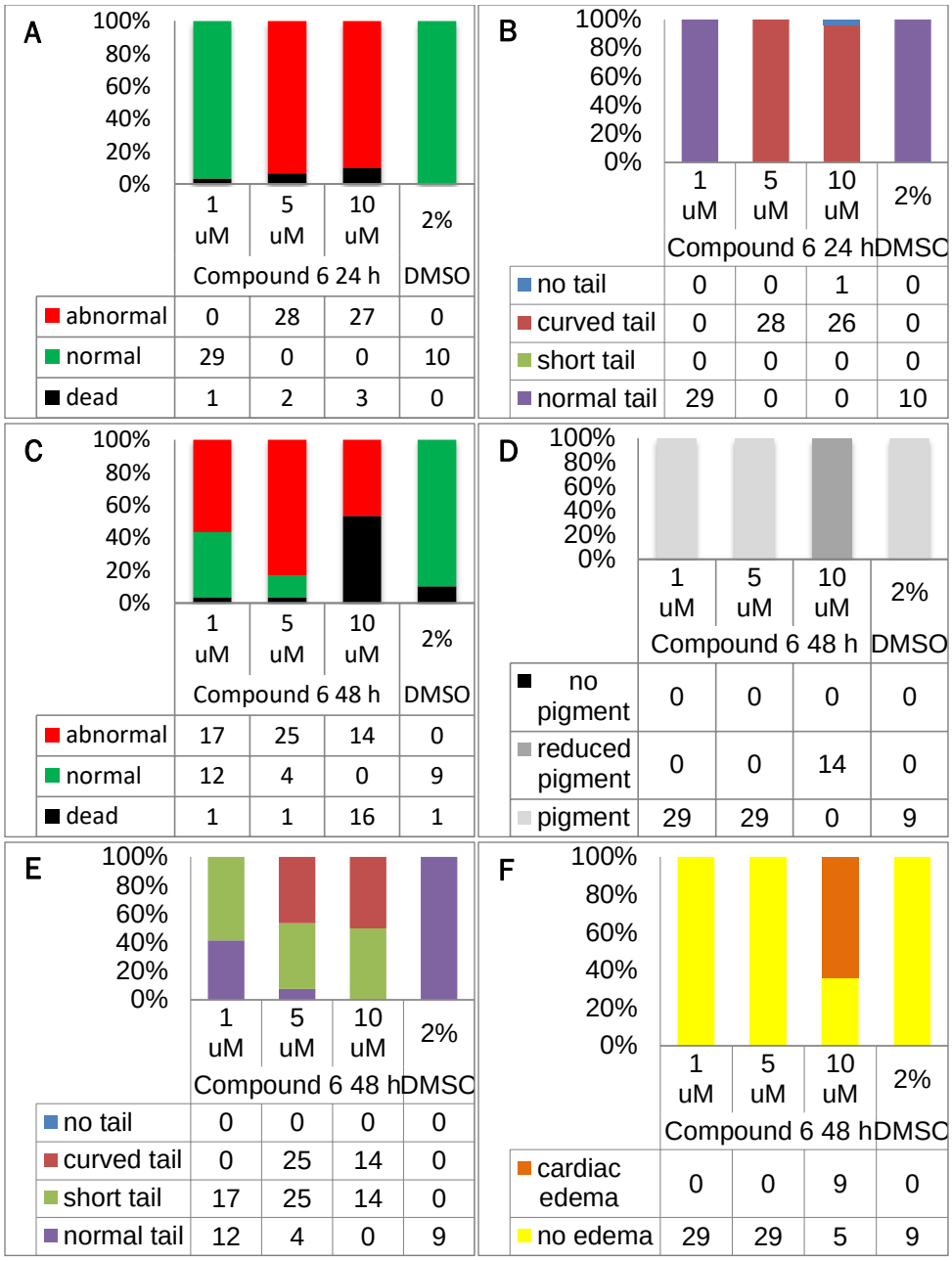

Figure 8: Screen compound 6 at different concentrations. General morphological observations of compound 6 at 24 hpf **A**) and 48 hpf **C**). Observations of tail morphology at 24 hpf B) and pigment **D**), tail morphology **E**) and presence of edema **F**) at 48 hpf.

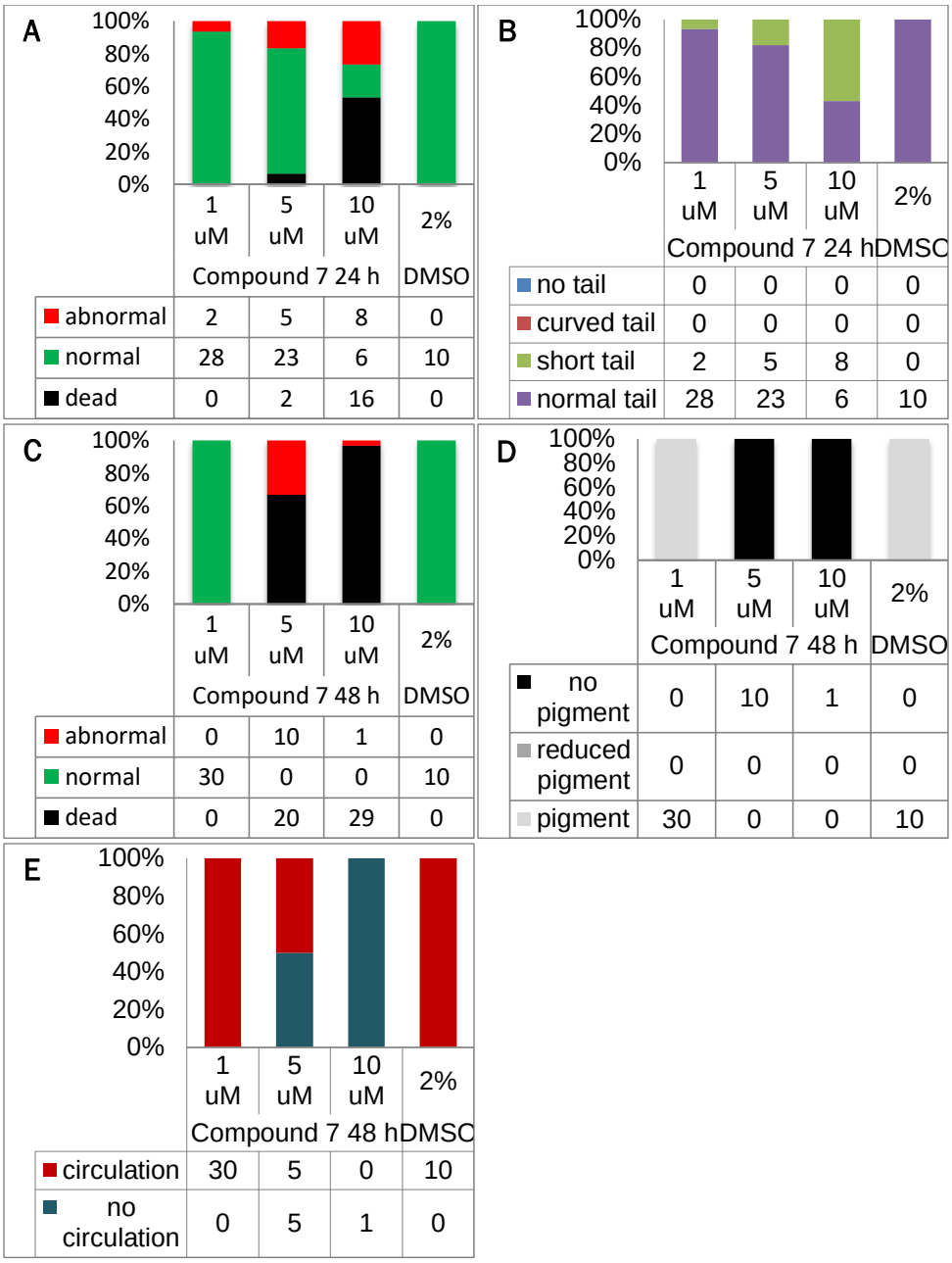

Figure 9: Screen compound 7 at different concentrations. General morphological observations of compound 7 at 24 hpf **A**) and 48 hpf **C**). Observations of tail morphology at 24 hpf **B**) and pigment **D**) and circulation **E**) at 48 hpf.

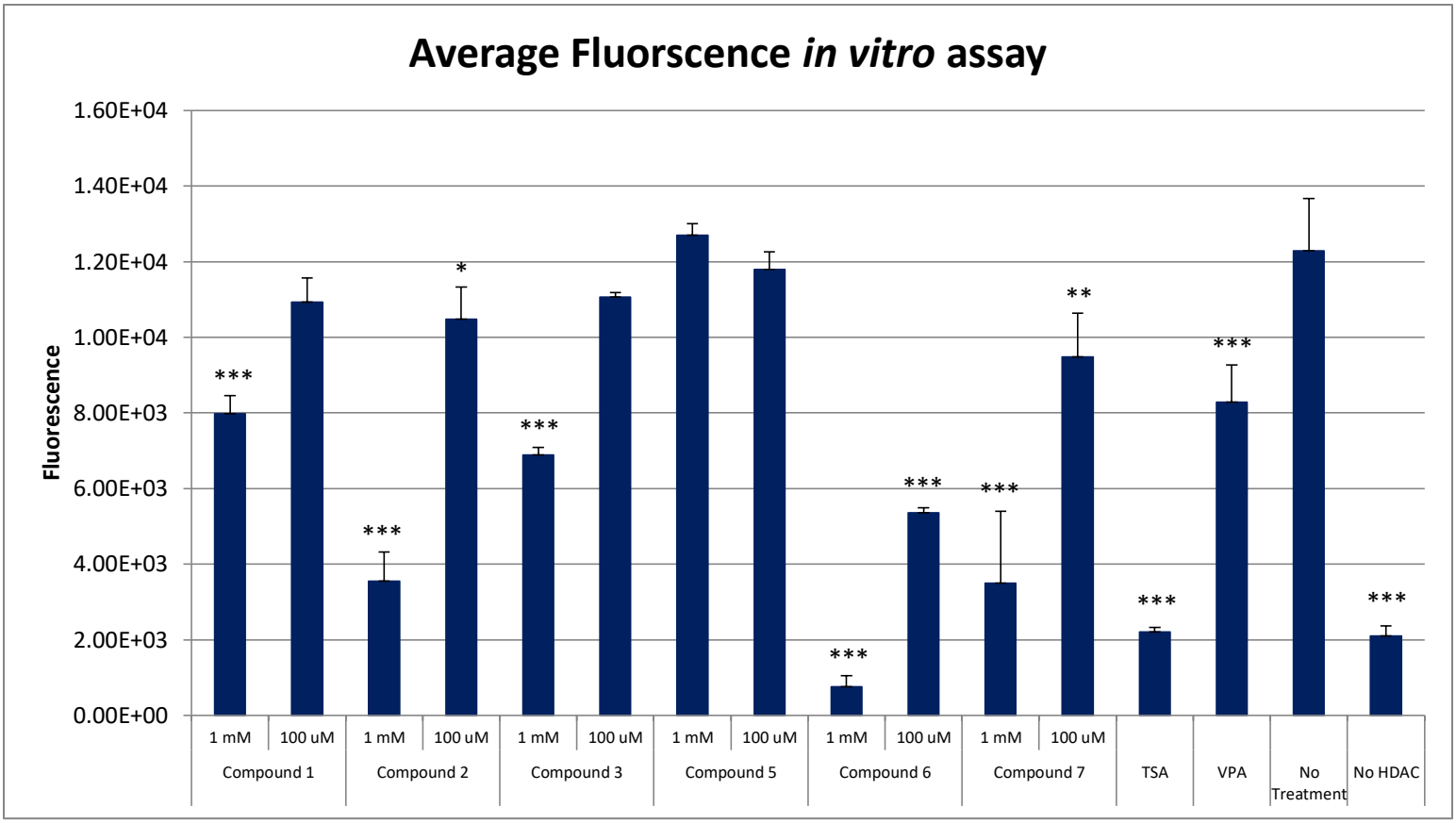

Figure 10: *In vitro* HDAC assay. Average fluorescence after 30 minutes past addition of the developer, as measured with a Promega GloMax®-Multi Detection System at an excitation wavelength of UV 365 and emission wavelength of 415-445. HeLa nuclear extract (containing HDAC) was treated with 1 mM and 100 uM of compounds 1, 2, 3, 5, 6 and 7, 20 uM TSA and 1 mM VPA. The positive control consisted of HDAC buffer instead of HeLa nuclear extract and treatment. The negative control consisted of HDAC buffer instead of treatment. Error bars represented by the standard deviation. *P<0.05, **P<0.005, ***P<0.0001.

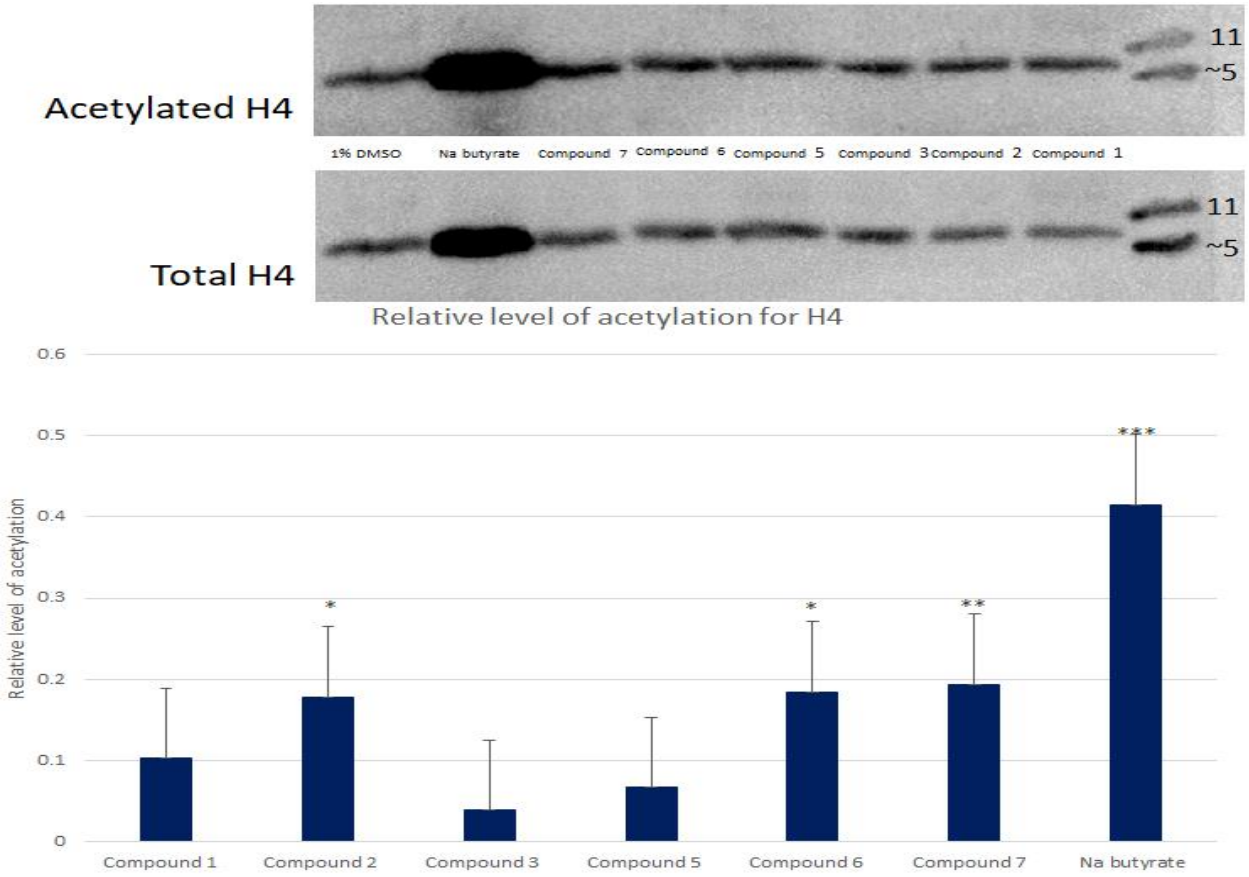

Figure 11: Western blot analysis for H4. Human umbilical vein endothelial cells (HUVEC) were treated with compounds of interest (treatment), DMSO (negative control) or sodium butyrate (positive control). The percentage difference to the negative control was calculated by comparing each compound to the negative control in the framework of ANOVA using arcsine transformed ratio with a randomized block design. Error bars represented by the standard error. *P<0.1, **P<0.05, ***P<0.01.

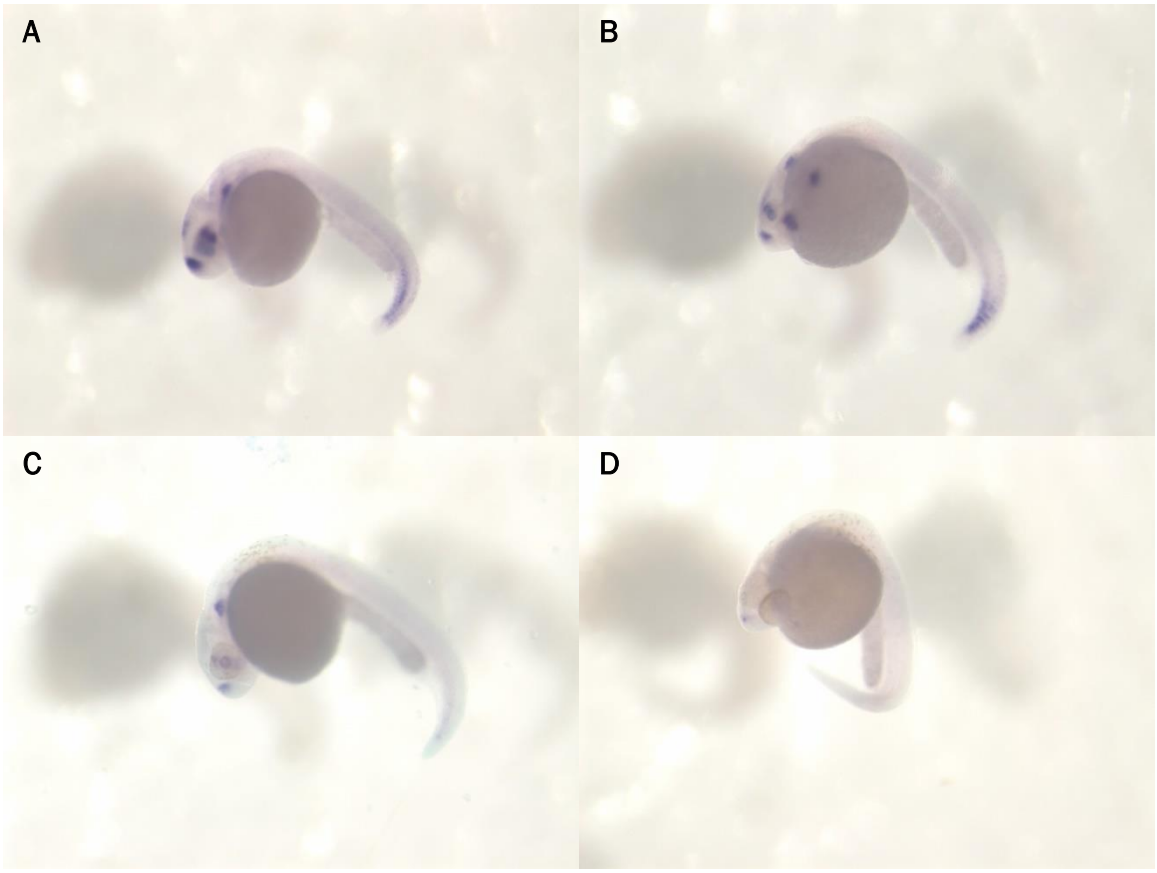

Figure 12: *in situ* for *efnb2a* marker. Expression pattern for wild type (WT) embryos and offspring of an *hdac1*$^{+/-}$ cross. The expression patter of WT embryos exhibits spots in the head region, and a streak in the tail A). The largest group looks like WT embryos **B**) the second largest group has spots on the head, but little to no expression the tail **C**) the smallest group has no expression **D**).

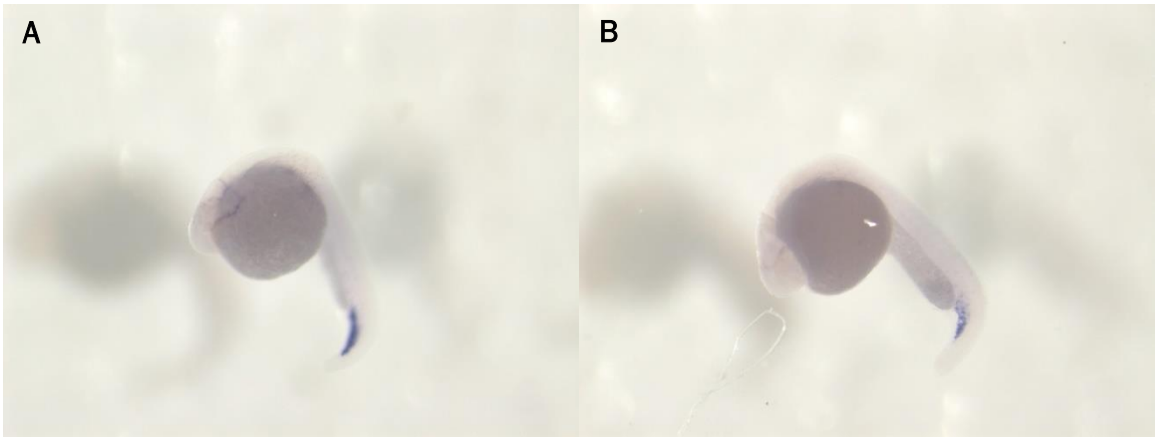

Figure 13: *in situ* for *flt4* marker. Expression pattern for wild type (WT) embryos and offspring of an *hdac1*$^{+/-}$ cross. The expression patter of WT embryos exhibits a streak in the tail **A**). Offspring of an *hdac1*$^{+/-}$ cross have similar patterns to WT embryos **B**).

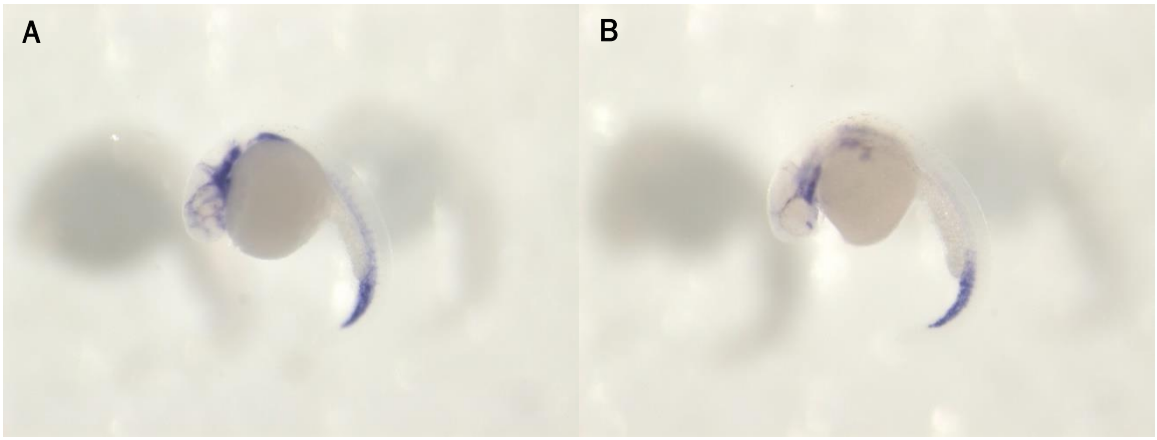

Figure 14: *in situ* for *fli1a* marker. Expression pattern for wild type (WT) embryos and offspring of an *hdac1*$^{+/-}$ cross. The expression patter of WT embryos exhibits streaks in the head region the tail **A**). Offspring of an *hdac1*$^{+/-}$ cross have similar patterns to WT embryos **B**).

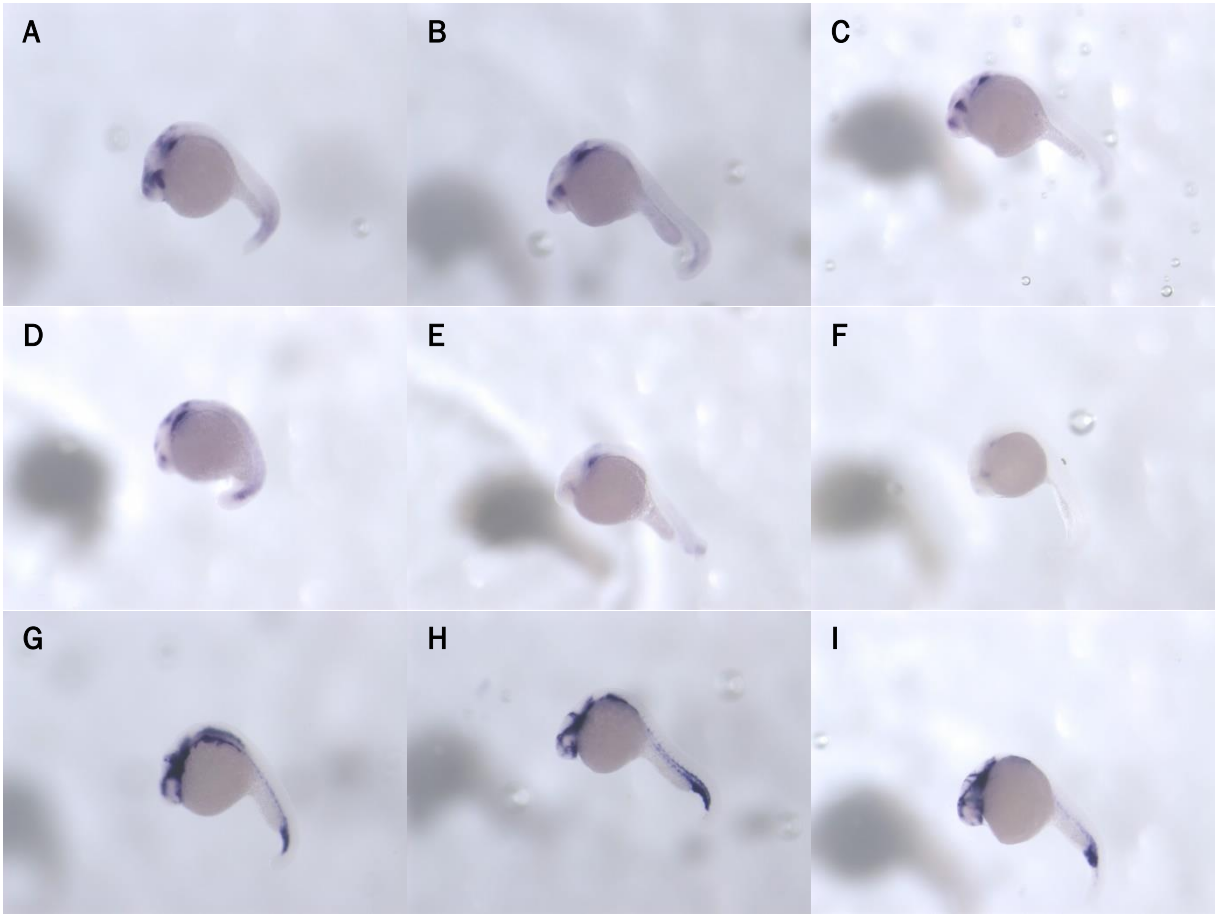

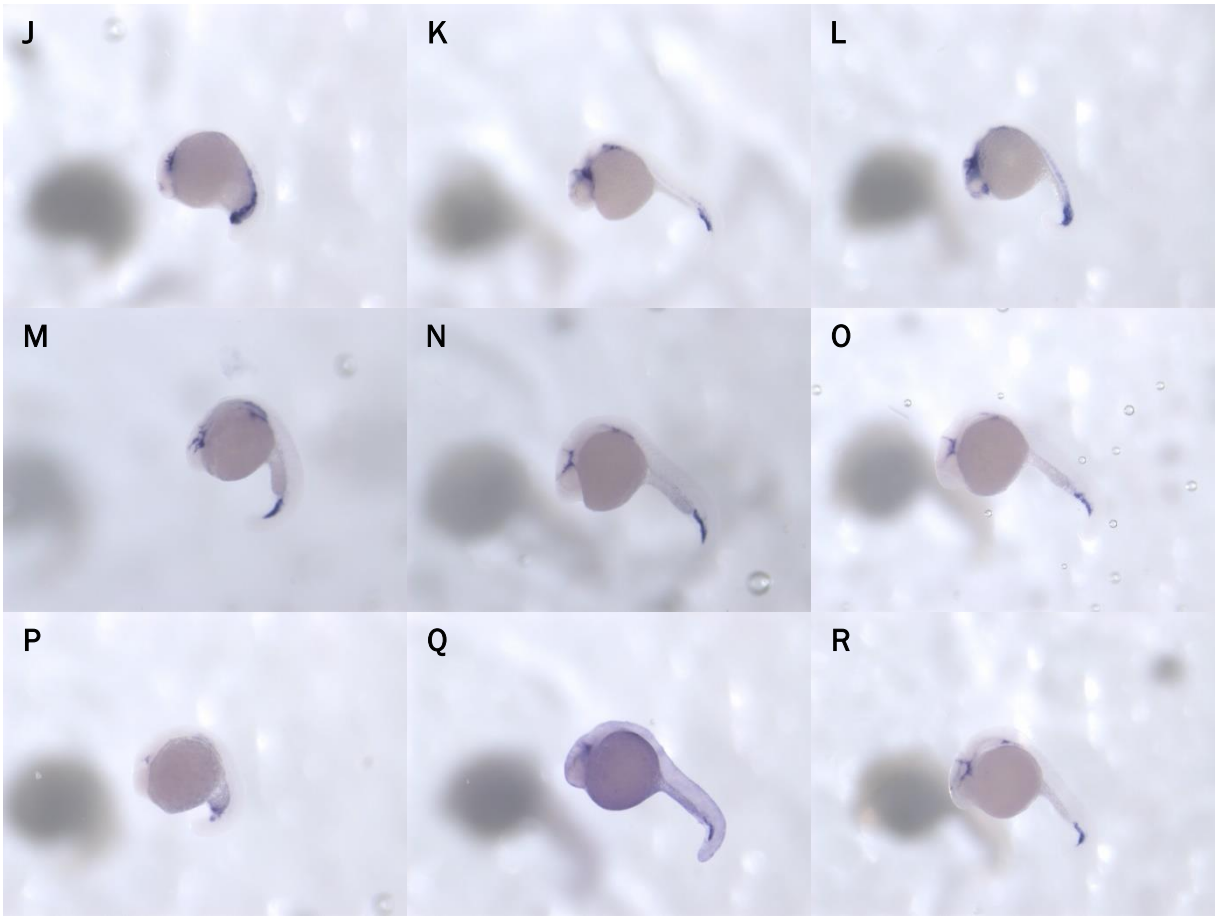

Figure 15: *in situ* for markers *efnb2a, fli1a* and *fl4* in embryos treated with compounds. *Efnb2a* expression for compounds treated with compound 1 **A**) compound 2 **B**) compound 3 **C**) compound 5 **D**) compound 6 **E**) compound 7 **F**). *Flia1* expression for compounds treated with compound 1 **G**) compound 2 **H**) compound 3 **I**) compound 5 **J**) compound 6 **K**) compound 7 **L**). *Flt4* expression for compounds treated with compound 1 **M**) compound 2 **N**) compound 3 **O**) compound 5 **P**) compound 6 **Q**) compound 7 **R**).

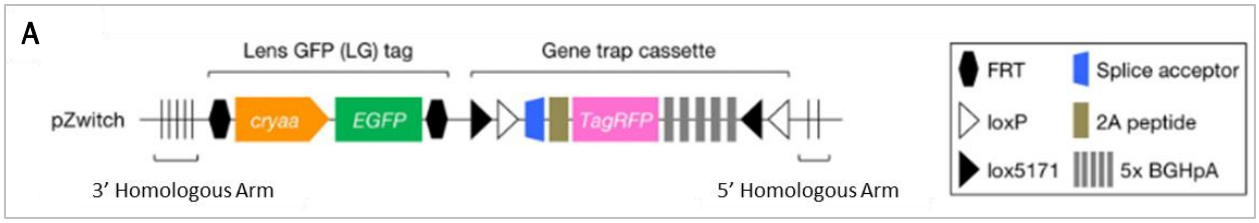

sg12	5′-taggGAGCATCATTCACACACGCT-3′ 3′-CTCGTAGTAAGTGTGTGCGAcaaa-5′	B
sg27	5′-taggCTGGCTTTGTGTCTAGTTGA-3′ 3′-GACCGAAACACAGATCAACTcaaa-5′	

cr17	5′-CGTGTGTGAATGATGCTCTAGTTATCTACACTTAGTAG-3′	C
cr21	5′-TCTAATAGGCCTTCAACTAGACAATCTACACTTAGTAG-3′	

Figure 16: Zwich, sgRNAs and crRNAs. Schematick of Zwich casette (Sugimoto, 2017) **A**). Sequence of the sgRNAs for injection with Cas9 **B**). Sequence of the crRNAs for injection with IbCpf1 **C**).

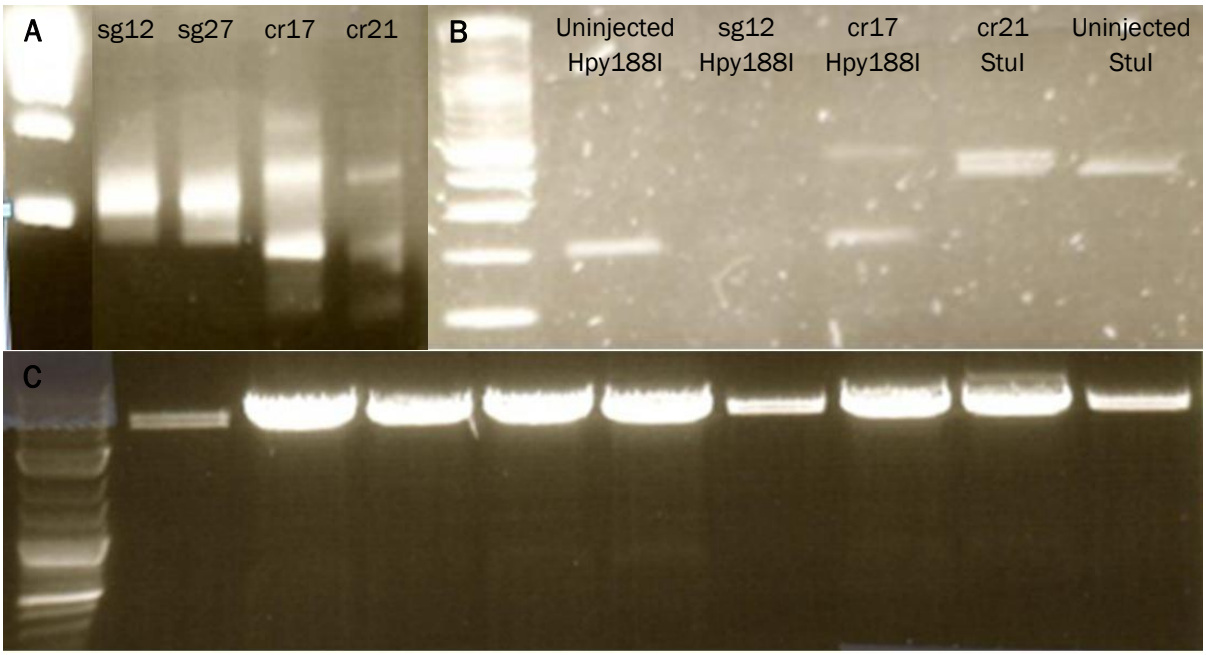

Figure 17: Agarose gels of RNAs, injected embryos and Zwich cassette. Agarose gel of sgRNAs 12 and 27, as well as crRNAs 17 and 21 after synthesis and purification **A**). Agarose gel of genomic DNA of uninjected and injected embryos after amplification and digestion **B**). Agarose gel of Zwich cassette after HiFi assembly with homologous arms, electroporation, purification and digestion with EcoRI **C**).

Supplementary Material

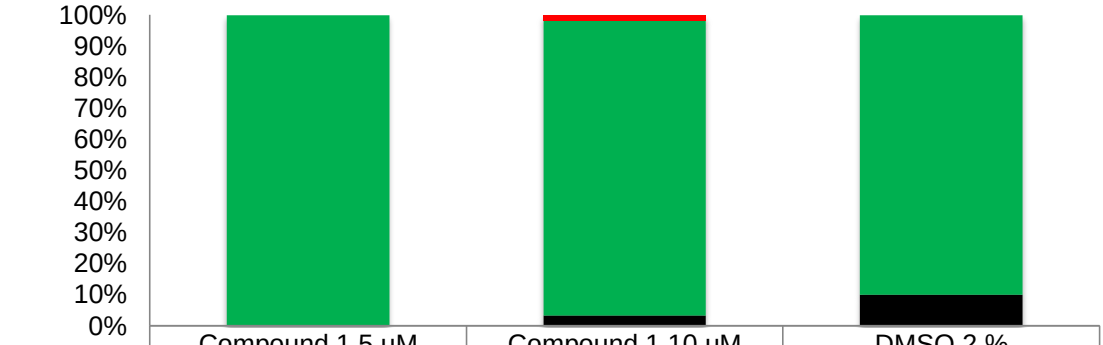

	Compound 1 5 uM	Compound 1 10 uM	DMSO 2 %
abnormal	0	1	0
normal	60	57	9
dead	0	2	1

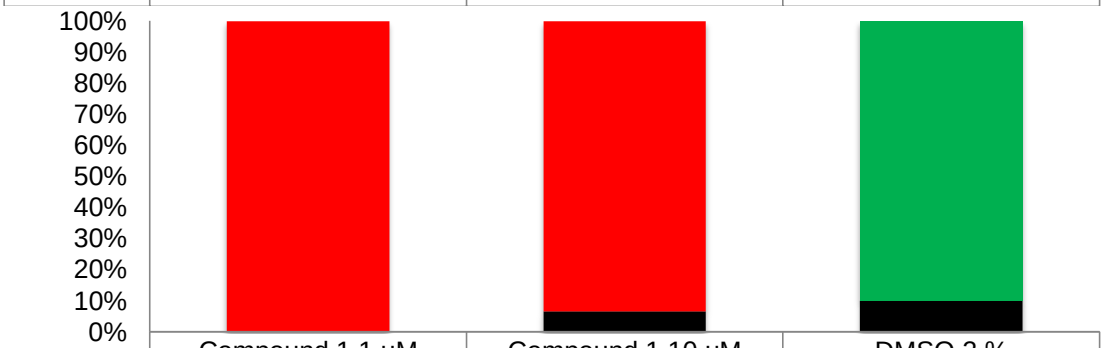

	Compound 1 1 uM	Compound 1 10 uM	DMSO 2 %
abnormal	60	56	0
normal	0	0	9
dead	0	4	1

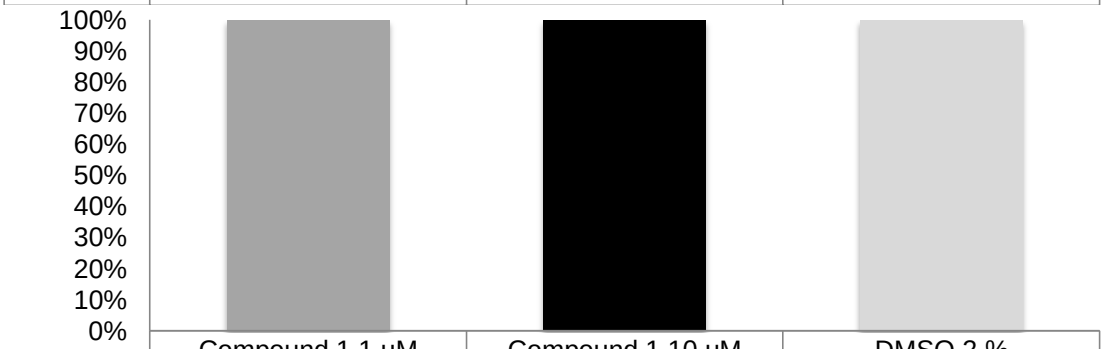

	Compound 1 1 uM	Compound 1 10 uM	DMSO 2 %
no pigment	0	56	0
reduced pigment	60	0	0
pigment	0	0	9

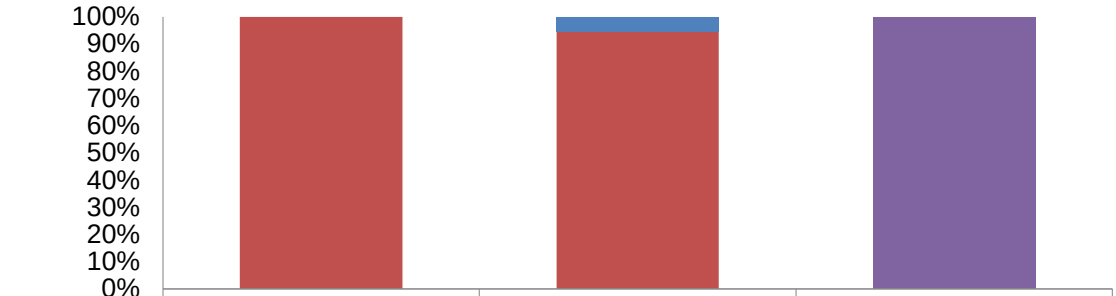

	Compound 1 1 uM	Compound 1 10 uM	DMSO 2 %
no tail	0	3	0
curved tail	60	53	0
short tail	0	0	0
normal tail	0	0	9

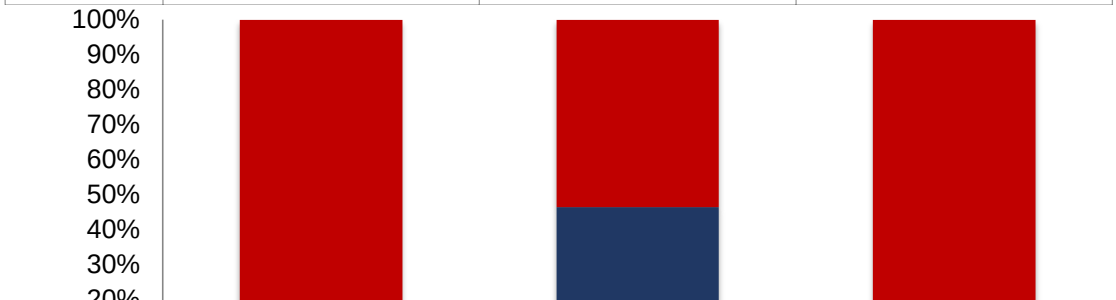

	Compound 1 1 uM	Compound 1 10 uM	DMSO 2 %
circulation	51	30	9
no circulation	9	26	0

	Compound 1 5 uM	Compound 1 10 uM	DMSO 2 %
abnormal	35	19	0
normal	0	0	9
dead	25	41	1

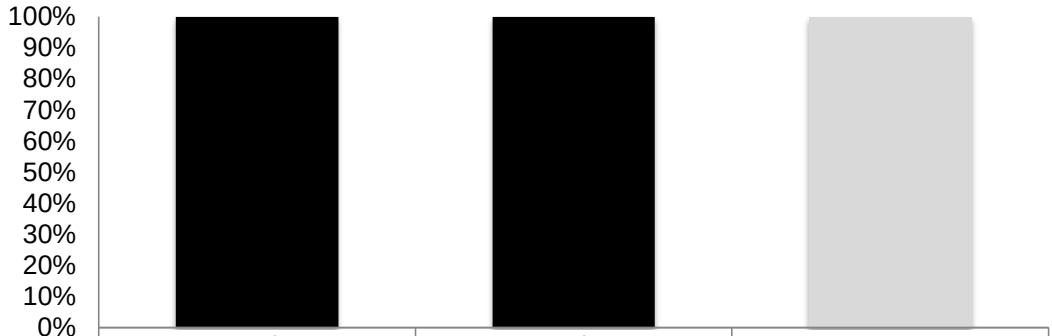

	Compound 1 5 uM	Compound 1 10 uM	DMSO 2 %
no pigment	35	19	0
reduced pigment	0	0	0
pigment	0	0	9

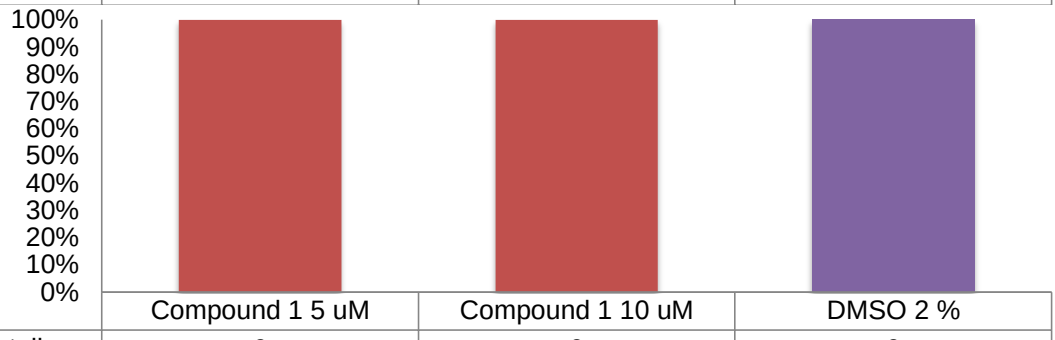

	Compound 1 5 uM	Compound 1 10 uM	DMSO 2 %
no tail	0	0	0
curved tail	35	19	0
short tail	0	0	0
normal tail	0	0	9

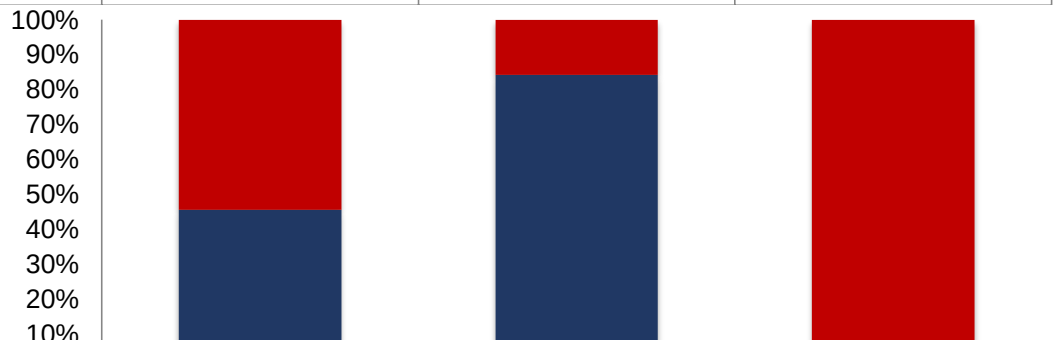

	Compound 1 5 uM	Compound 1 10 uM	DMSO 2 %
circulation	19	3	9
no circulation	16	16	0

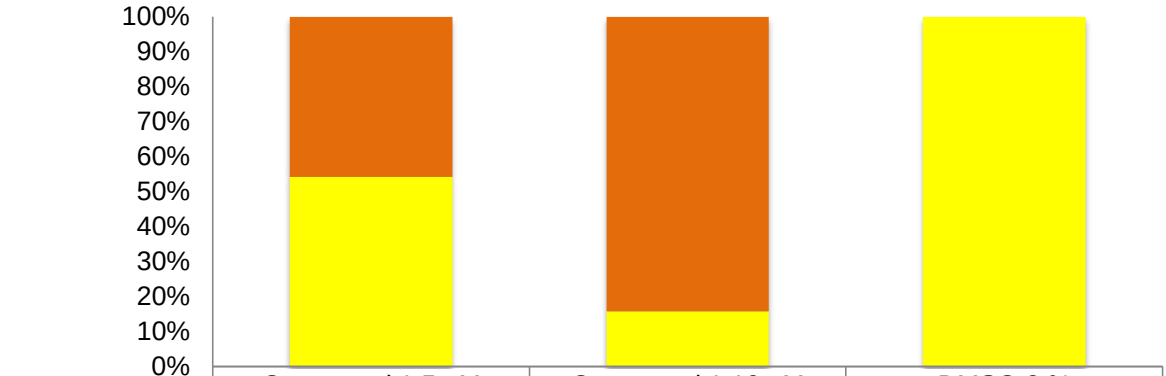

	Compound 1 5 uM	Compound 1 10 uM	DMSO 2 %
cardiac edema	16	16	0
no edema	19	3	9

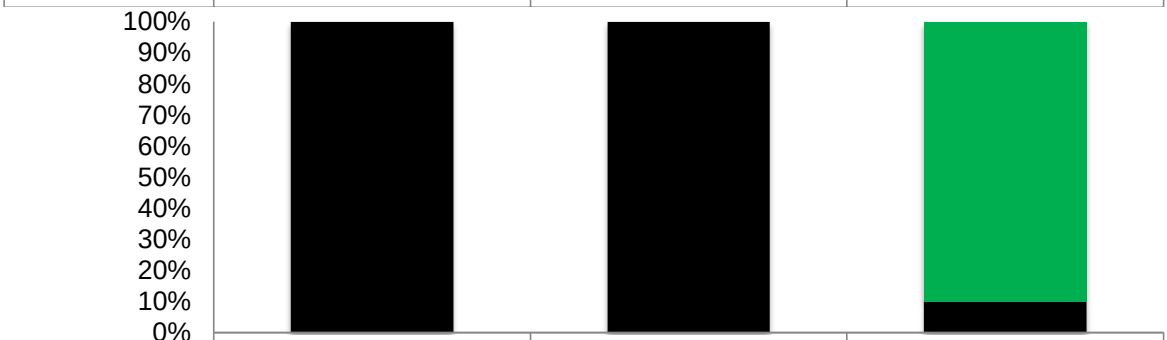

	Compound 1 5 uM	Compound 1 10 uM	DMSO 2 %
abnormal	0	0	0
normal	0	0	9
dead	60	60	1

Supplementary Figure 1: Time Screen for treatment at 24 hours post fertilization with compound 1.

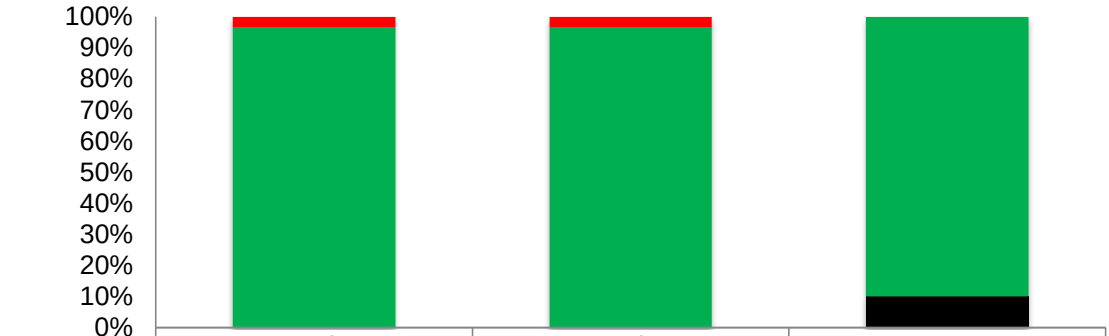

	Compound 1 5 uM	Compound 1 10 uM	DMSO 2 %
abnormal	2	2	0
normal	58	58	9
dead	0	0	1

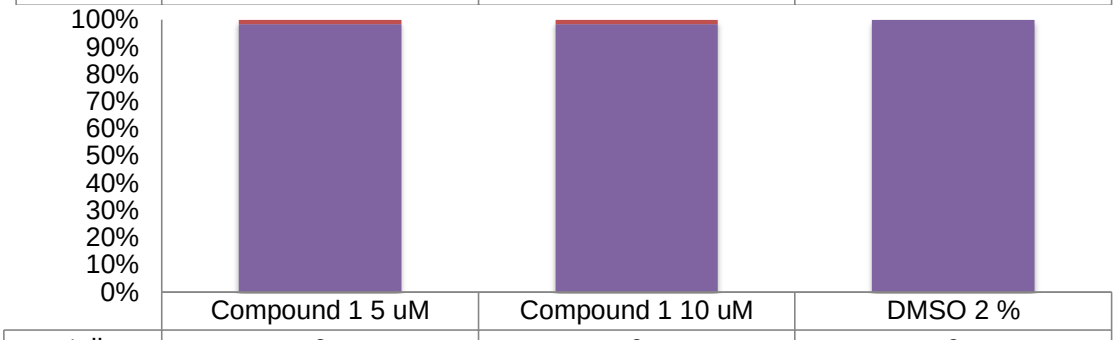

	Compound 1 5 uM	Compound 1 10 uM	DMSO 2 %
no tail	0	0	0
curved tail	1	1	0
short tail	0	0	0
normal tail	59	59	9

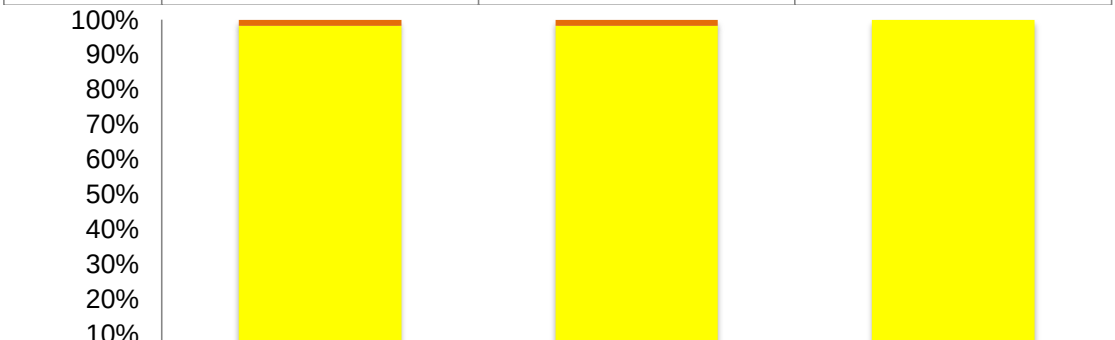

	Compound 1 5 uM	Compound 1 10 uM	DMSO 2 %
cardiac edema	1	1	0
no edema	59	59	9

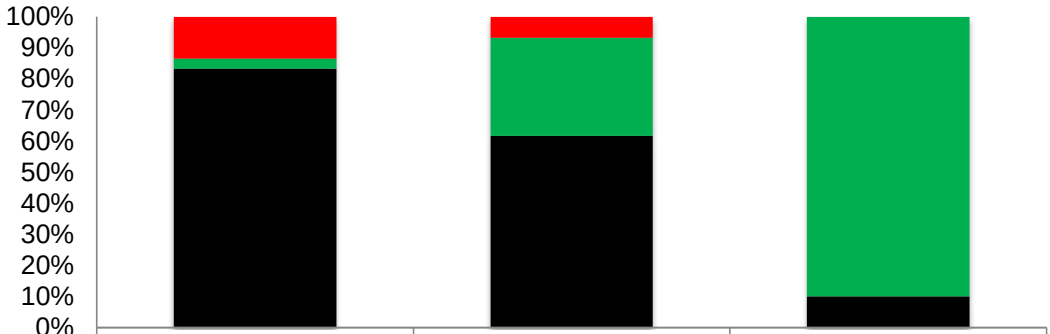

	Compound 1 5 uM	Compound 1 10 uM	DMSO 2 %
abnormal	8	4	0
normal	2	19	9
dead	50	37	1

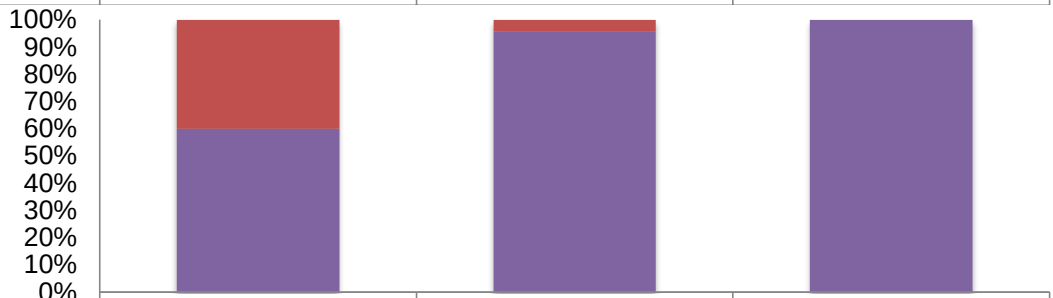

	Compound 1 5 uM	Compound 1 10 uM	DMSO 2 %
no tail	0	0	0
curved tail	4	1	0
short tail	0	0	0
normal tail	6	22	9

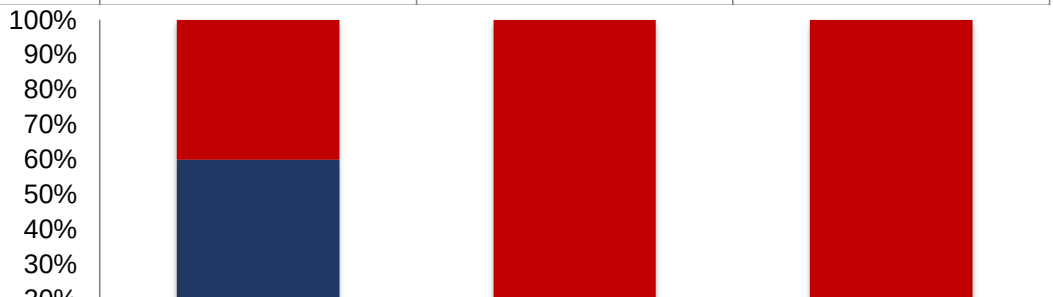

	Compound 1 5 uM	Compound 1 10 uM	DMSO 2 %
circulation	4	20	9
no circulation	6	3	0

Supplementary Figure 2: Time Screen for treatment at 48 hours post fertilization with compound 1.

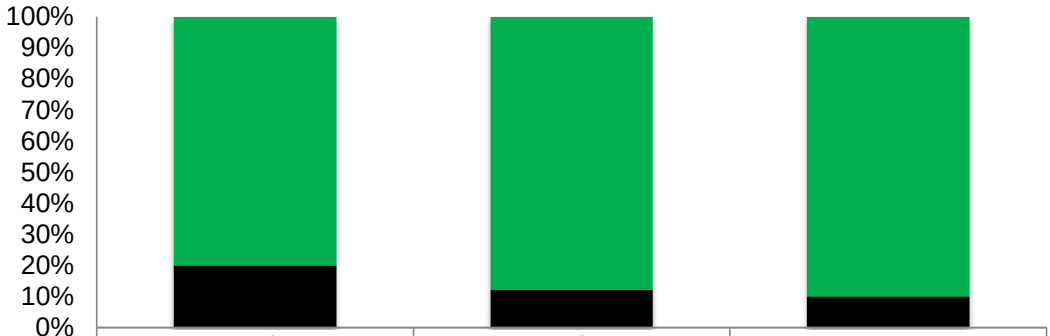

	Compound 2 5 uM	Compound 2 10 uM	DMSO 2 %
abnormal	0	0	0
normal	72	79	9
dead	18	11	1

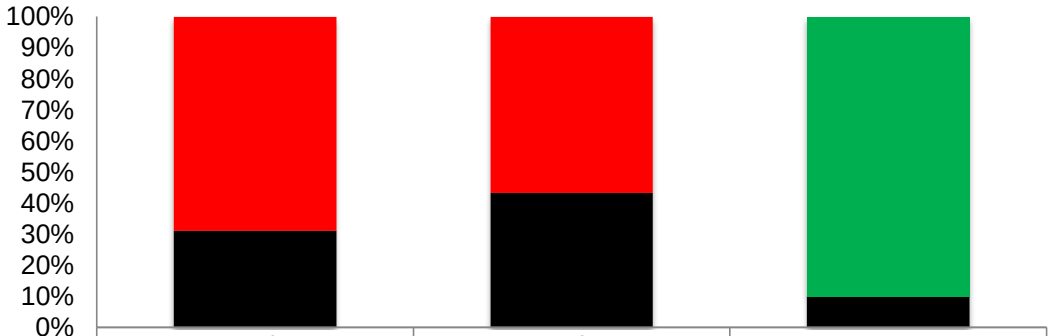

	Compound 2 5 uM	Compound 2 10 uM	DMSO 2 %
abnormal	62	51	0
normal	0	0	9
dead	28	39	1

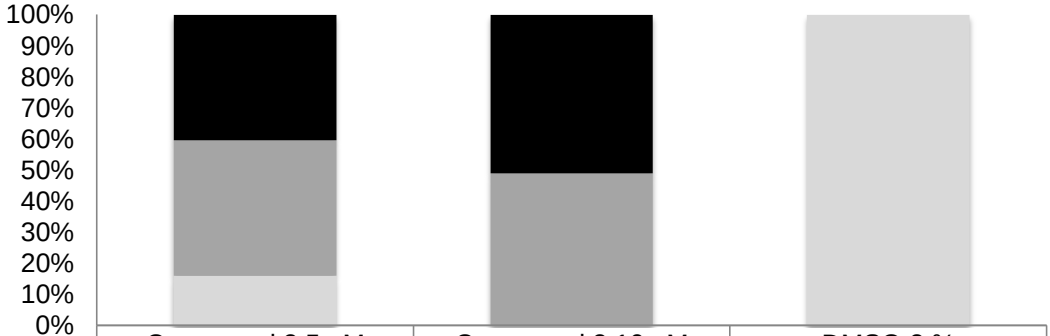

	Compound 2 5 uM	Compound 2 10 uM	DMSO 2 %
no pigment	25	26	0
reduced pigment	27	25	0
pigment	10	0	9

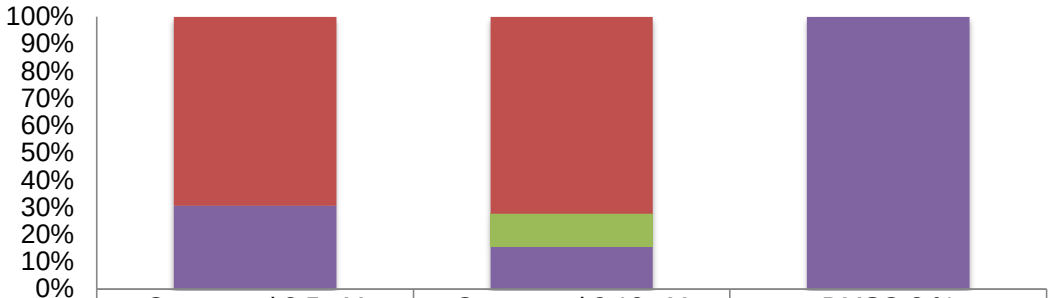

	Compound 2 5 uM	Compound 2 10 uM	DMSO 2 %
no tail	0	0	0
curved tail	43	42	0
short tail	0	7	0
normal tail	19	9	9

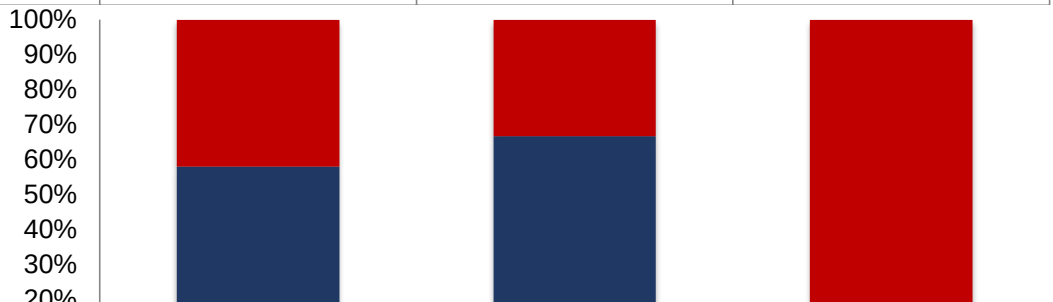

	Compound 2 5 uM	Compound 2 10 uM	DMSO 2 %
circulation	26	17	9
no circulation	36	34	0

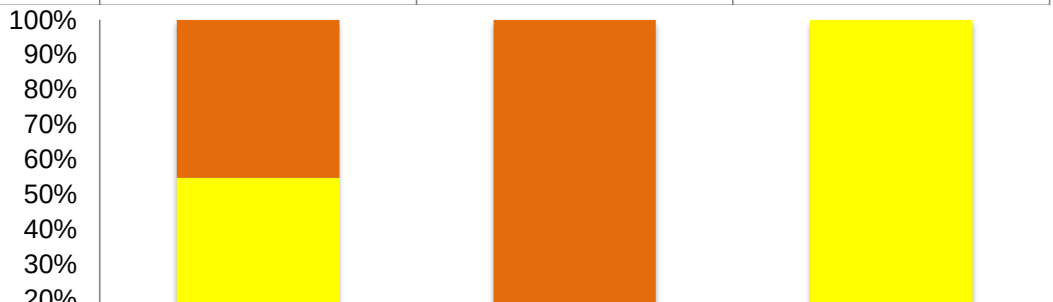

	Compound 2 5 uM	Compound 2 10 uM	DMSO 2 %
cardiac edema	28	44	0
no edema	34	7	9

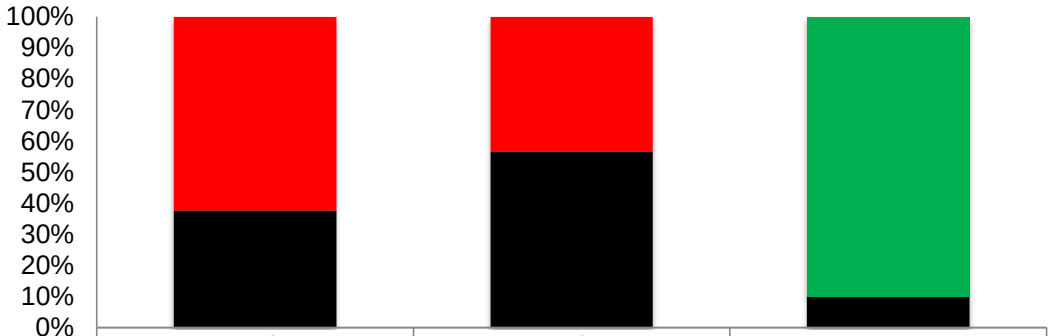

	Compound 2 5 uM	Compound 2 10 uM	DMSO 2 %
abnormal	56	39	0
normal	0	0	9
dead	34	51	1

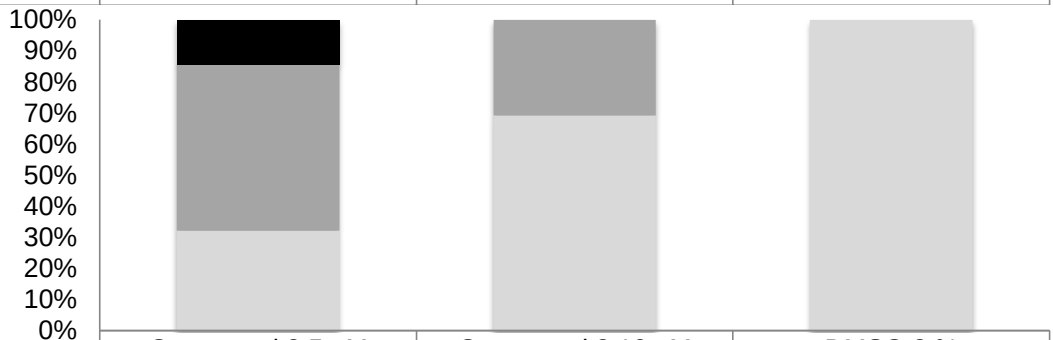

	Compound 2 5 uM	Compound 2 10 uM	DMSO 2 %
no pigment	8	0	0
reduced pigment	30	12	0
pigment	18	27	9

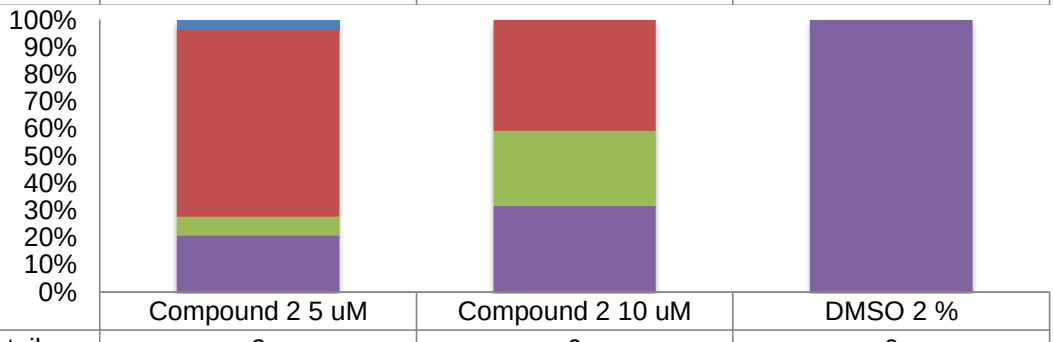

	Compound 2 5 uM	Compound 2 10 uM	DMSO 2 %
no tail	2	0	0
curved tail	40	22	0
short tail	4	15	0
normal tail	12	17	9

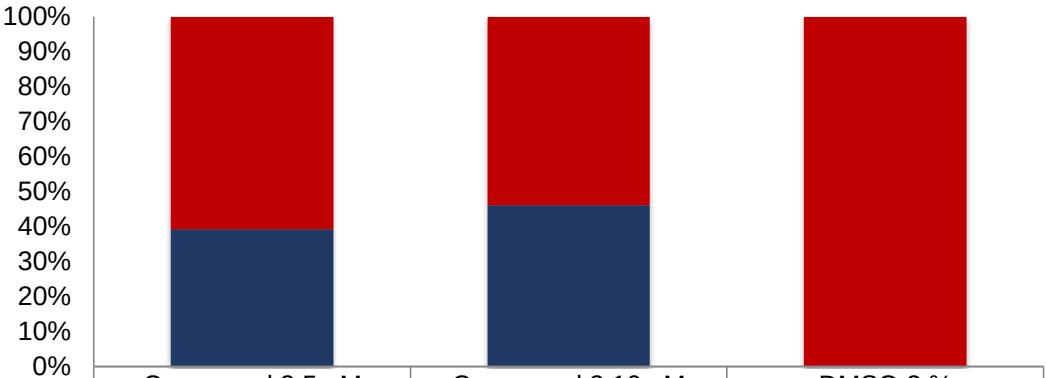

	Compound 2 5 uM	Compound 2 10 uM	DMSO 2 %
circulation	34	21	9
no circulation	22	18	0

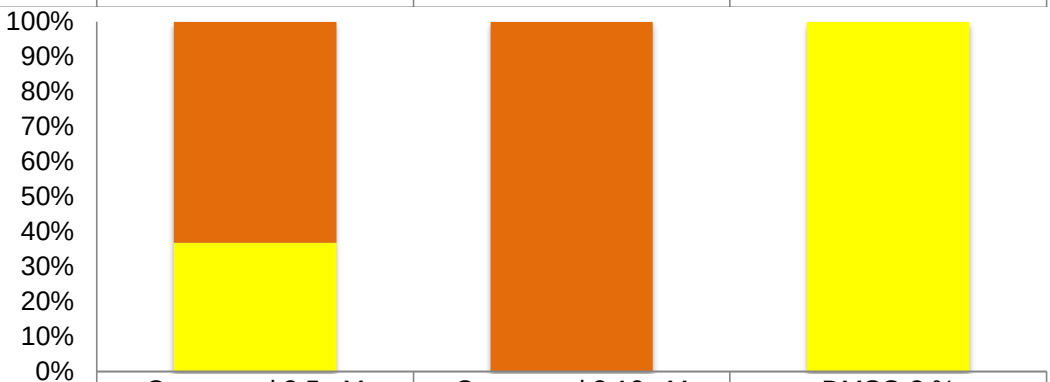

	Compound 2 5 uM	Compound 2 10 uM	DMSO 2 %
cardiac edema	36	39	0
no edema	21	0	9

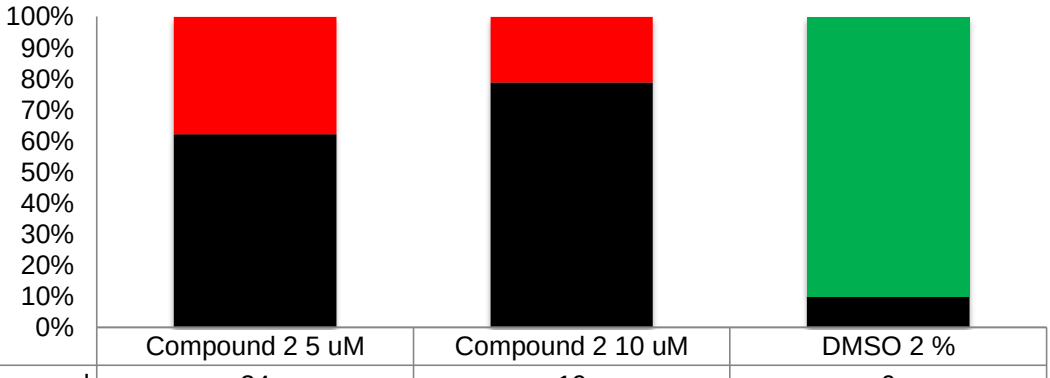

	Compound 2 5 uM	Compound 2 10 uM	DMSO 2 %
abnormal	34	19	0
normal	0	0	9
dead	56	71	1

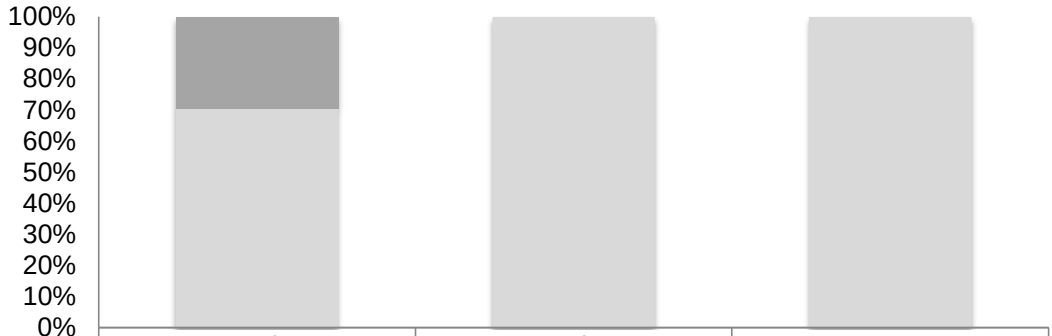

	Compound 2 5 uM	Compound 2 10 uM	DMSO 2 %
no pigment	0	0	0
reduced pigment	10	0	0
pigment	24	19	9

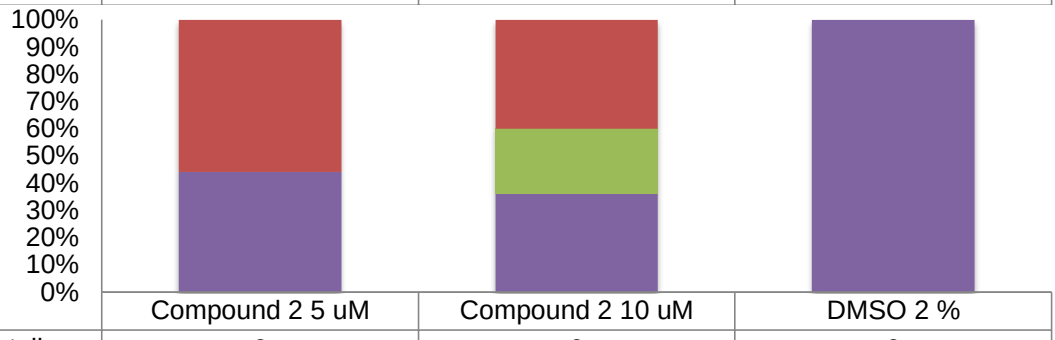

	Compound 2 5 uM	Compound 2 10 uM	DMSO 2 %
no tail	0	0	0
curved tail	19	10	0
short tail	0	6	0
normal tail	15	9	9

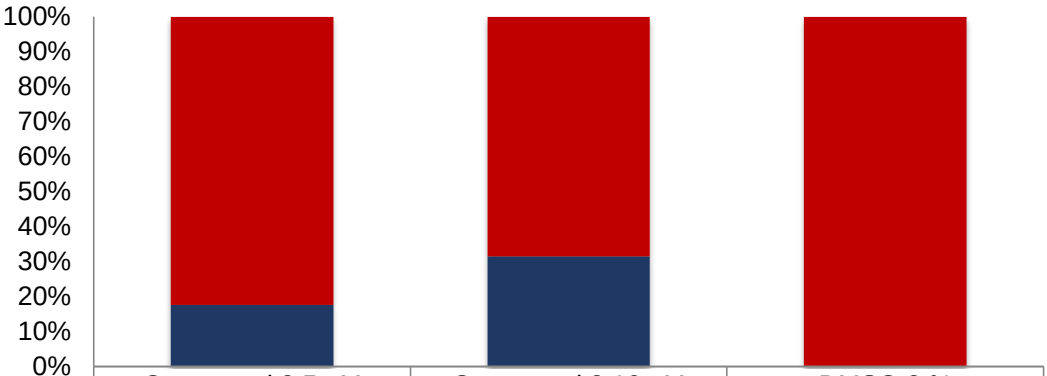

	Compound 2 5 uM	Compound 2 10 uM	DMSO 2 %
circulation	28	13	9
no circulation	6	6	0

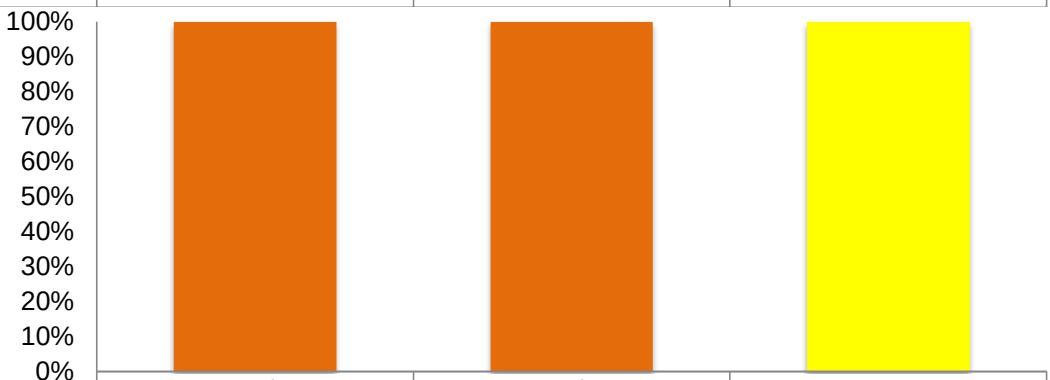

	Compound 2 5 uM	Compound 2 10 uM	DMSO 2 %
cardiac edema	34	19	0
no edema	0	0	9

Supplementary Figure 3: Time Screen for treatment at 12 hours post fertilization with compound 2.

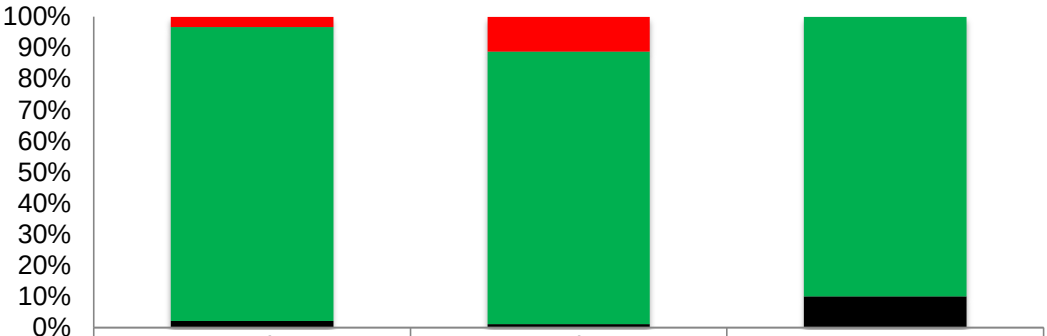

	Compound 2 5 uM	Compound 2 10 uM	DMSO 2 %
abnormal	3	10	0
normal	85	79	9
dead	2	1	1

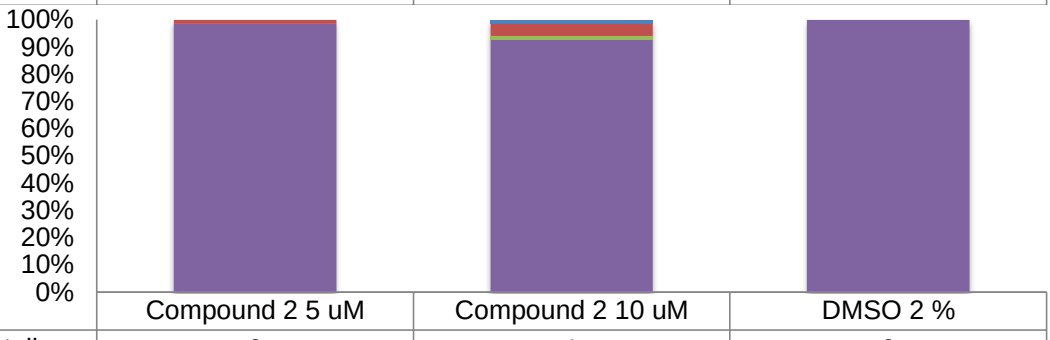

	Compound 2 5 uM	Compound 2 10 uM	DMSO 2 %
no tail	0	1	0
curved tail	1	4	0
short tail	0	1	0
normal tail	85	79	9

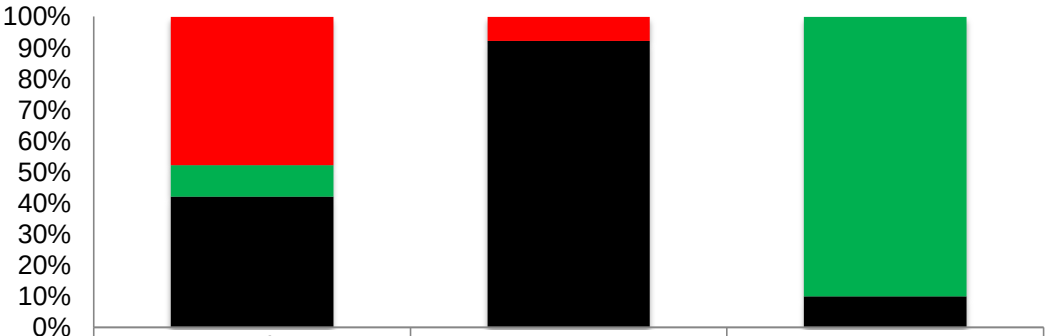

	Compound 2 5 uM	Compouns 2 10 uM	DMSO 2 %
abnormal	43	7	0
normal	9	0	9
dead	38	83	1

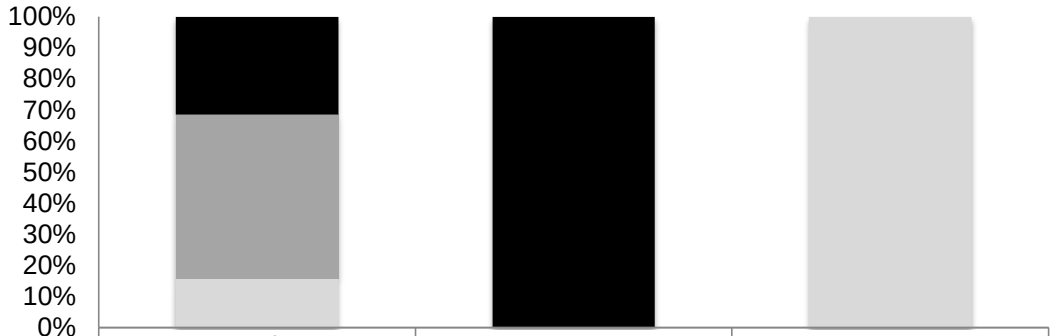

	Compound 2 5 uM	Compouns 2 10 uM	DMSO 2 %
no pigment	16	7	0
reduced pigment	27	0	0
pigment	8	0	9

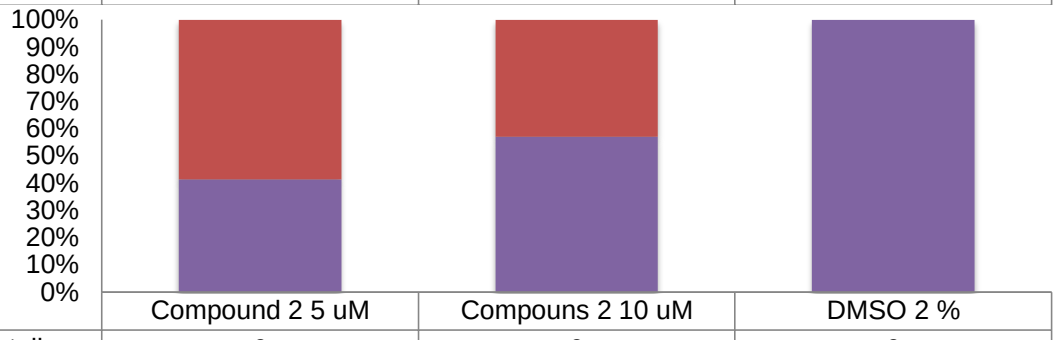

	Compound 2 5 uM	Compouns 2 10 uM	DMSO 2 %
no tail	0	0	0
curved tail	27	3	0
short tail	0	0	0
normal tail	19	4	9

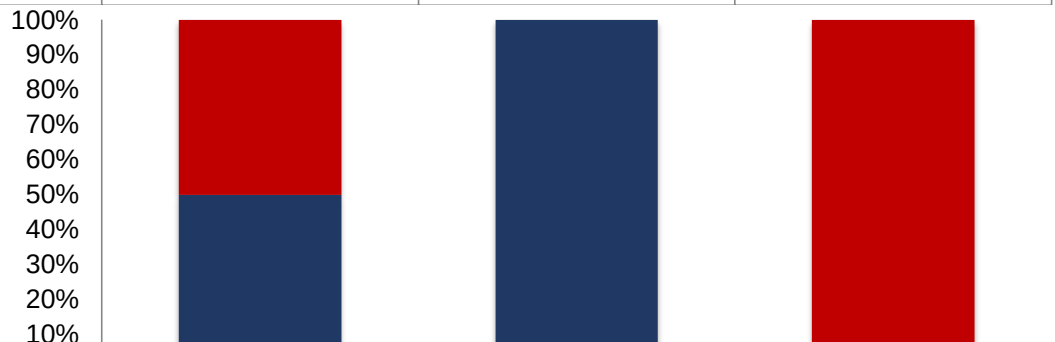

	Compound 2 5 uM	Compouns 2 10 uM	DMSO 2 %
circulation	26	0	9
no circulation	26	7	0

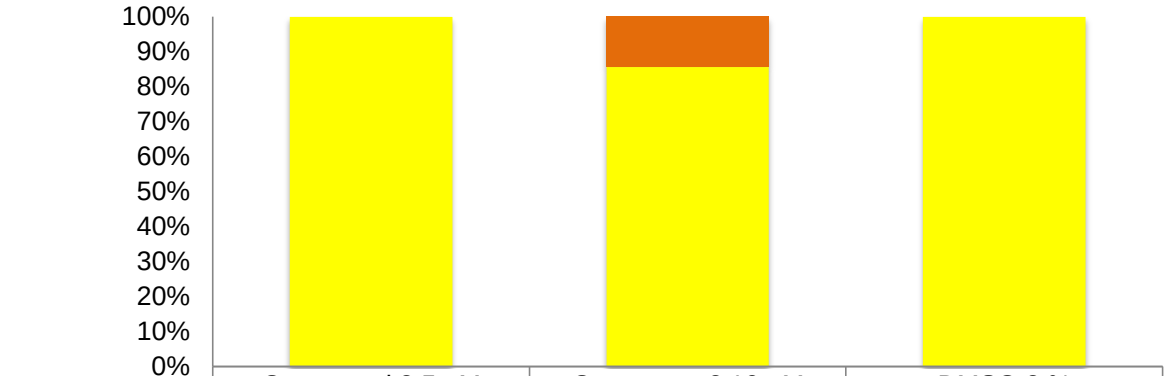

	Compound 2 5 uM	Compouns 2 10 uM	DMSO 2 %
cardiac edema	0	1	0
no edema	52	6	9

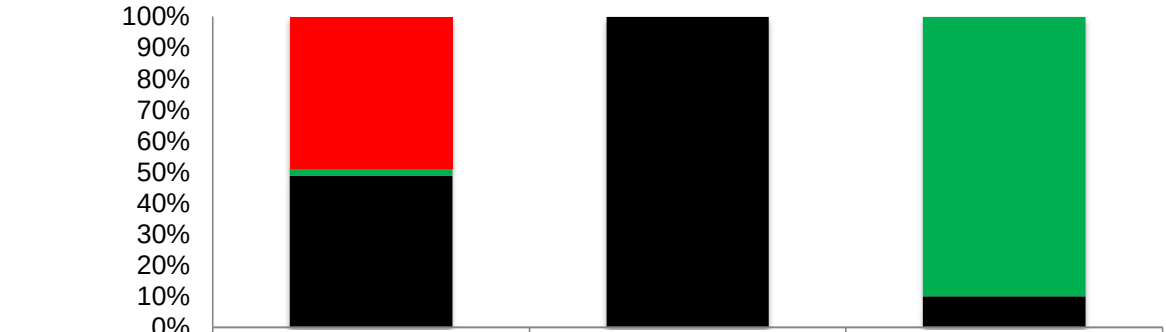

	Compound 2 5 uM	Compound 2 10 uM	DMSO 2 %
abnormal	44	0	0
normal	2	0	9
dead	44	90	1

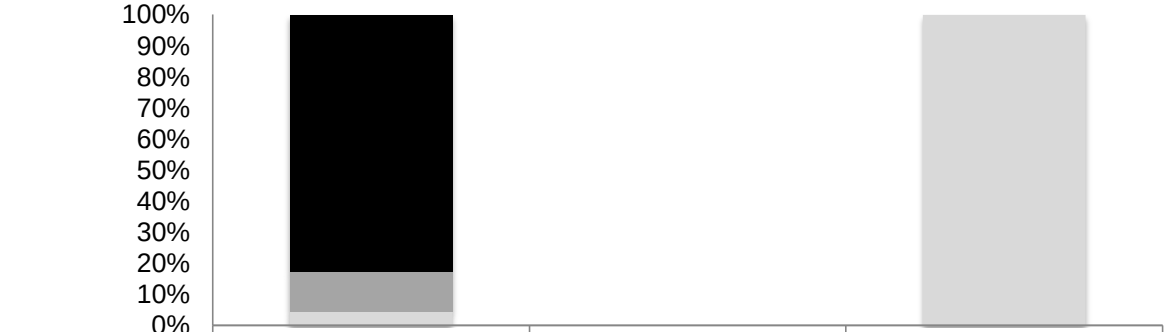

	Compound 2 5 uM	Compound 2 10 uM	DMSO 2 %
no pigment	38	0	0
reduced pigment	6	0	0
pigment	2	0	9

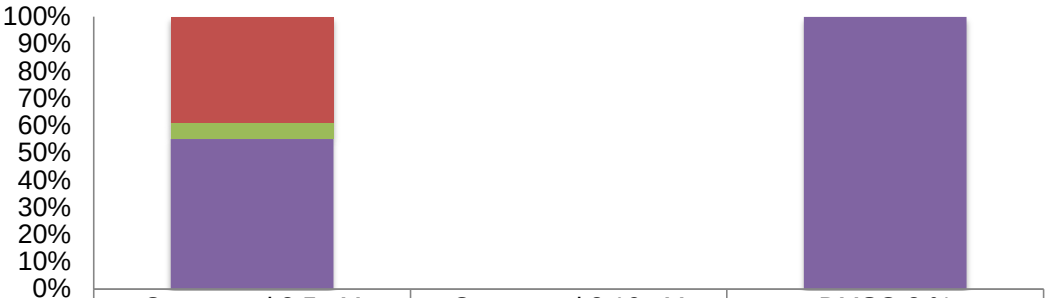

	Compound 2 5 uM	Compound 2 10 uM	DMSO 2 %
no tail	0	0	0
curved tail	19	0	0
short tail	3	0	0
normal tail	27	0	9

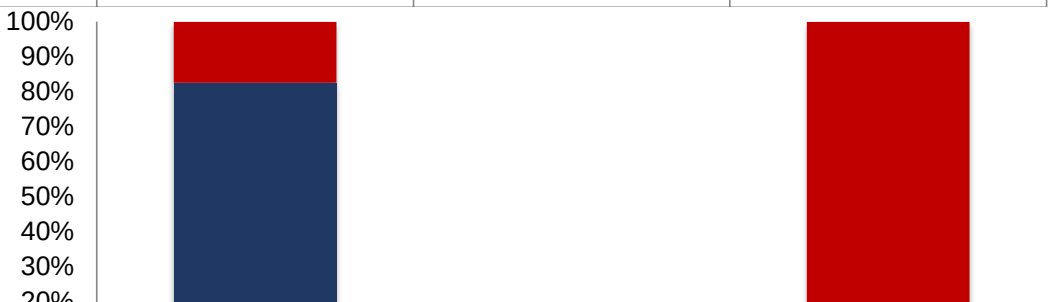

	Compound 2 5 uM	Compound 2 10 uM	DMSO 2 %
circulation	8	0	9
no circulation	38	0	0

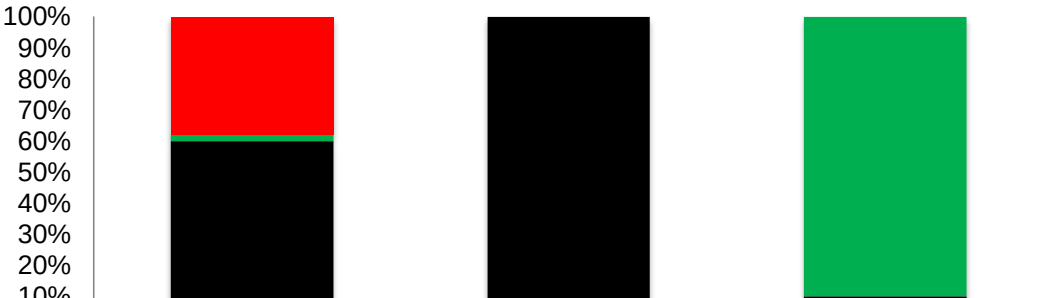

	Compound 2 5 uM	Compound 2 10 uM	DMSO 2 %
abnormal	34	0	0
normal	2	0	9
dead	54	90	1

	Compound 2 5 uM	Compound 2 10 uM	DMSO 2 %
no pigment	0	0	0
reduced pigment	30	0	0
pigment	6	0	9

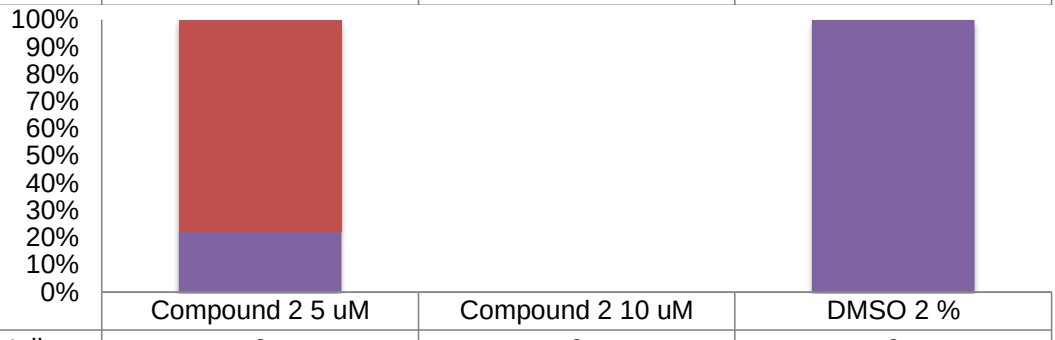

	Compound 2 5 uM	Compound 2 10 uM	DMSO 2 %
no tail	0	0	0
curved tail	28	0	0
short tail	0	0	0
normal tail	8	0	9

	Compound 2 5 uM	Compound 2 10 uM	DMSO 2 %
circulation	22	0	9
no circulation	14	0	0

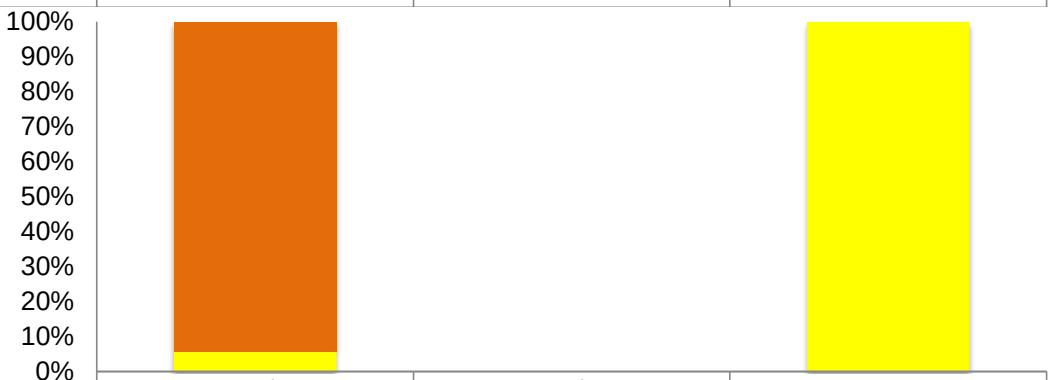

	Compound 2 5 uM	Compound 2 10 uM	DMSO 2 %
cardiac edema	33	0	0
no edema	2	0	9

Supplementary Figure 4: Time Screen for treatment at 24 hours post fertilization with compound 2.

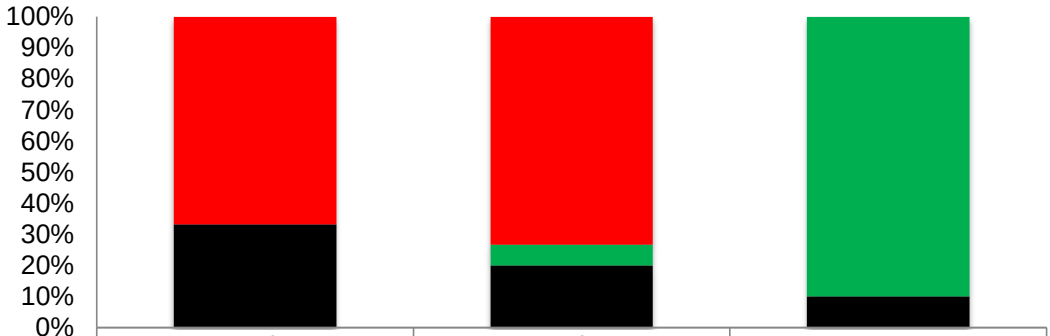

	Compound 2 5 uM	Compound 2 10 uM	DMSO 2 %
abnormal	20	22	0
normal	0	2	9
dead	10	6	1

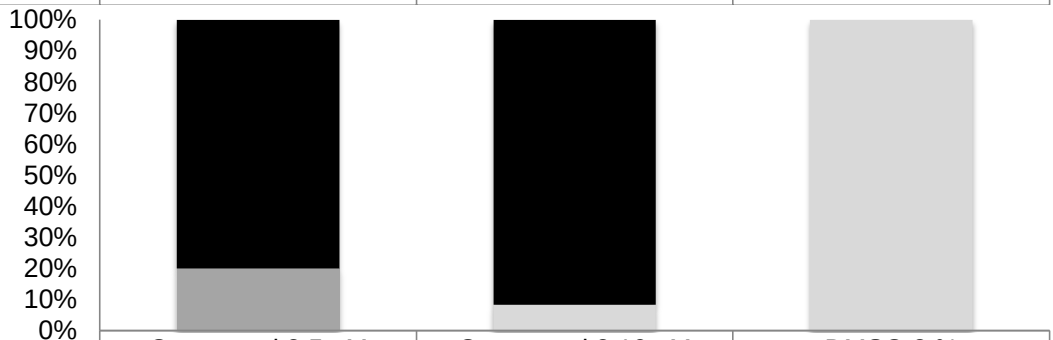

	Compound 2 5 uM	Compound 2 10 uM	DMSO 2 %
no pigment	16	22	0
reduced pigment	4	0	0
pigment	0	2	9

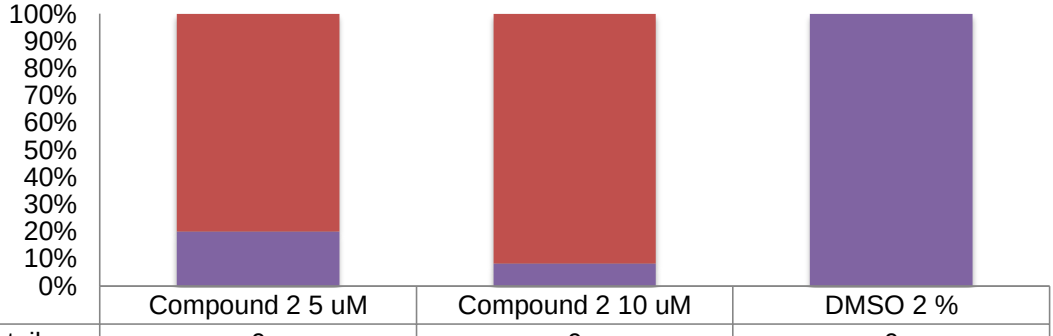

	Compound 2 5 uM	Compound 2 10 uM	DMSO 2 %
no tail	0	0	0
curved tail	16	22	0
short tail	0	0	0
normal tail	4	2	9

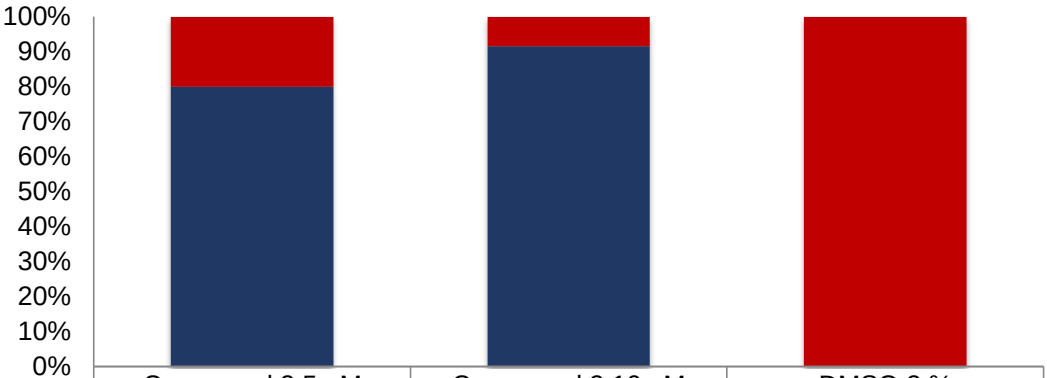

	Compound 2 5 uM	Compound 2 10 uM	DMSO 2 %
circulation	4	2	9
no circulation	16	22	0

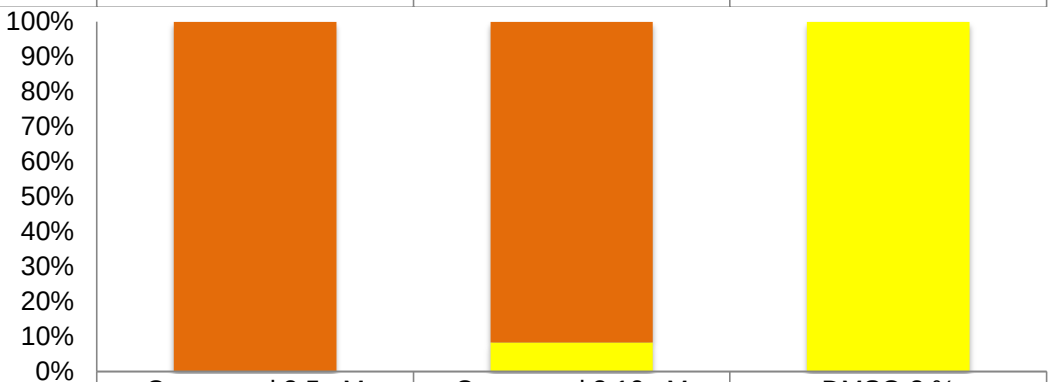

	Compound 2 5 uM	Compound 2 10 uM	DMSO 2 %
cardiac edema	20	22	0
no edema	0	2	9

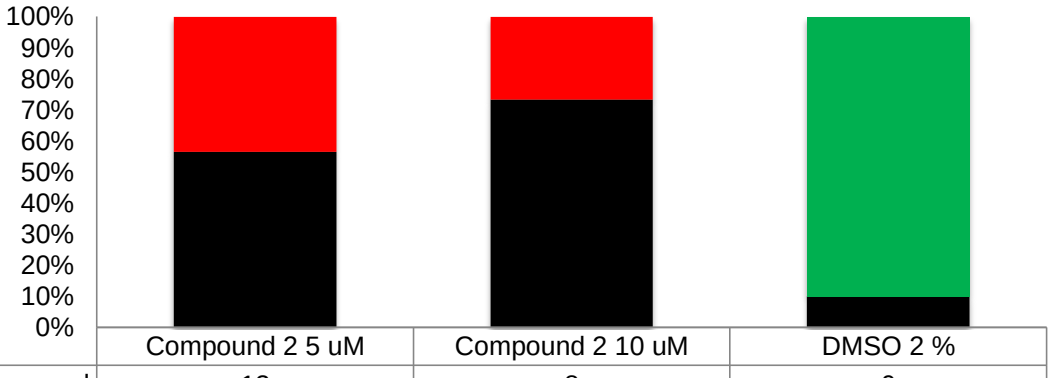

	Compound 2 5 uM	Compound 2 10 uM	DMSO 2 %
abnormal	13	8	0
normal	0	0	9
dead	17	22	1

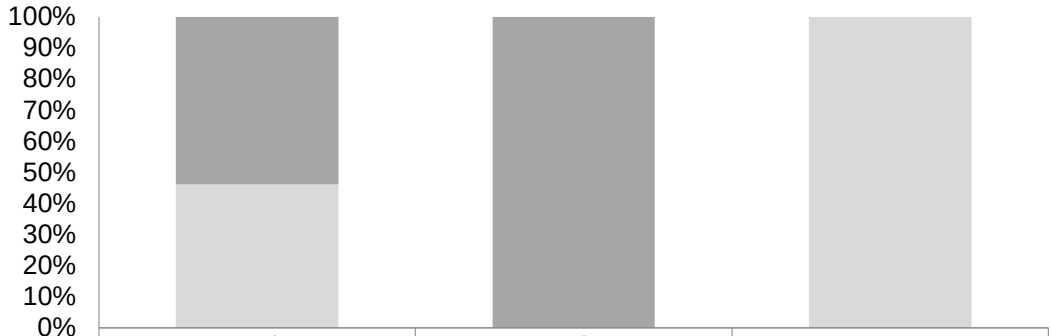

	Compound 2 5 uM	Compound 2 10 uM	DMSO 2 %
no pigment	0	0	0
reduced pigment	7	8	0
pigment	6	0	9

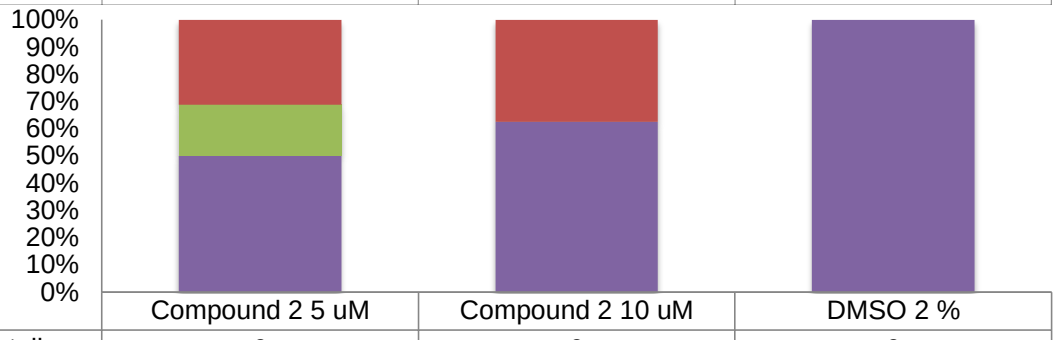

	Compound 2 5 uM	Compound 2 10 uM	DMSO 2 %
no tail	0	0	0
curved tail	5	3	0
short tail	3	0	0
normal tail	8	5	9

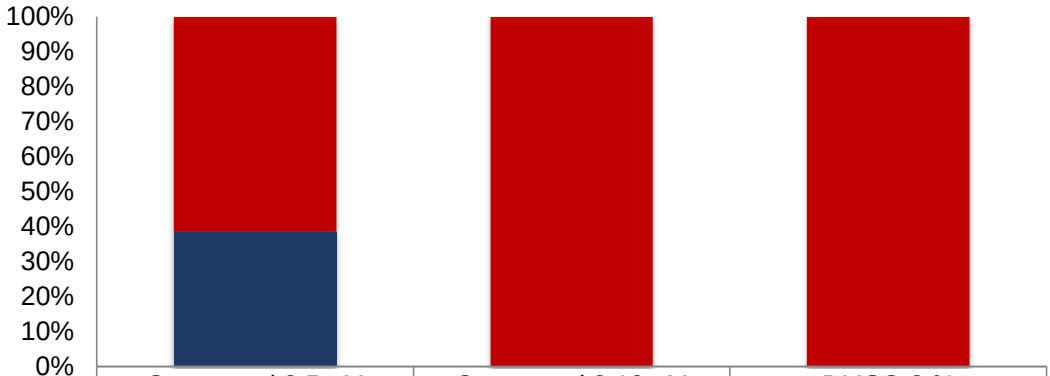

	Compound 2 5 uM	Compound 2 10 uM	DMSO 2 %
circulation	8	8	9
no circulation	5	0	0

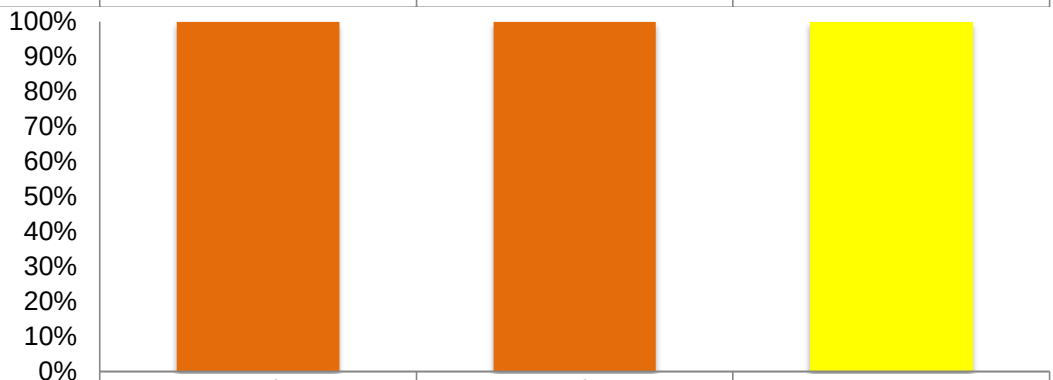

	Compound 2 5 uM	Compound 2 10 uM	DMSO 2 %
cardiac edema	13	8	0
no edema	0	0	9

Supplementary Figure 5: Time Screen for treatment at 36 hours post fertilization with compound 2.

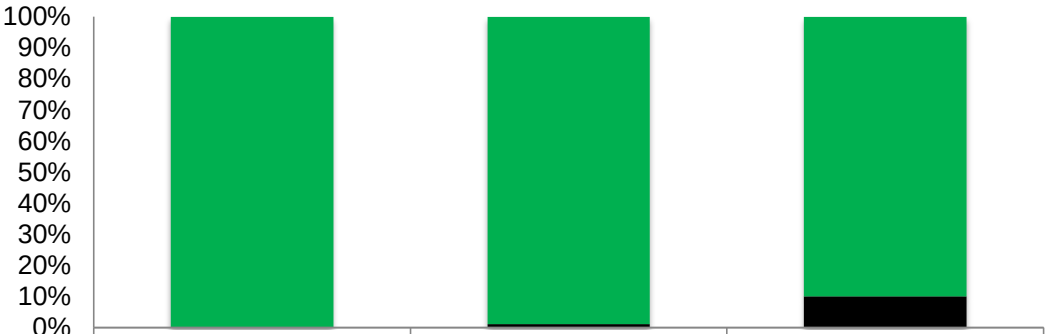

	Compound 2 5 uM	Compound 2 10 uM	DMSO 2 %
abnormal	0	0	0
normal	90	89	9
dead	0	1	1

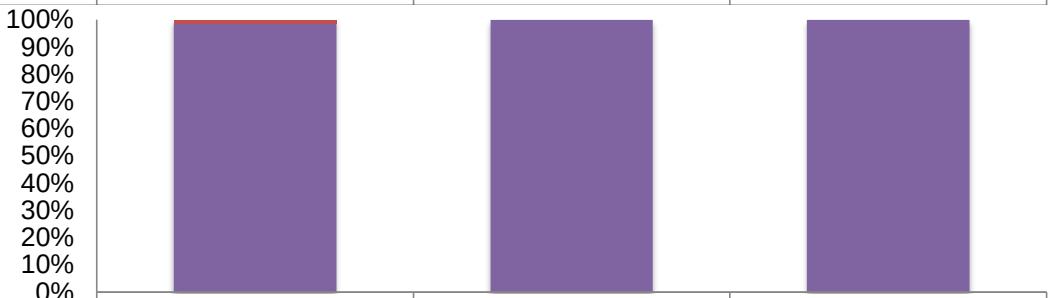

	Compound 2 5 uM	Compound 2 10 uM	DMSO 2 %
no tail	0	0	0
curved tail	1	0	0
short tail	0	0	0
normal tail	89	89	9

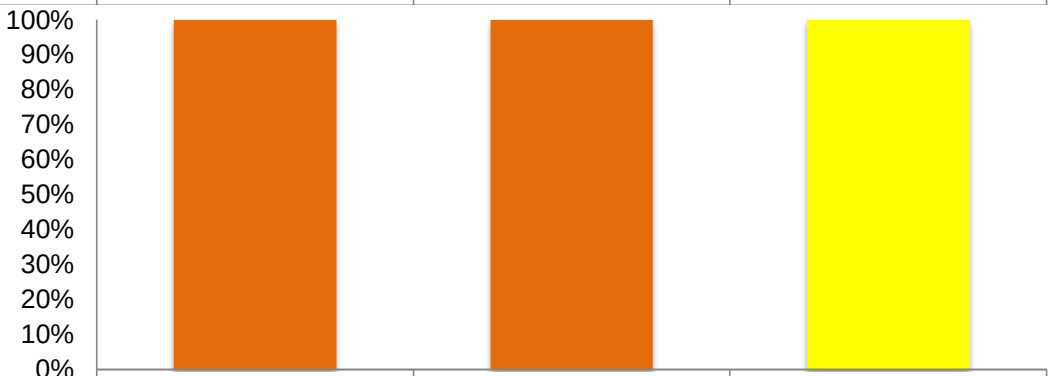

	Compound 2 5 uM	Compound 2 10 uM	DMSO 2 %
cardiac edema	90	89	0
no edema	0	0	9

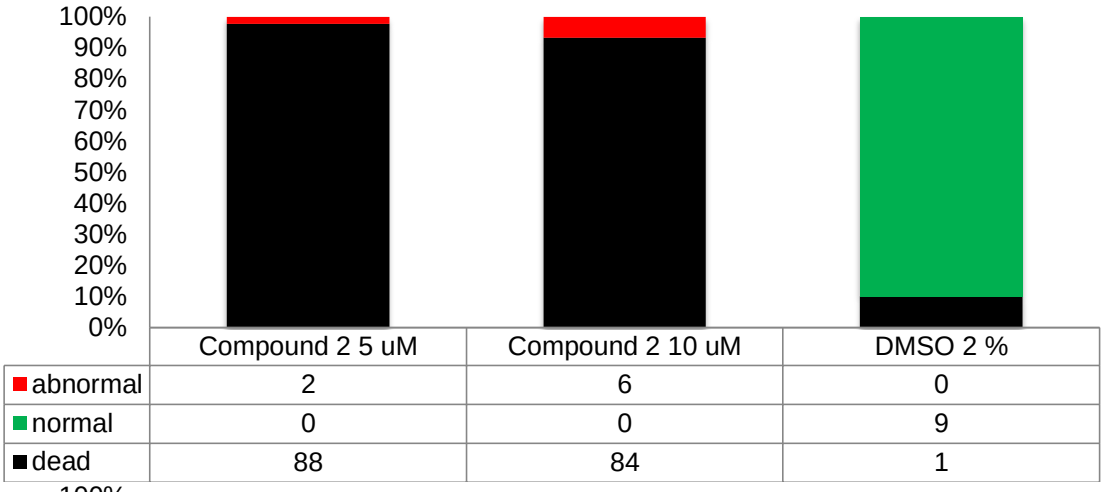

	Compound 2 5 uM	Compound 2 10 uM	DMSO 2 %
abnormal	2	6	0
normal	0	0	9
dead	88	84	1

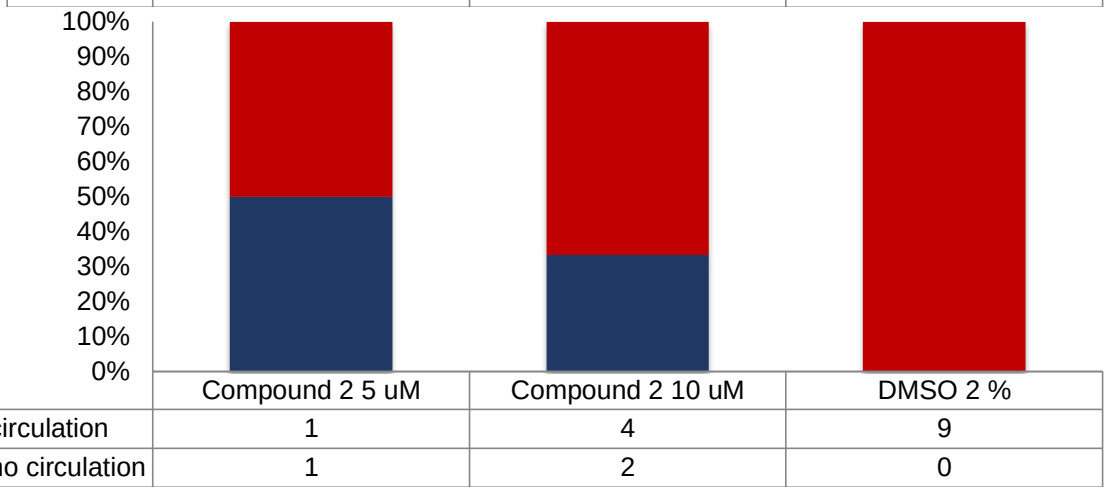

	Compound 2 5 uM	Compound 2 10 uM	DMSO 2 %
circulation	1	4	9
no circulation	1	2	0

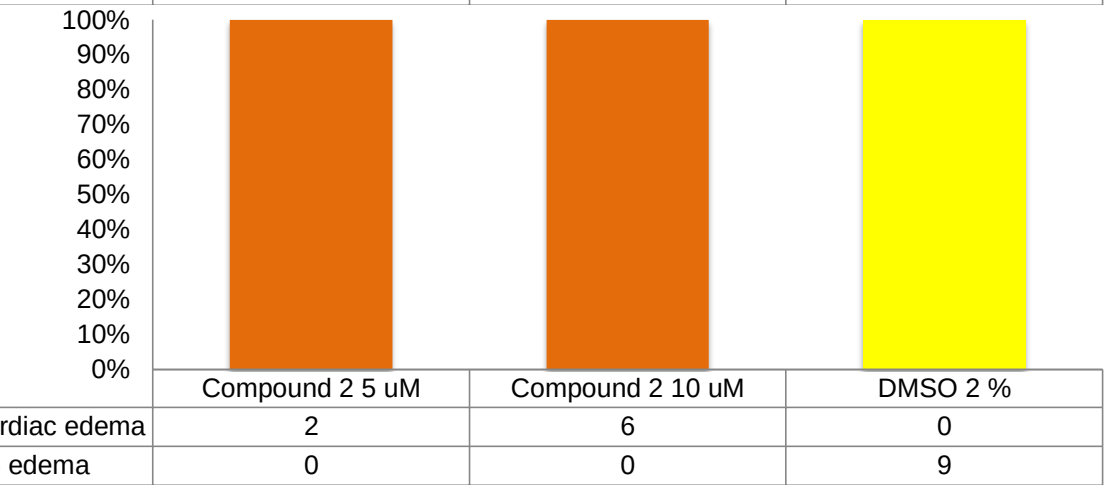

	Compound 2 5 uM	Compound 2 10 uM	DMSO 2 %
cardiac edema	2	6	0
no edema	0	0	9

Supplementary Figure 6: Development Screen for treatment at 48 hours post fertilization Compound 2.

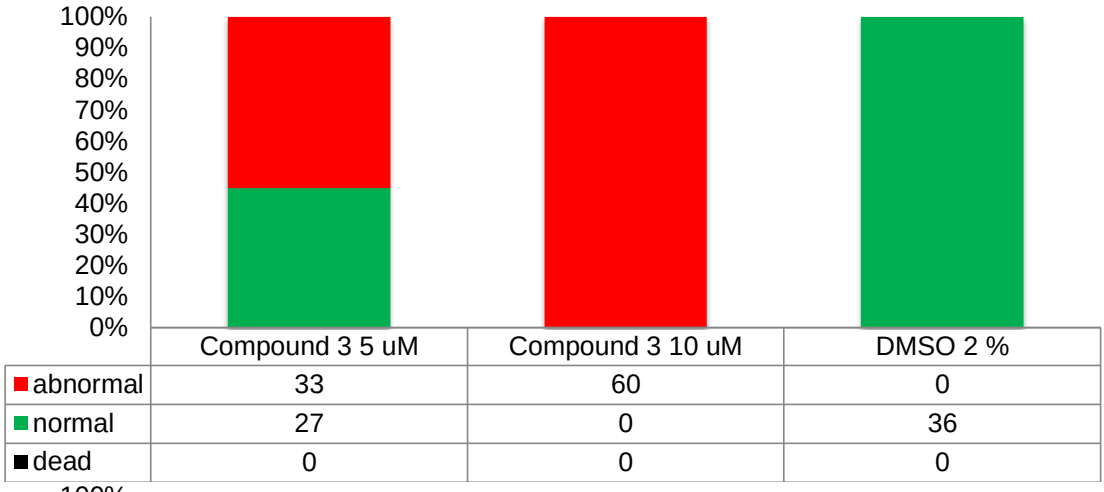

	Compound 3 5 uM	Compound 3 10 uM	DMSO 2 %
abnormal	33	60	0
normal	27	0	36
dead	0	0	0

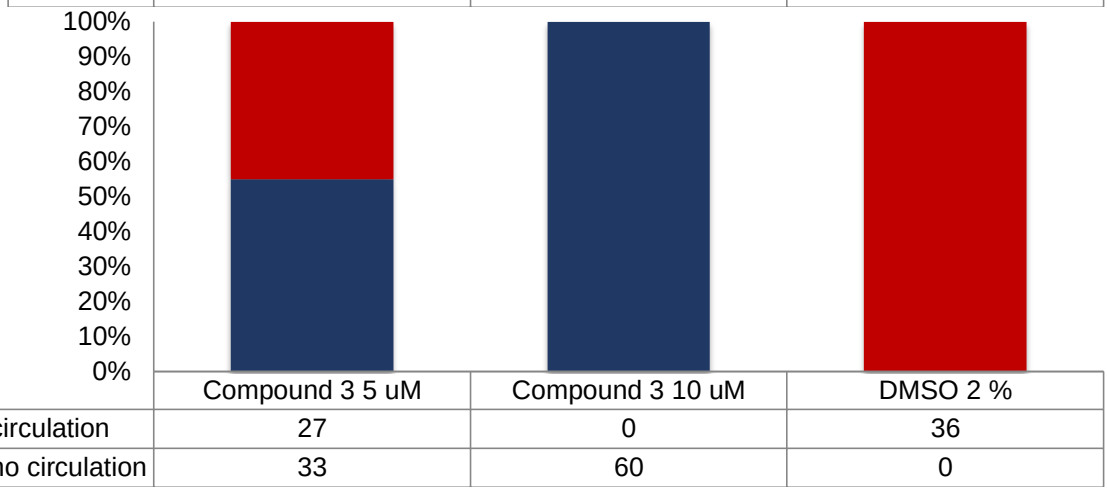

	Compound 3 5 uM	Compound 3 10 uM	DMSO 2 %
circulation	27	0	36
no circulation	33	60	0

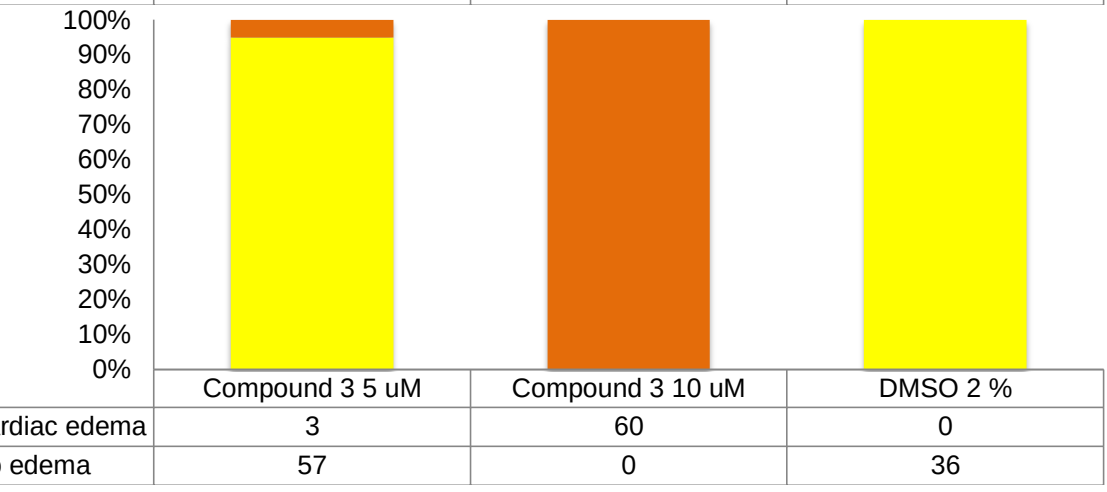

	Compound 3 5 uM	Compound 3 10 uM	DMSO 2 %
cardiac edema	3	60	0
no edema	57	0	36

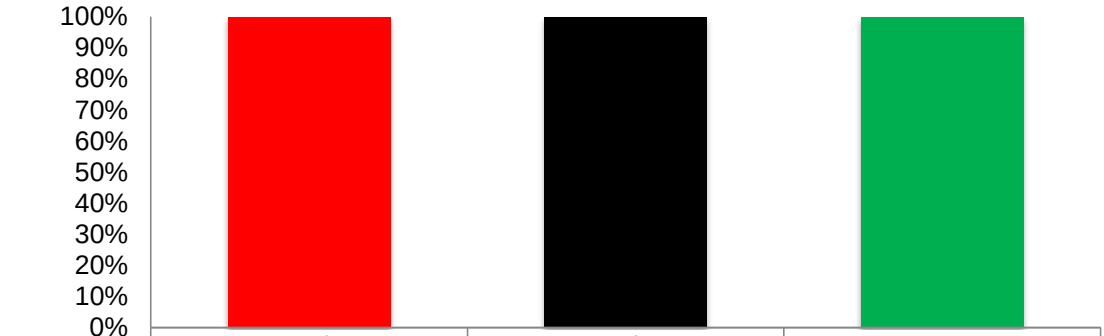

	Compound 3 5 uM	Compound 3 10 uM	DMSO 2 %
abnormal	60	0	0
normal	0	0	36
dead	0	60	0

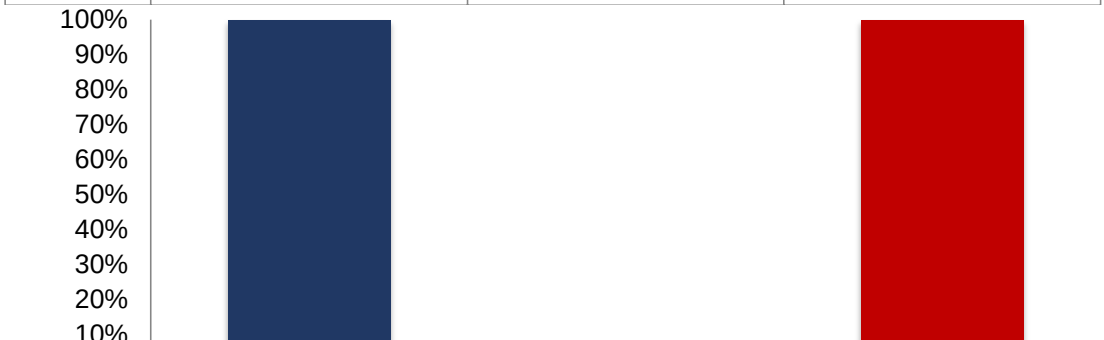

	Compound 3 5 uM	Compound 3 10 uM	DMSO 2 %
circulation	0	0	36
no circulation	60	0	0

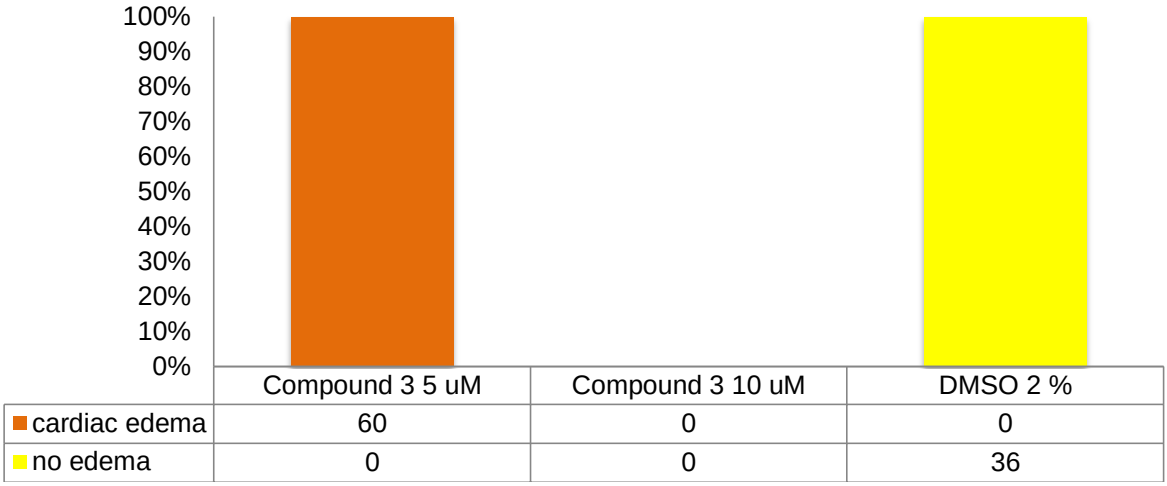

	Compound 3 5 uM	Compound 3 10 uM	DMSO 2 %
cardiac edema	60	0	0
no edema	0	0	36

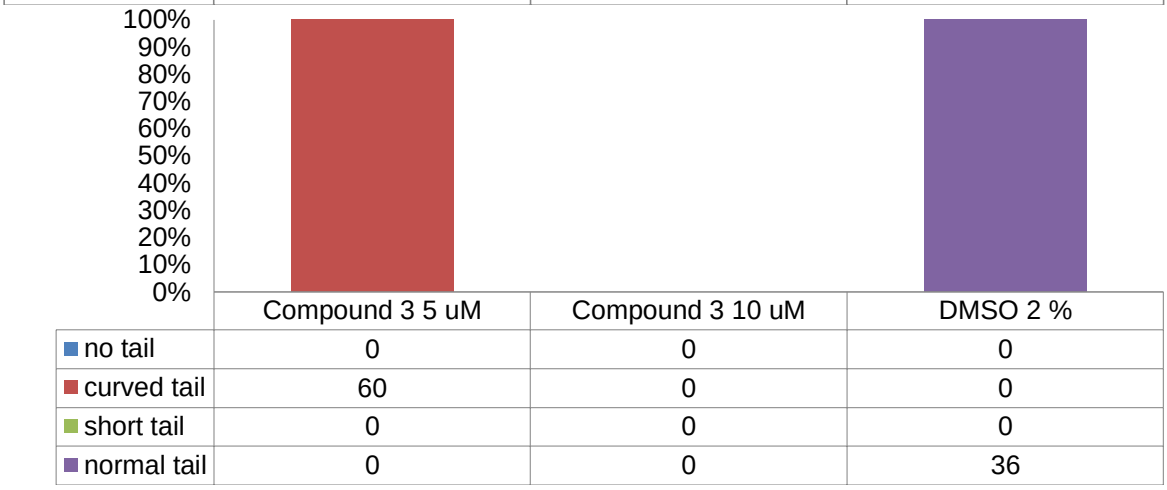

	Compound 3 5 uM	Compound 3 10 uM	DMSO 2 %
no tail	0	0	0
curved tail	60	0	0
short tail	0	0	0
normal tail	0	0	36

Supplementary Figure 7: Time Screen for treatment at 24 hours post fertilization with compound 3.

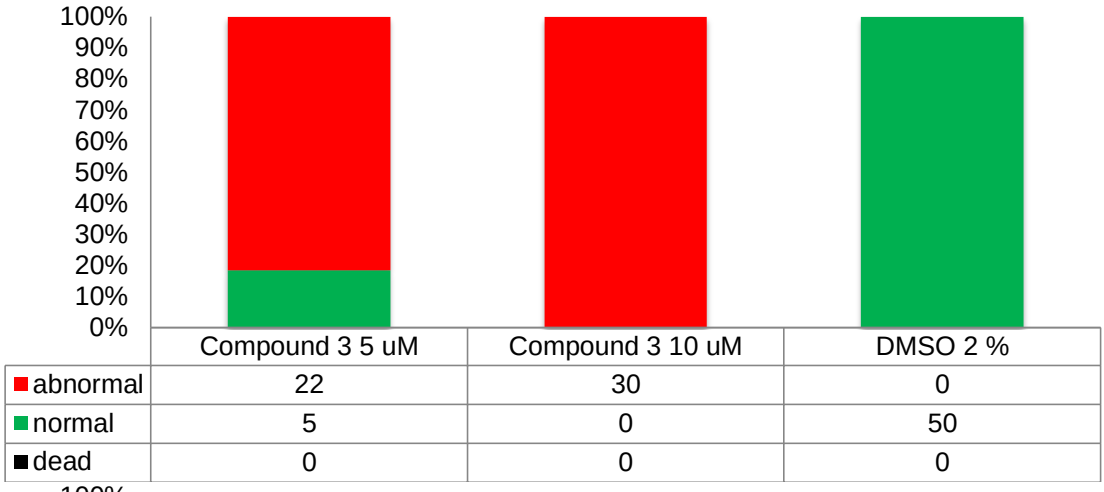

	Compound 3 5 uM	Compound 3 10 uM	DMSO 2 %
abnormal	22	30	0
normal	5	0	50
dead	0	0	0

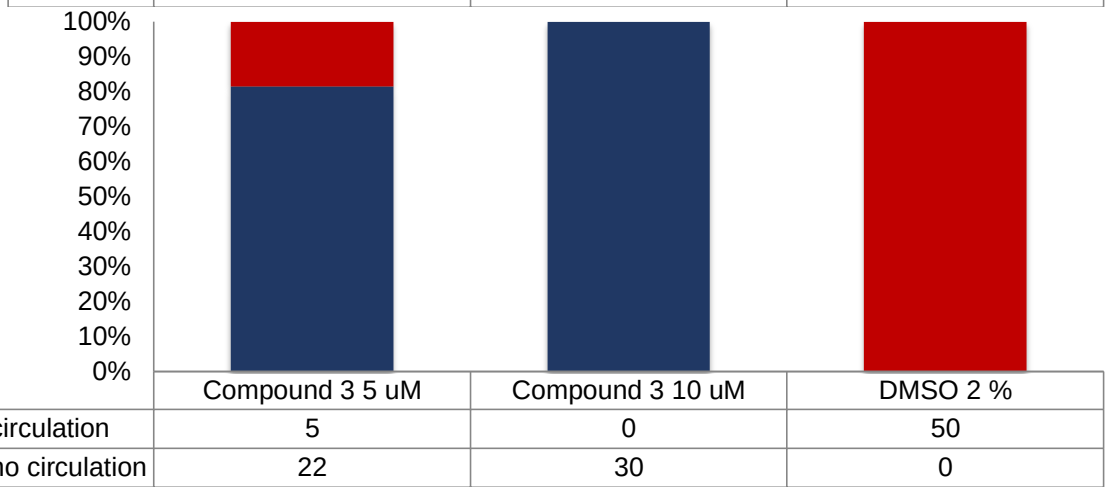

	Compound 3 5 uM	Compound 3 10 uM	DMSO 2 %
circulation	5	0	50
no circulation	22	30	0

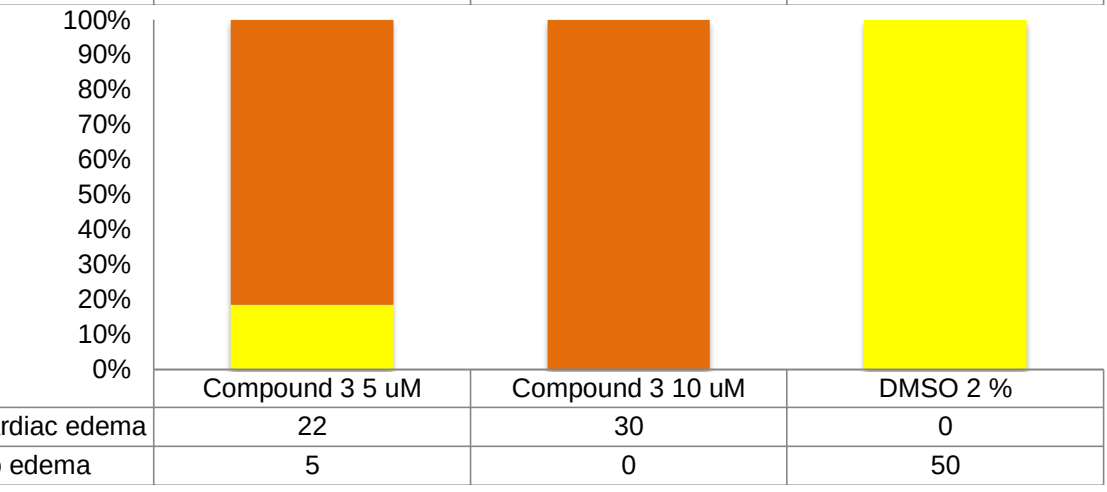

	Compound 3 5 uM	Compound 3 10 uM	DMSO 2 %
cardiac edema	22	30	0
no edema	5	0	50

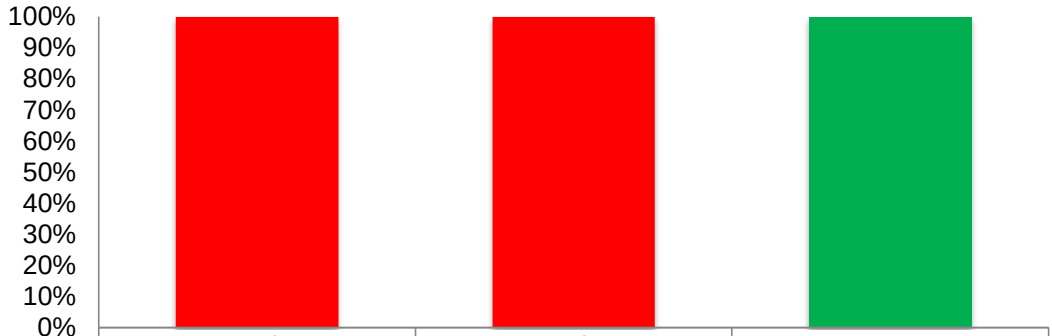

	Compound 3 5 uM	Compound 3 10 uM	DMSO 2 %
abnormal	27	30	0
normal	0	0	50
dead	0	0	0

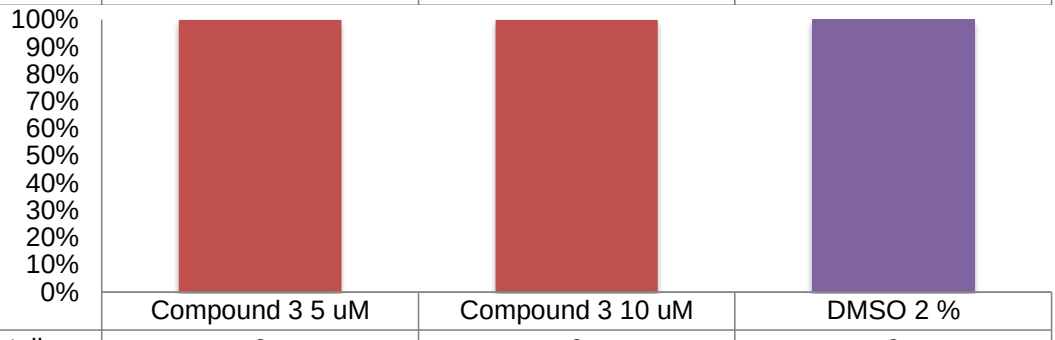

	Compound 3 5 uM	Compound 3 10 uM	DMSO 2 %
no tail	0	0	0
curved tail	27	30	0
short tail	0	0	0
normal tail	0	0	50

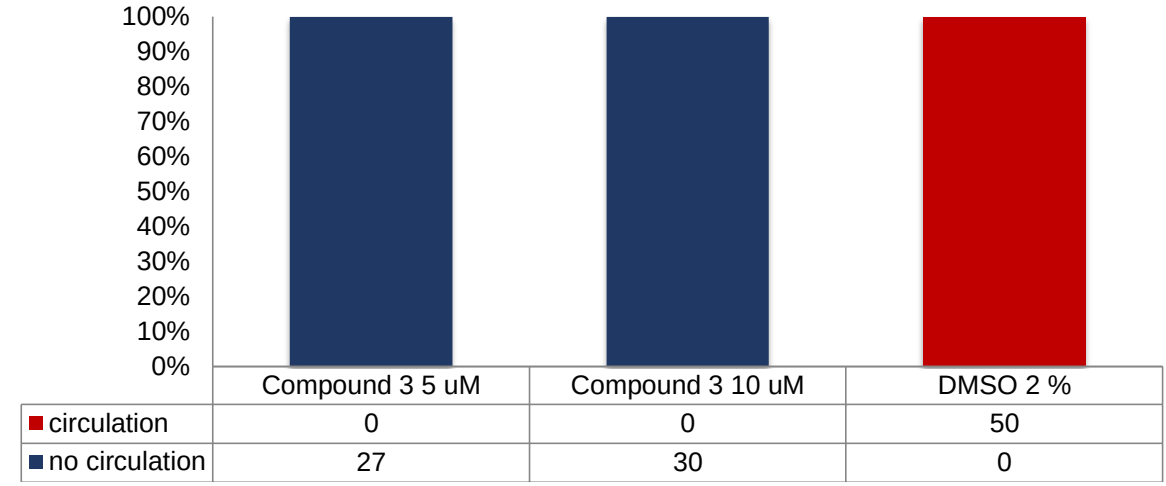

	Compound 3 5 uM	Compound 3 10 uM	DMSO 2 %
circulation	0	0	50
no circulation	27	30	0

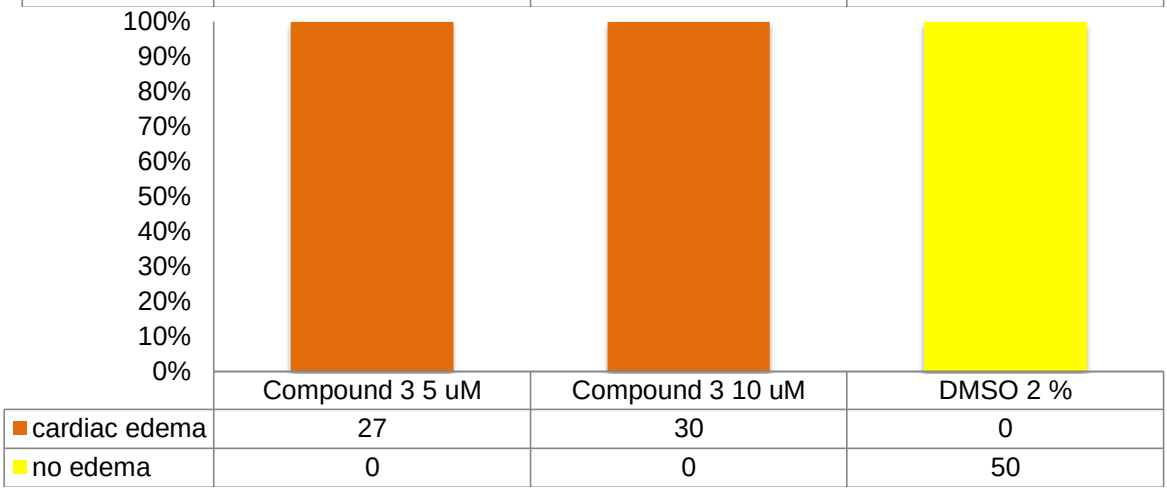

	Compound 3 5 uM	Compound 3 10 uM	DMSO 2 %
cardiac edema	27	30	0
no edema	0	0	50

Supplementary Figure 8: Time Screen for treatment at 48 hours post fertilization with compound 3.

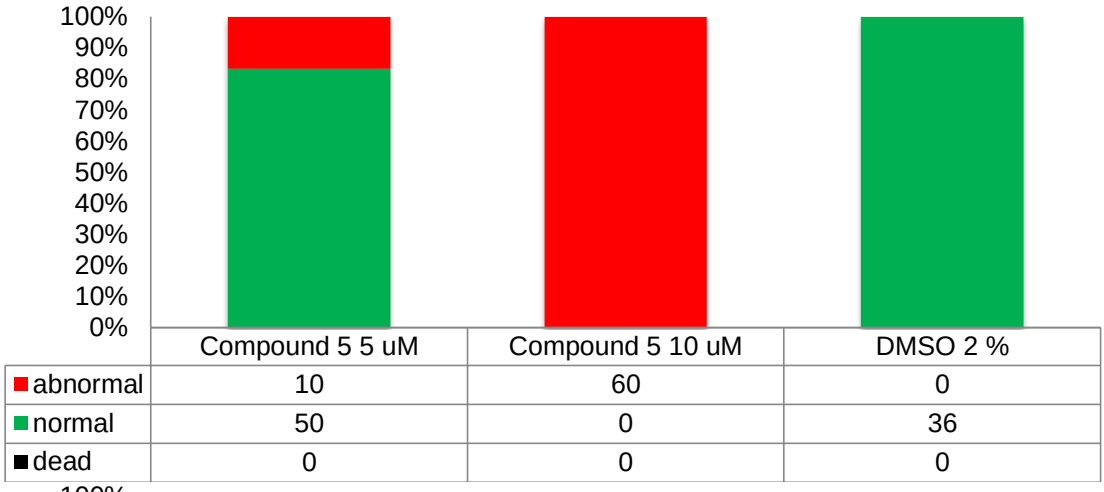

	Compound 5 5 uM	Compound 5 10 uM	DMSO 2 %
abnormal	10	60	0
normal	50	0	36
dead	0	0	0

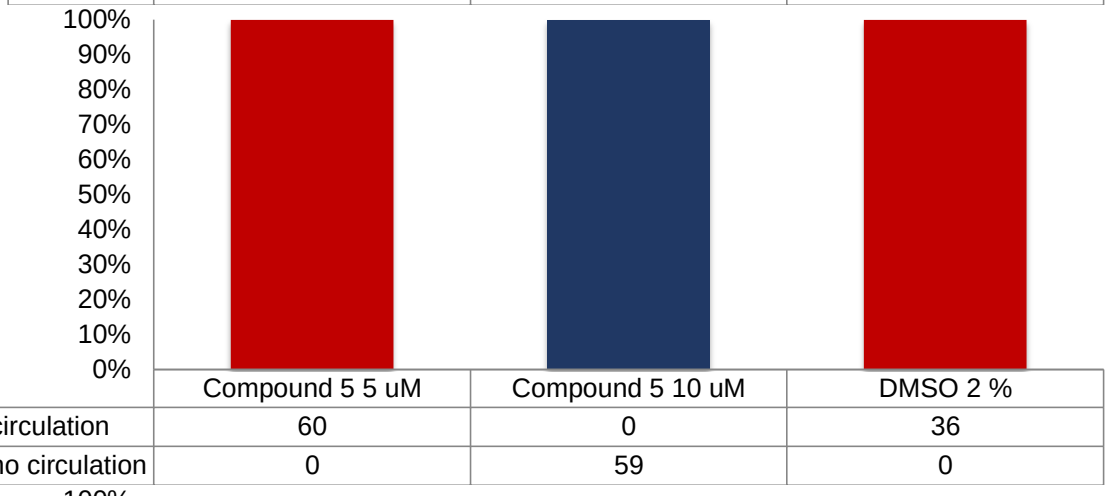

	Compound 5 5 uM	Compound 5 10 uM	DMSO 2 %
circulation	60	0	36
no circulation	0	59	0

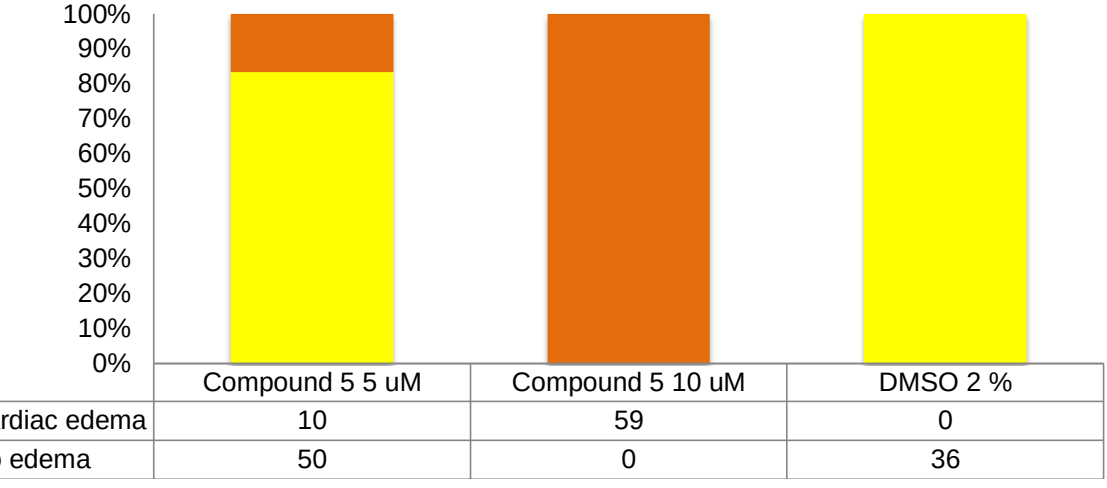

	Compound 5 5 uM	Compound 5 10 uM	DMSO 2 %
cardiac edema	10	59	0
no edema	50	0	36

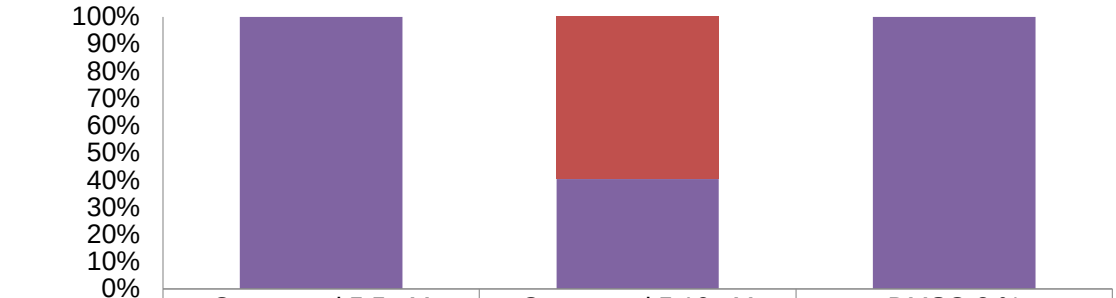

	Compound 5 5 uM	Compound 5 10 uM	DMSO 2 %
no tail	0	0	0
curved tail	0	59	0
short tail	0	0	0
normal tail	60	40	36

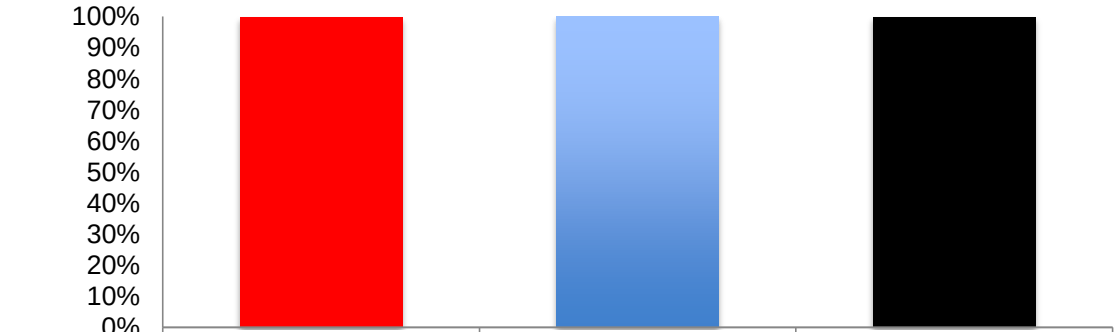

	Compound 5 5 uM	Compound 5 10 uM	DMSO 2 %
abnormal	60	0	0
normal	0	0	36
dead	0	60	0

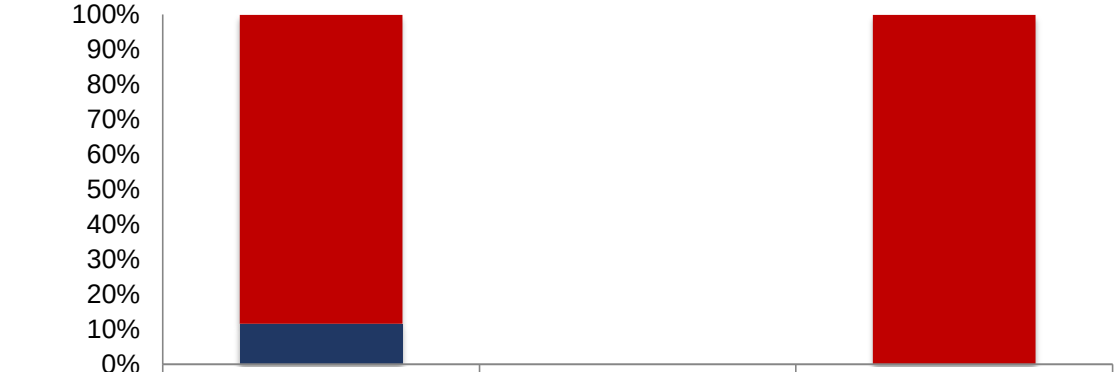

	Compound 5 5 uM	Compound 5 10 uM	DMSO 2 %
circulation	53	0	36
no circulation	7	0	0

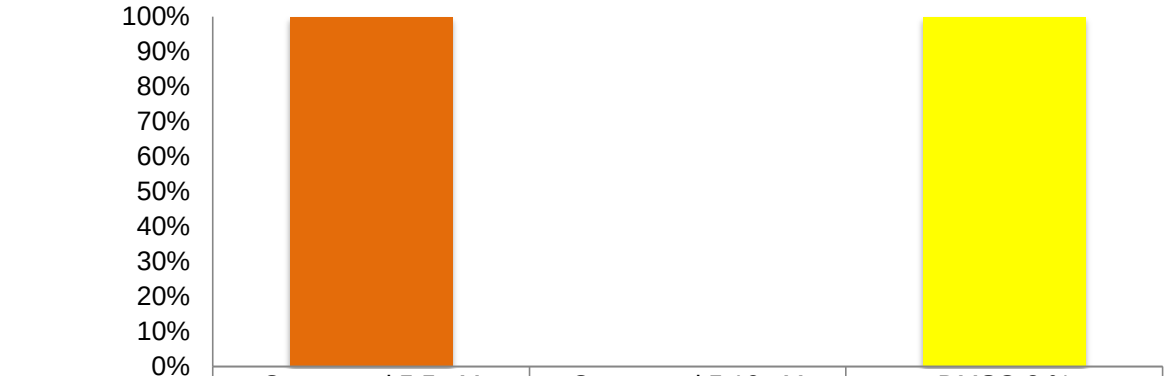

	Compound 5 5 uM	Compound 5 10 uM	DMSO 2 %
cardiac edema	60	0	0
no edema	0	0	36

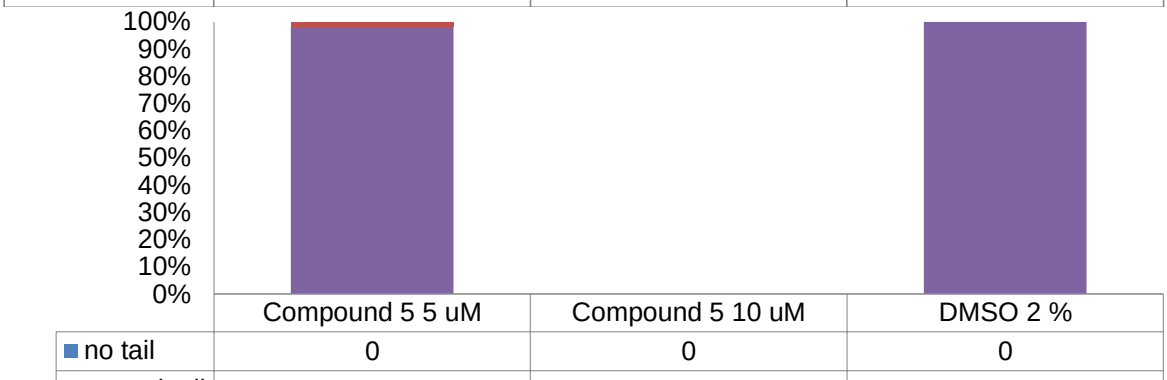

	Compound 5 5 uM	Compound 5 10 uM	DMSO 2 %
no tail	0	0	0
curved tail	1	0	0
short tail	0	0	0
normal tail	59	0	36

Supplementary Figure 9: Time Screen for treatment at 24 hours post fertilization with compound 5.

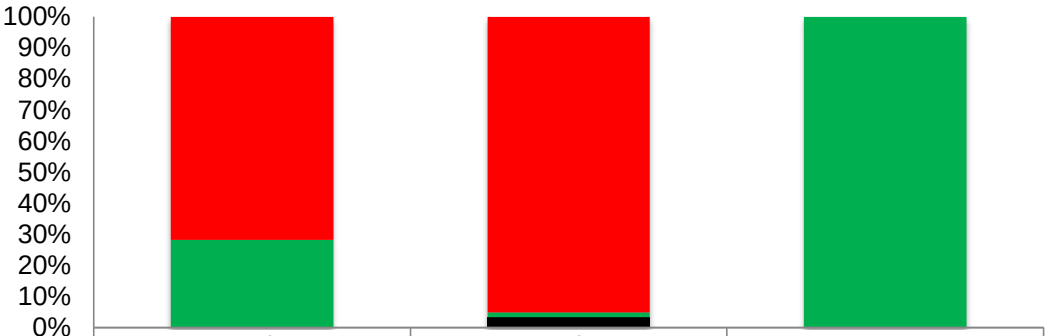

	Compound 6 5 uM	Compound 6 10 uM	DMSO 2 %
abnormal	43	57	0
normal	17	1	36
dead	0	2	0

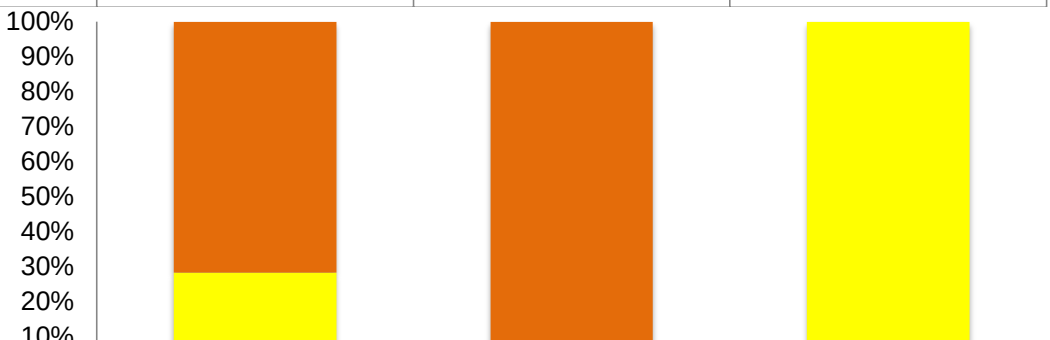

	Compound 6 5 uM	Compound 6 10 uM	DMSO 2 %
cardiac edema	43	57	0
no edema	17	1	36

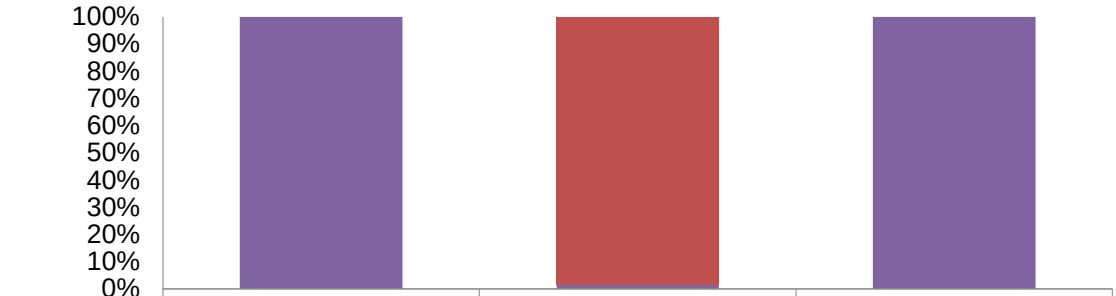

	Compound 6 5 uM	Compound 6 10 uM	DMSO 2 %
no tail	0	0	0
curved tail	0	57	0
short tail	0	0	0
normal tail	60	1	36

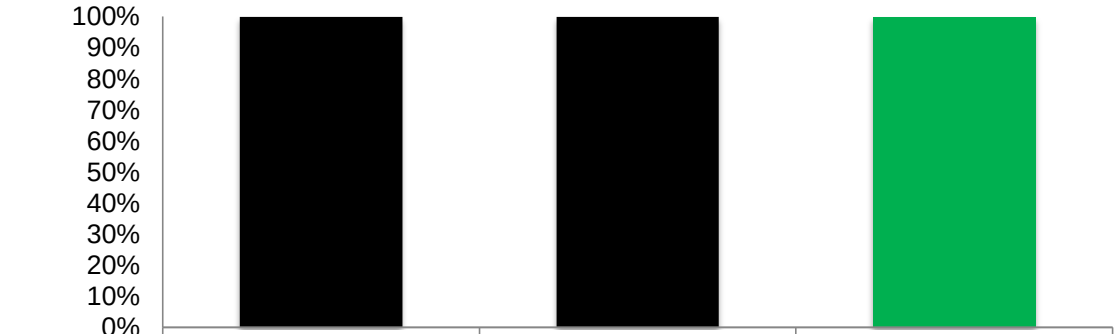

	Compound 6 5 uM	Compound 6 10 uM	DMSO 2 %
abnormal	0	0	0
normal	0	0	36
dead	60	60	0

Supplementary Figure 10: Time Screen for treatment at 24 hours post fertilization with compound 6.

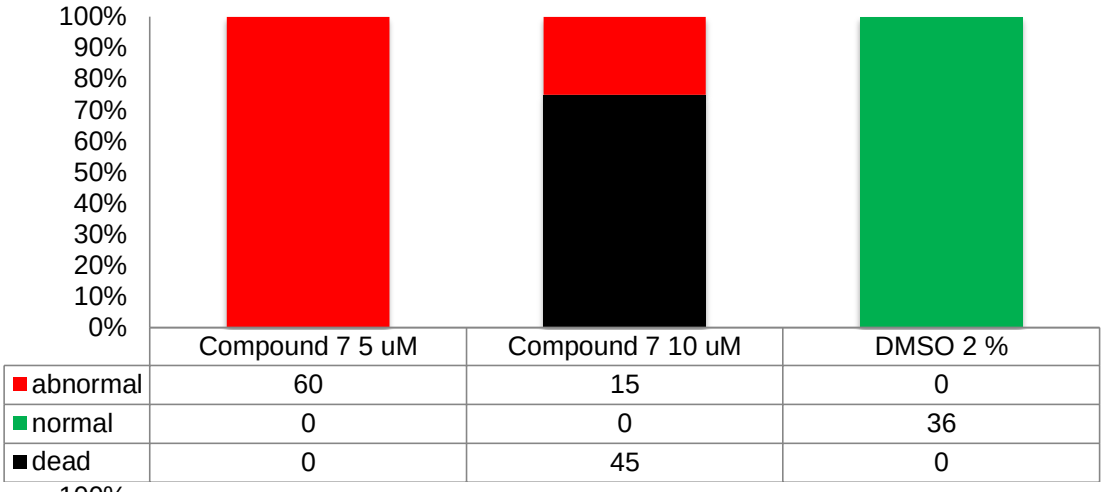

	Compound 7 5 uM	Compound 7 10 uM	DMSO 2 %
abnormal	60	15	0
normal	0	0	36
dead	0	45	0

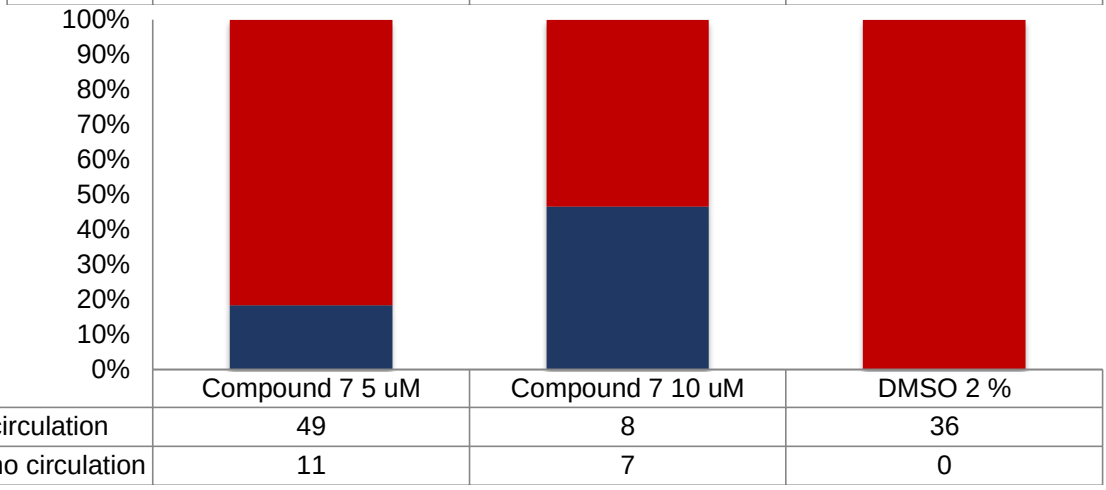

	Compound 7 5 uM	Compound 7 10 uM	DMSO 2 %
circulation	49	8	36
no circulation	11	7	0

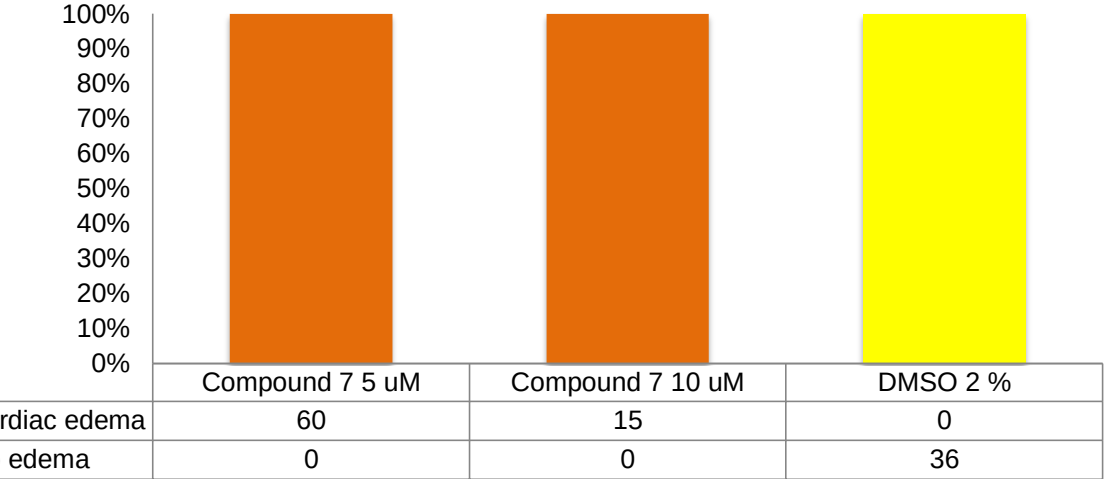

	Compound 7 5 uM	Compound 7 10 uM	DMSO 2 %
cardiac edema	60	15	0
no edema	0	0	36

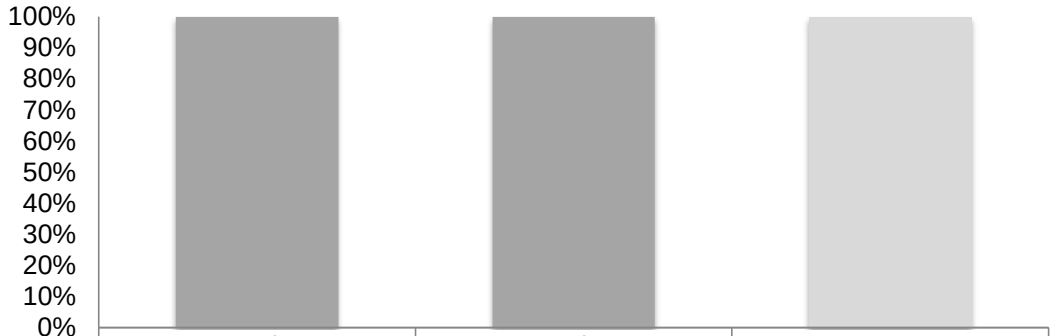

	Compound 7 5 uM	Compound 7 10 uM	DMSO 2 %
no pigment	0	0	0
reduced pigment	60	15	0
pigment	0	0	36

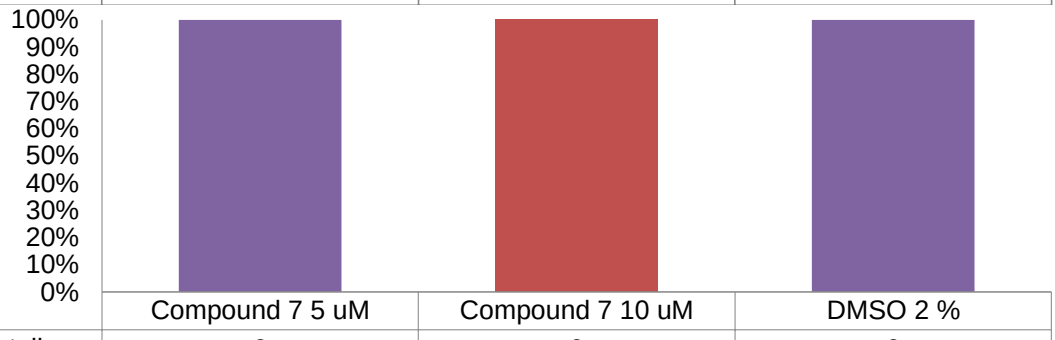

	Compound 7 5 uM	Compound 7 10 uM	DMSO 2 %
no tail	0	0	0
curved tail	0	15	0
short tail	0	0	0
normal tail	60	0	36

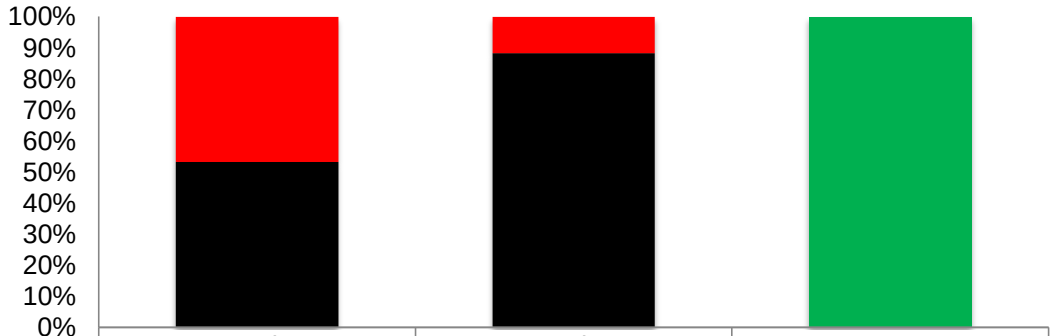

	Compound 7 5 uM	Compound 7 10 uM	DMSO 2 %
abnormal	28	7	0
normal	0	0	36
dead	32	53	0

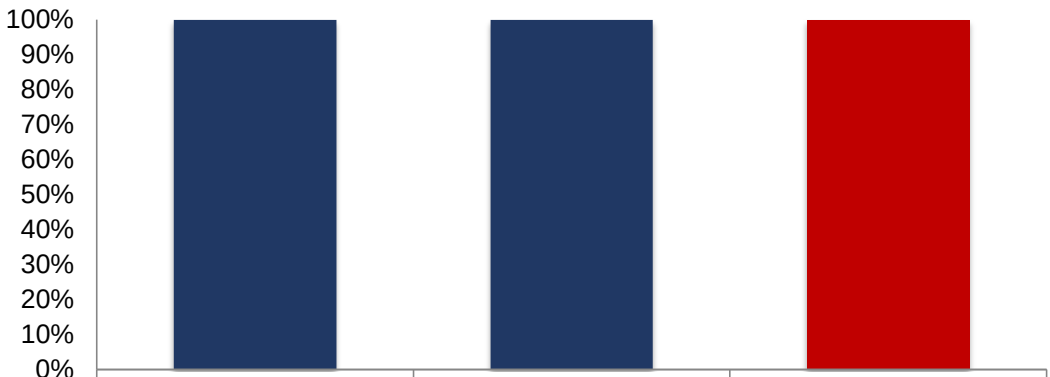

	Compound 7 5 uM	Compound 7 10 uM	DMSO 2 %
circulation	0	0	36
no circulation	28	7	0

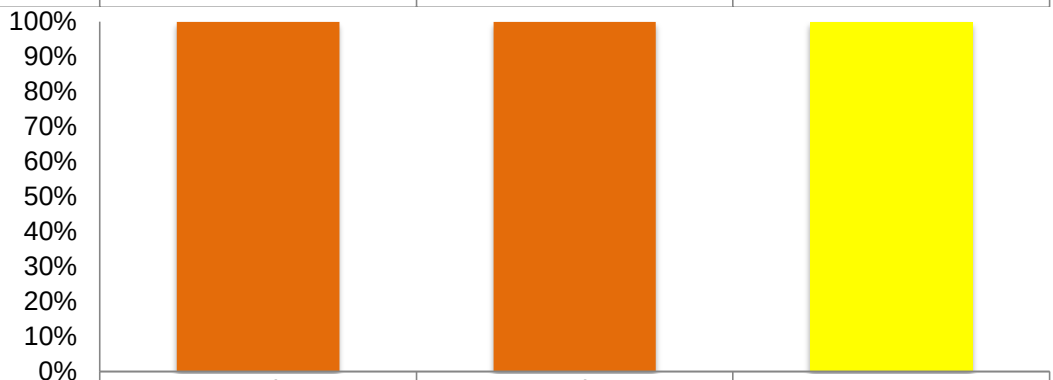

	Compound 7 5 uM	Compound 7 10 uM	DMSO 2 %
cardiac edema	28	7	0
no edema	0	0	36

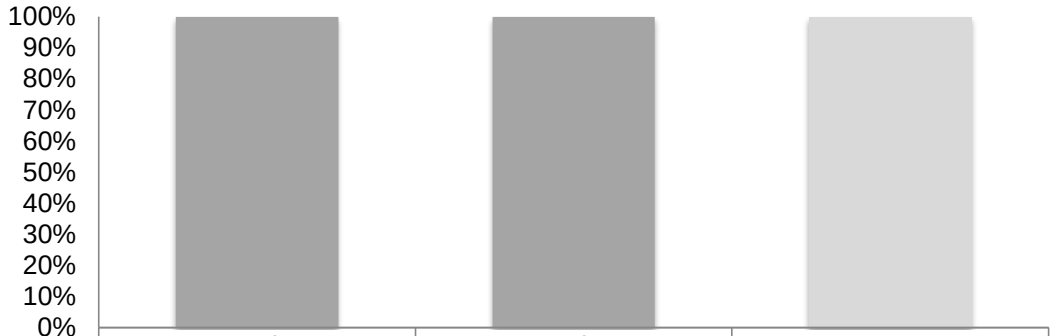

	Compound 7 5 uM	Compound 7 10 uM	DMSO 2 %
no pigment	0	0	0
reduced pigment	28	7	0
pigment	0	0	36

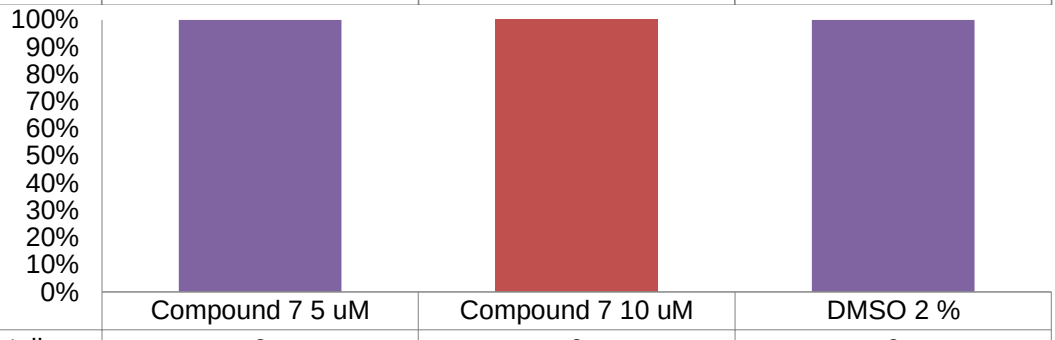

	Compound 7 5 uM	Compound 7 10 uM	DMSO 2 %
no tail	0	0	0
curved tail	0	7	0
short tail	0	0	0
normal tail	28	0	36

Supplementary Figure 11: Time Screen for treatment at 24 hours post fertilization with compound 7.